Time Dependent Methods in Spectroscopy

- What do spectra tell us about dynamics?
- How can we easily calculate spectra?
- Case studies
  - *MIME effect (with J. Zink)*
  - *Benzophenone (with John Frederick)*
  - *Scars*

In the beginning (Schrödinger) ...

$$i\hbar\frac{\partial\psi(x,t)}{\partial t} = H\psi(x,t)$$

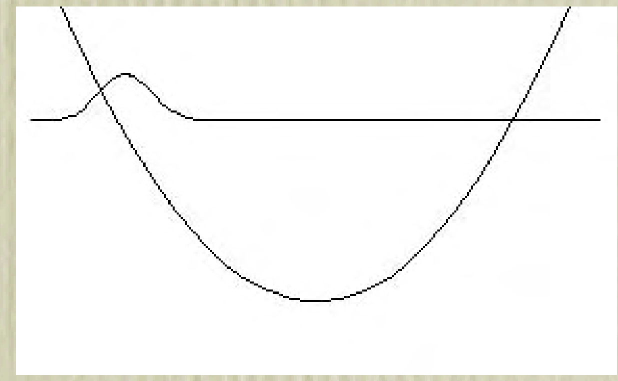

Many years of focus on stationary states followed

$$i\hbar \frac{\partial \psi(x,t)}{\partial t} = H\psi(x,t)$$

$$H\psi_n(x) = E\psi_n(x)$$

Map complex phase into color

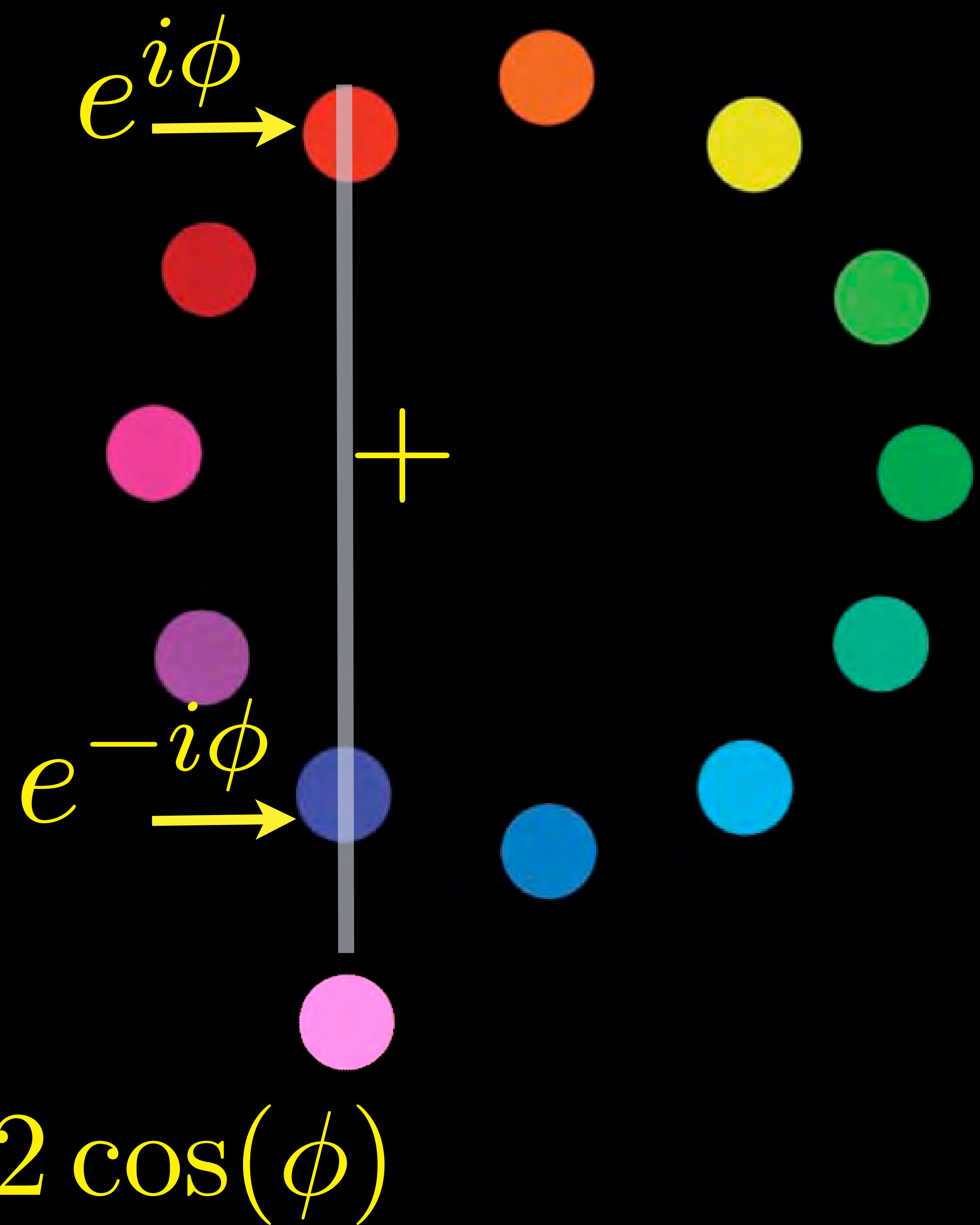

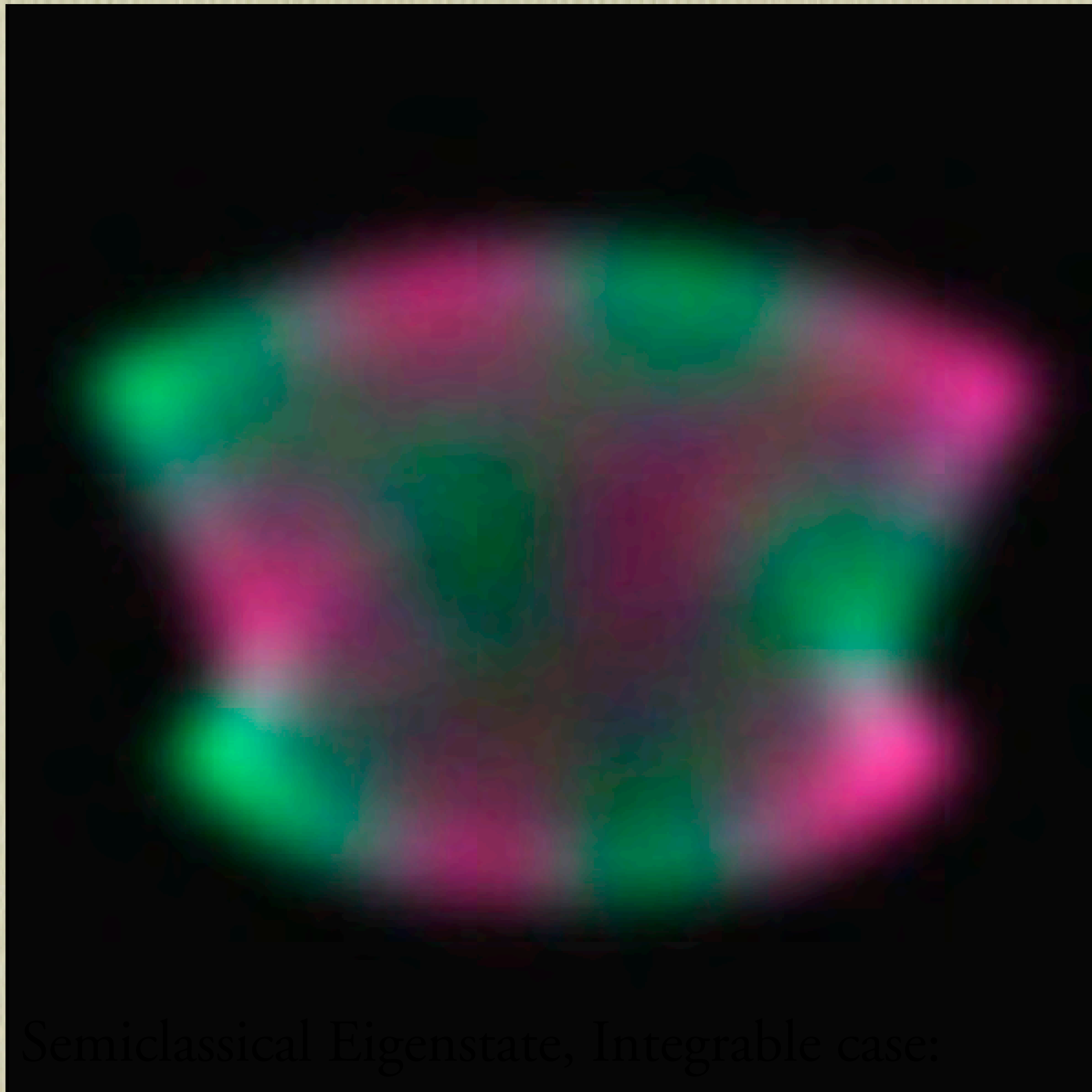

$$\psi(\vec{x}, \vec{J}) = (2\pi i \hbar)^{-n/2} \sum_k \left| \frac{\partial^2 S_k}{\partial \vec{x} \partial \vec{J}} \right|^{1/2} \exp\left[i S_k(\vec{x}, \vec{J})/\hbar - i\, \mu_k\, \pi/2 \right]$$

The focus on stationary states was understandable...

- low energy

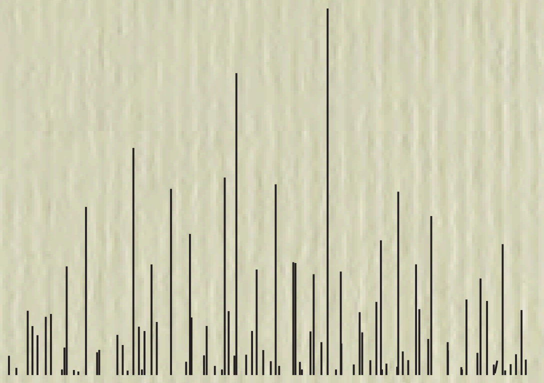

- high resolution “line” spectra
- i.e. evidence of individual eigenstates predominated

Franck-Condon formula

$$\sigma(\omega) = \sum_n f_n^a \; \delta(\hbar\omega - E_n)$$

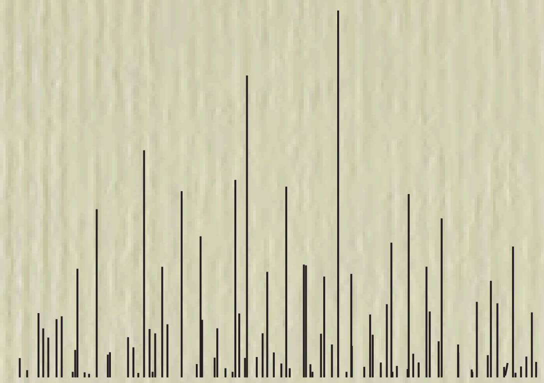

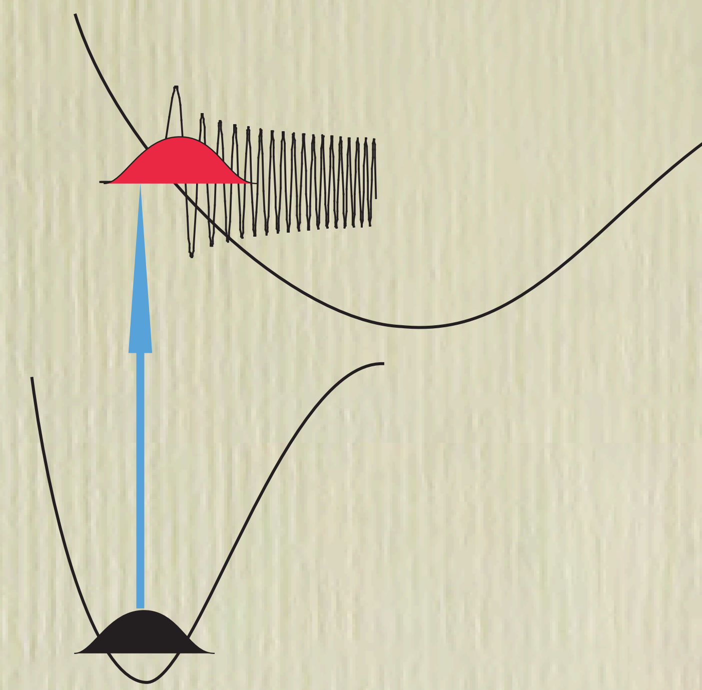

$$f_n^a = |\langle \chi_{e,n} | \mu_{ge} | \chi_{g,a} \rangle|^2$$

Time dependent version

$$\sigma(\omega) = \int_{-\infty}^{\infty} dt \; e^{i\omega t} \langle \phi_a | \phi_a(t) \rangle$$

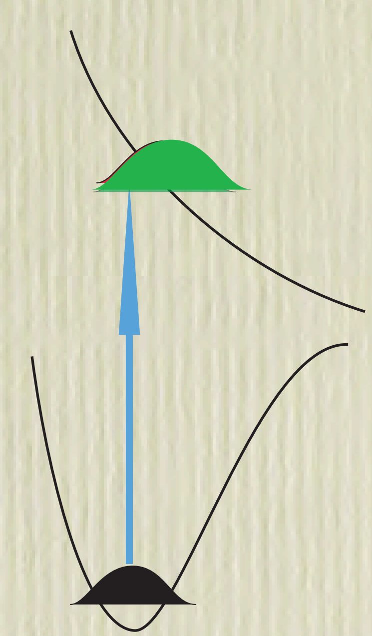

$$|\phi_a\rangle \equiv \mu_{ge} |\chi_{g,a}\rangle$$

$$|\phi_a(t)\rangle = e^{-iH_e t/\hbar} |\phi_a\rangle$$

Exact! not semiclassical

It's begging a Semiclassical Wavepacket Implementation

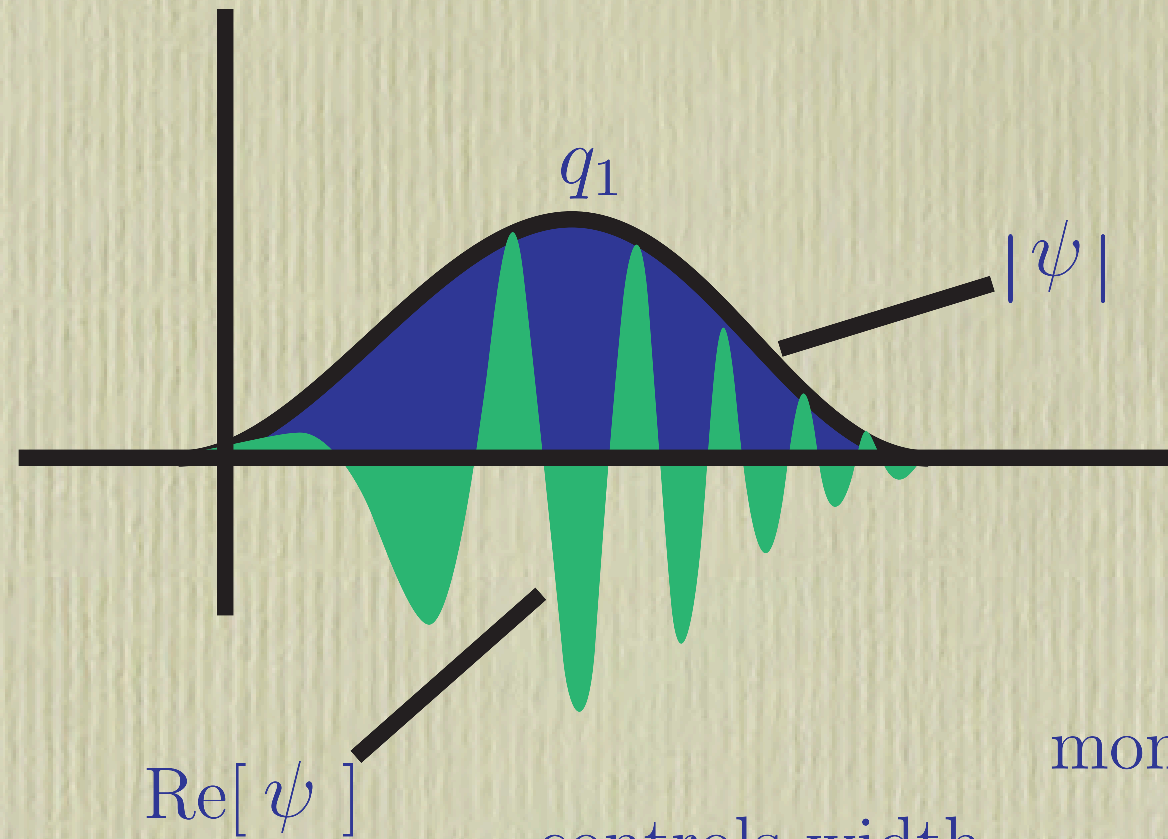

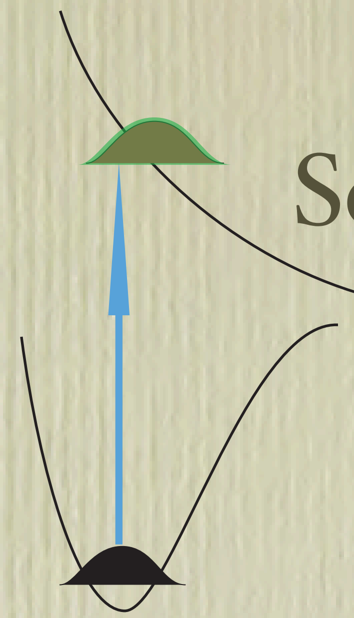

Implementation

position-momentum correlation

controls width

average momentum

$$\psi_{\mathbf{t}}(q) = \left(\frac{2\,a_{\mathbf{t}}}{\pi\hbar}\right)^{1/4} \exp\left[-\frac{a_{\mathbf{t}} + i b_{\mathbf{t}}}{\hbar}(q - q_{\mathbf{t}})^2 + \frac{i}{\hbar} p_1 (q - q_{\mathbf{t}}) + \frac{i}{\hbar}\phi_{\mathbf{t}}\right]$$

normalization factor

average position

phase

Thawed gaussian approximation

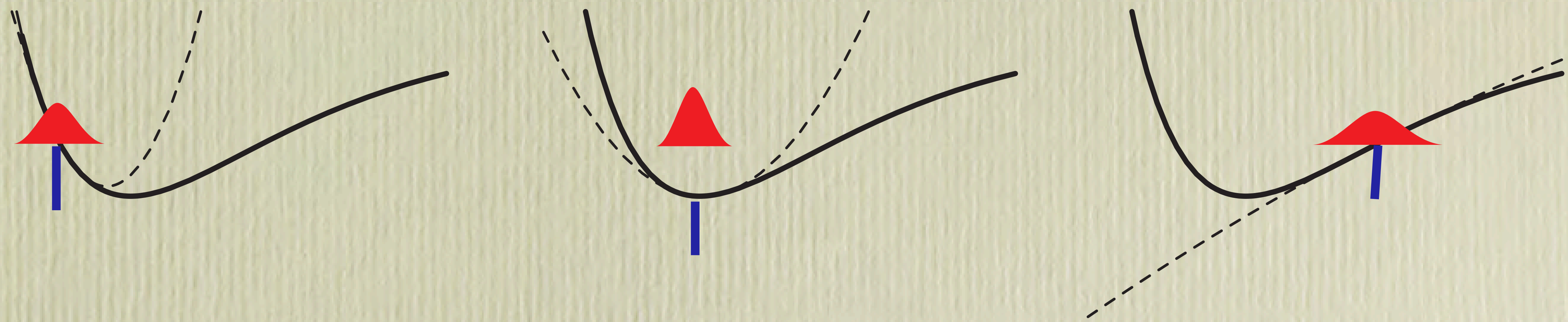

-- Center guided

Other gaussian wavepacket propagation schemes

Frozen Gaussians
Off-center guiding

The dream: provide a physically motivated basis set for chemical dynamics

- semiclassical Gaussian wavepackets are locally correct solutions to the time dependent Schroedinger equation
- they are a complete set - expand in semiclassical Gaussian basis
- they individually are guided by and act like classical trajectories; easy to run in many degrees of freedom

Many strategies and variants....

- Thawed Gaussians, frozen gaussians, Herman-Kluk, variational (Huber - EJH), off center guiding (Tomsovic - EJH), Jackson & Metiu (B.O. surface crossing), van Vleck cellular dynamics,...
- Promising recent work:, Ben-Nun & Martinez (spawning, surface crossing); Child & Shlashilin (variational swarm), H-K by many workers, van Voorhis & EJH (nearly real), Rossky & Co, Batista ...
- Related work by Miller & Co, Makri & Co,

Time-Frequency Correspondence

$$\sigma(\omega) = \int_{-\infty}^{\infty} dt\; e^{i\omega t} \langle \phi_a | \phi_a(t) \rangle$$

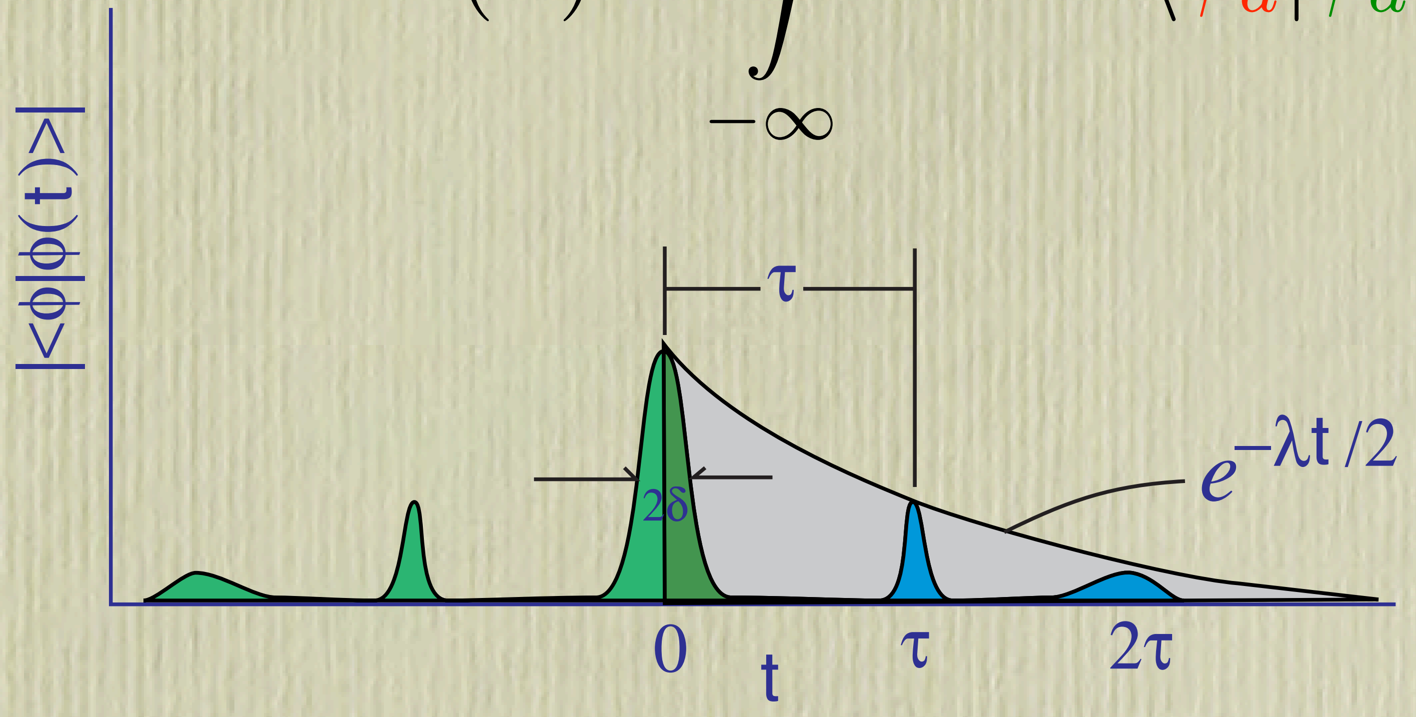

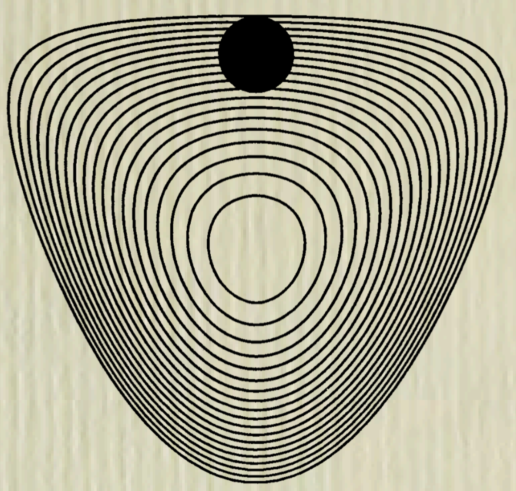

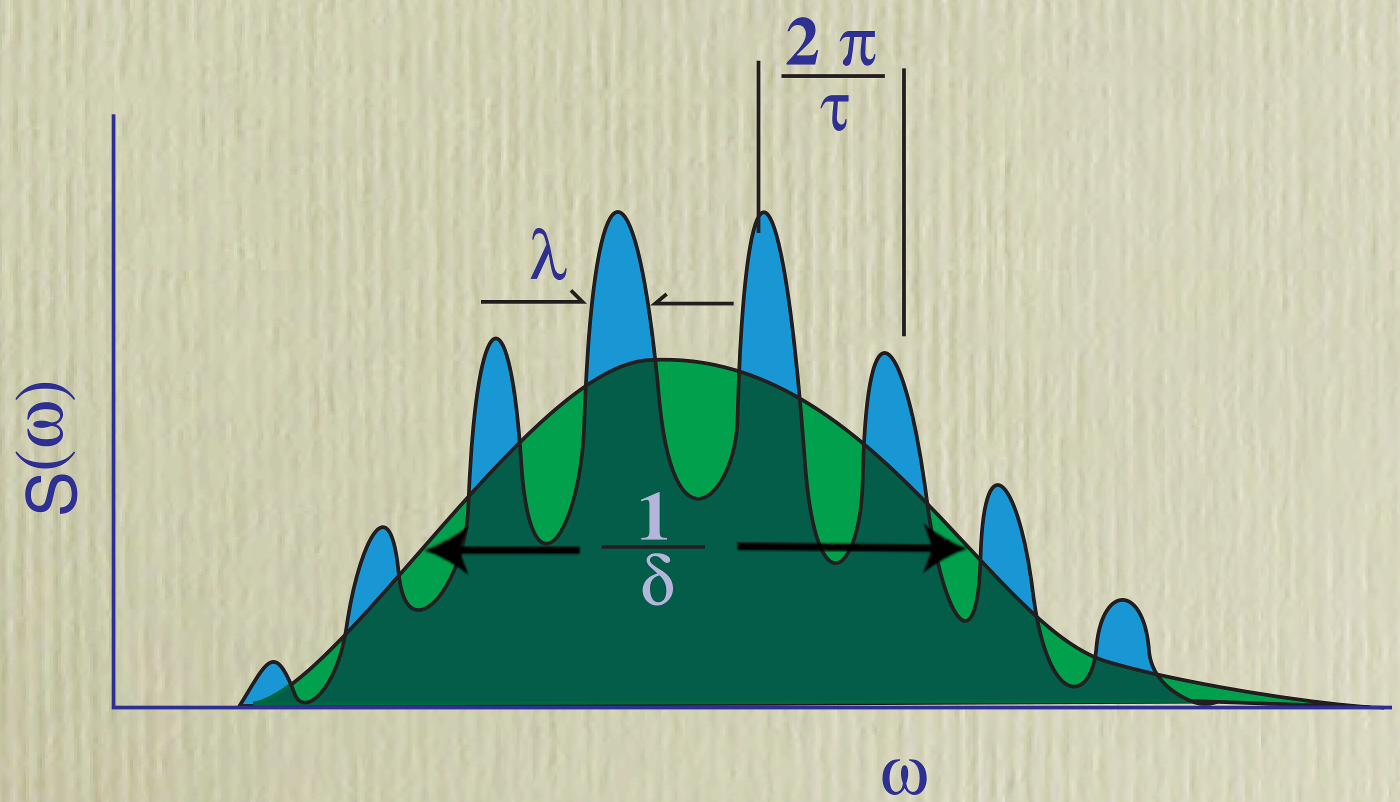

$$\langle \phi_a | \phi_a(t) \rangle = \frac{1}{2\pi} \int_{-\infty}^{\infty} e^{-i\omega t} \sigma(\omega) d\omega$$

$$\sigma(\omega) = \int_{-\infty}^{\infty} dt\ e^{i\omega t} \langle \phi_a | \phi_a(t) \rangle$$

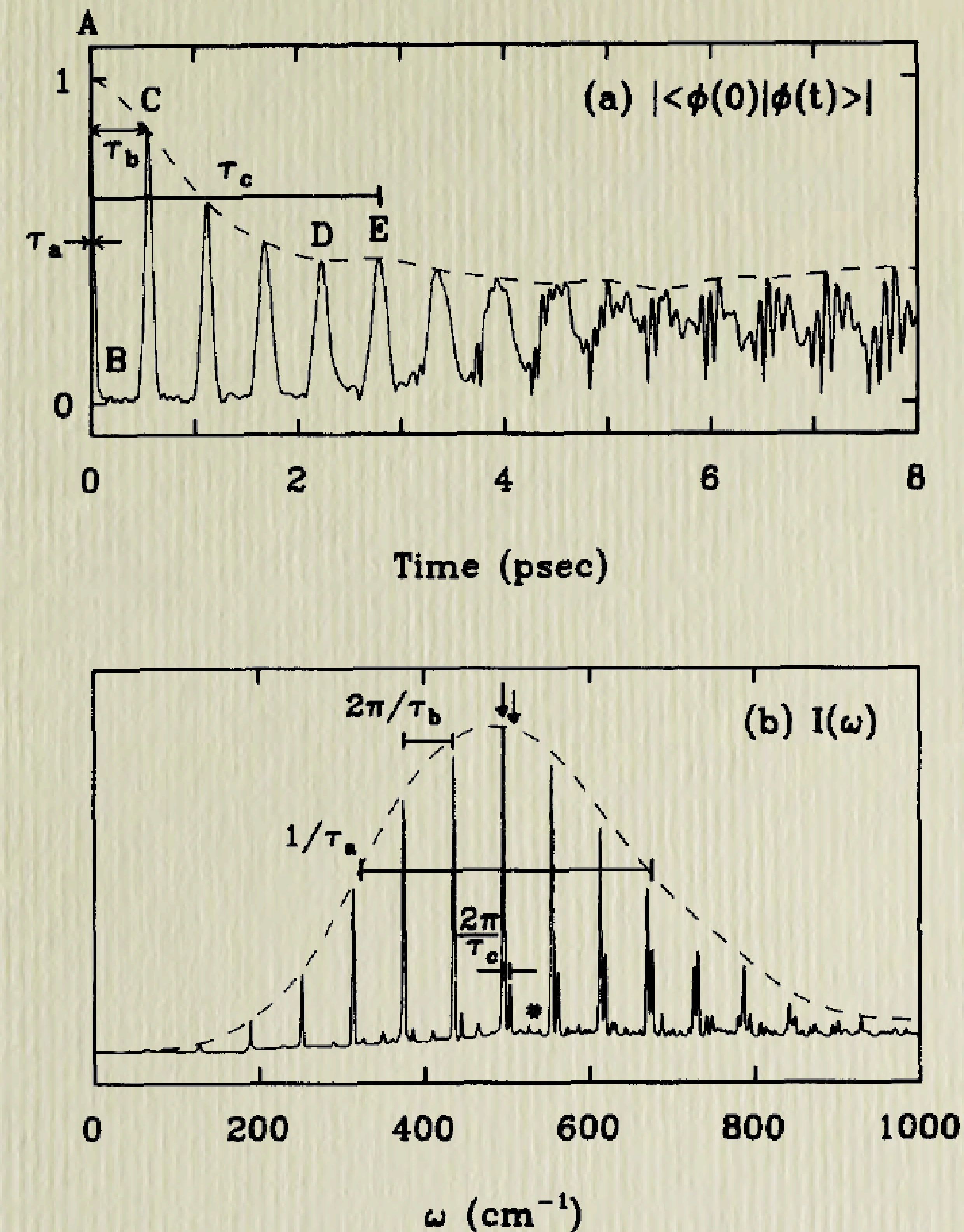

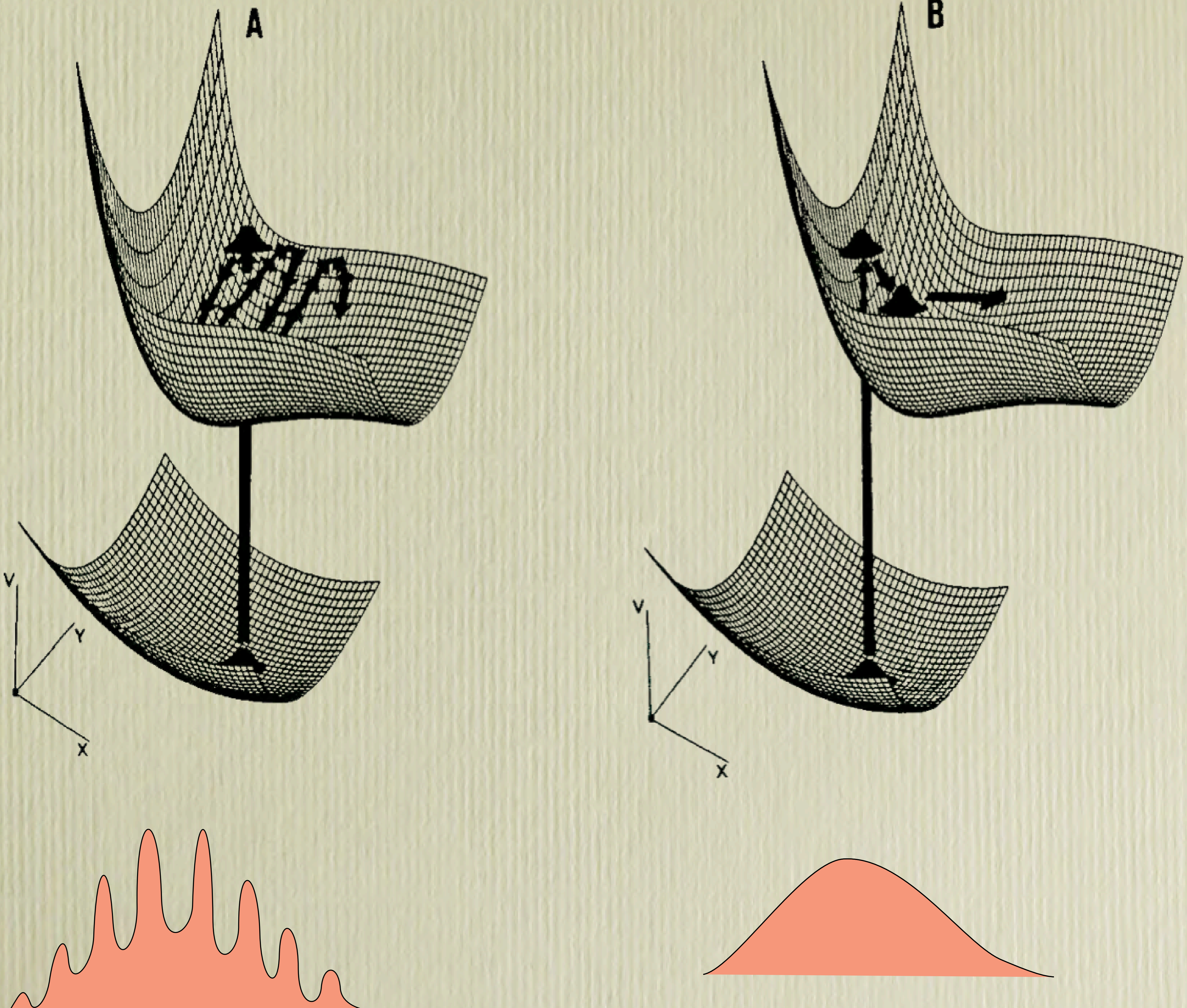
A
B
V
Y
X
V
Y
X

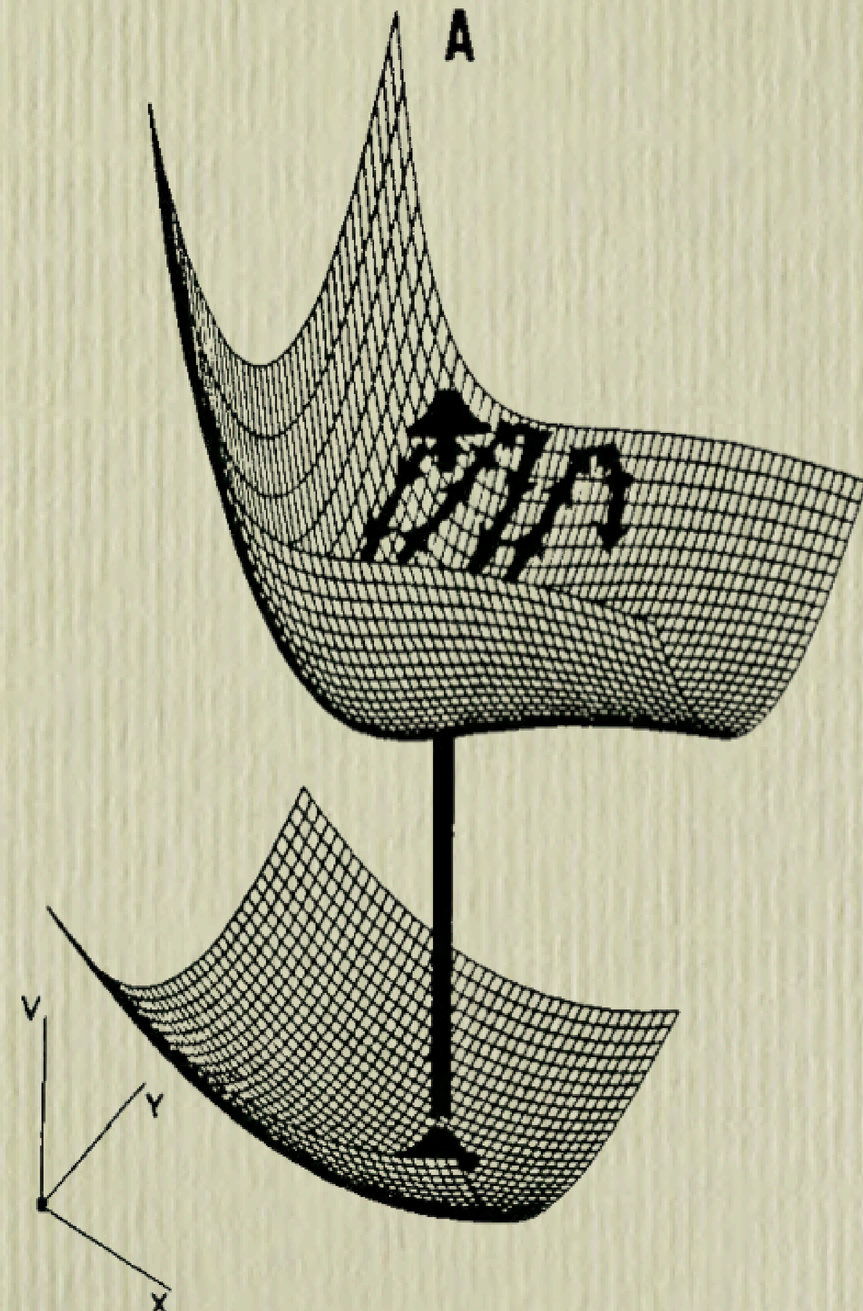
A
V
Y
X
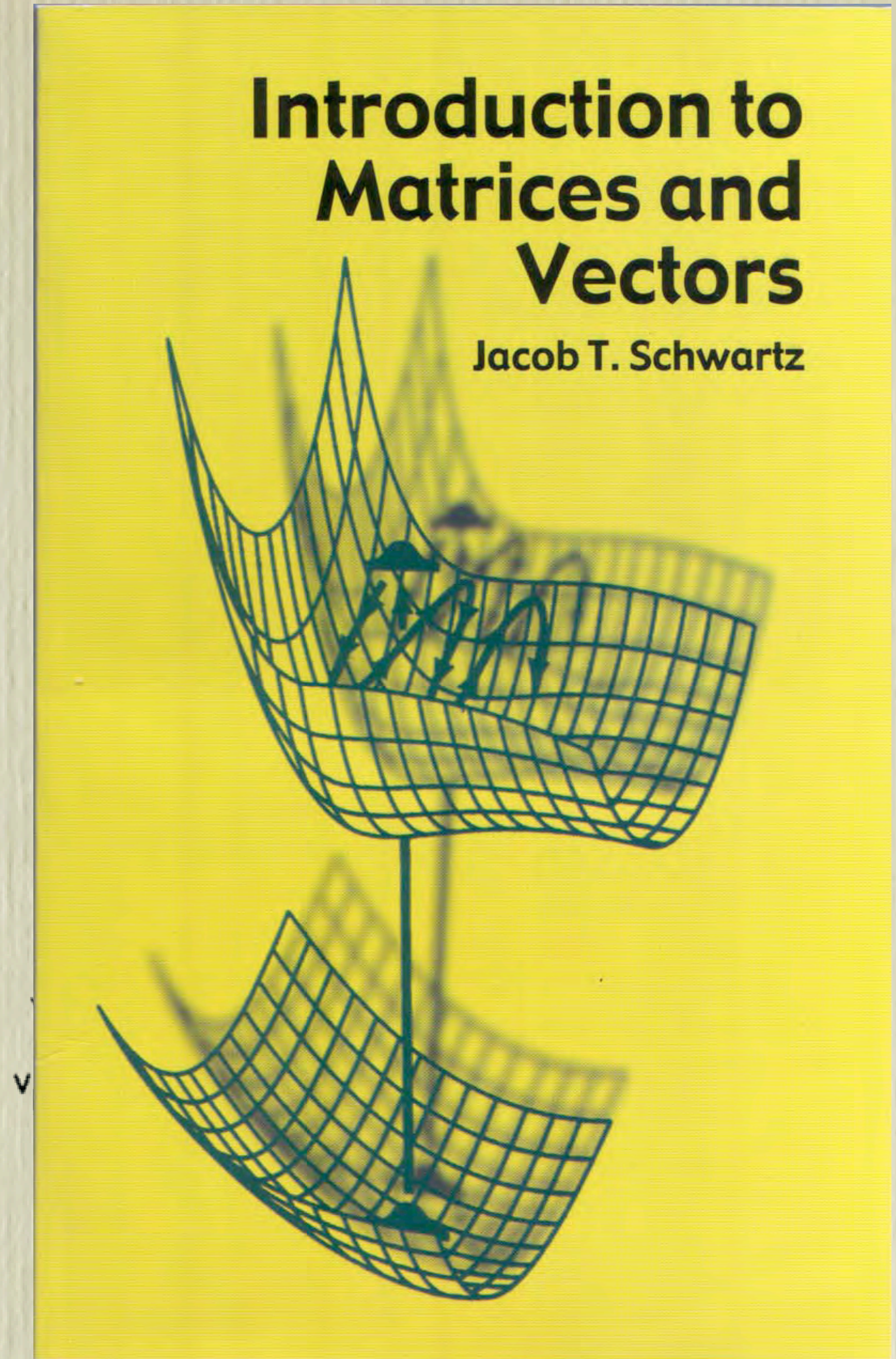
Introduction to
Matrices and
Vectors
Jacob T. Schwartz

Wavepacket, autocorrelation, spectrum

Eigenstates by Fourier Transform

$$\psi_E(\vec{x}) = \lim_{T\to\infty} \frac{1}{T} \int_{-T}^{T} e^{iEt/\hbar} \psi(\vec{x}, t)\ dt$$

{RUN MOVIE}

Wavepacket, autocorrelation, spectrum, eigenfunction

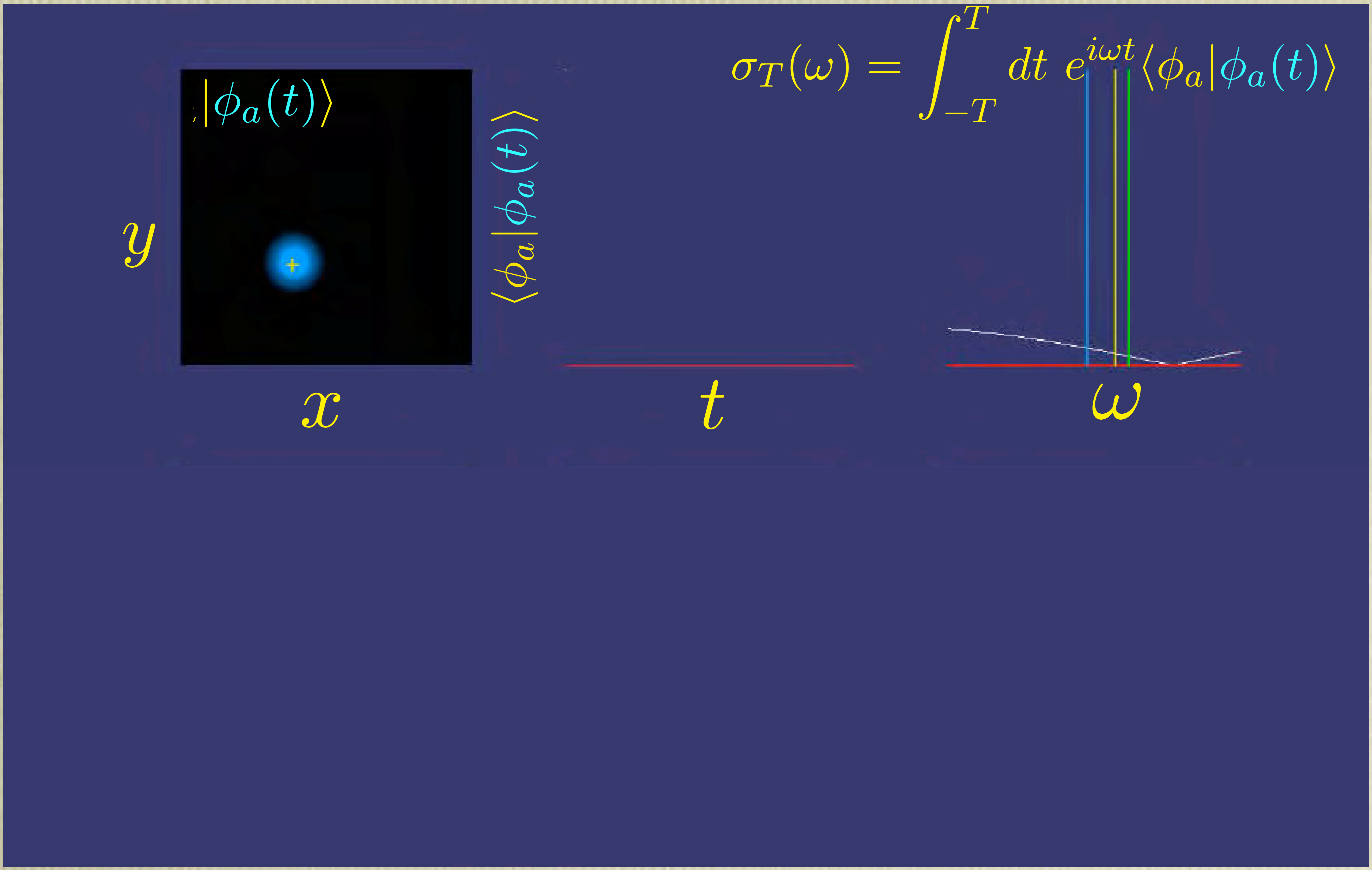

$$\sigma(\omega) = \int_{-\infty}^{\infty} dt\ e^{i\omega t} \langle \phi_a | \phi_a(t) \rangle$$

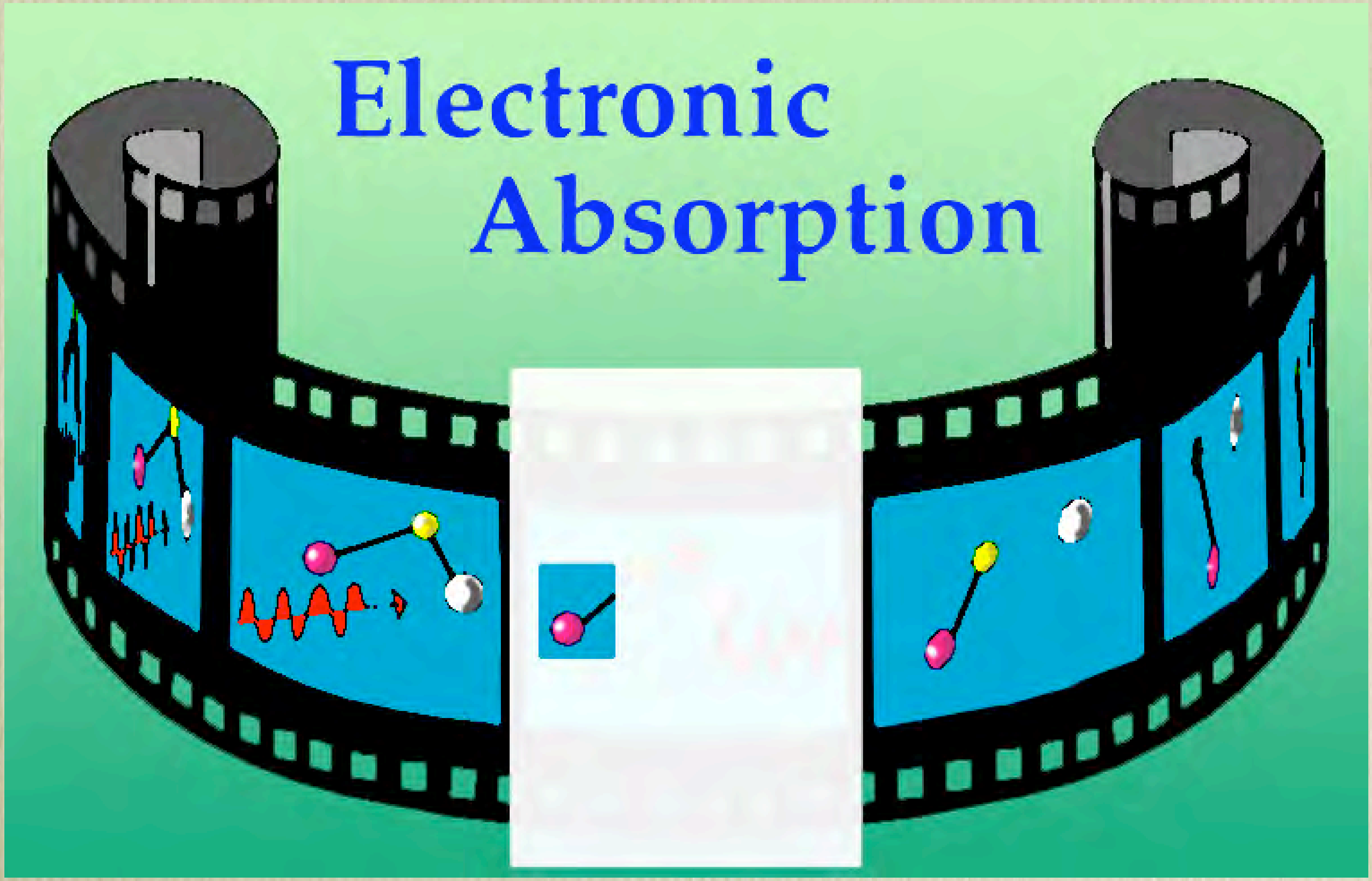

From a spectrum to dynamics

$$\langle \phi_a | \phi_a(t) \rangle = \frac{1}{2\pi} \int_{-\infty}^{\infty} e^{-i\omega t} \sigma(\omega) d\omega$$

correlation function

$$P_a(t) = |\langle \phi_a | \phi_a(t) \rangle|^2$$

survival probability

$$P(a|a) = \lim_{T \to \infty} \int_0^T P_a(t)\; dt$$

measure of phase space flow

Measuring ergodicity with one state

$$P(a|a) = \lim_{T\to\infty} \int_0^T P_a(t)\ dt$$

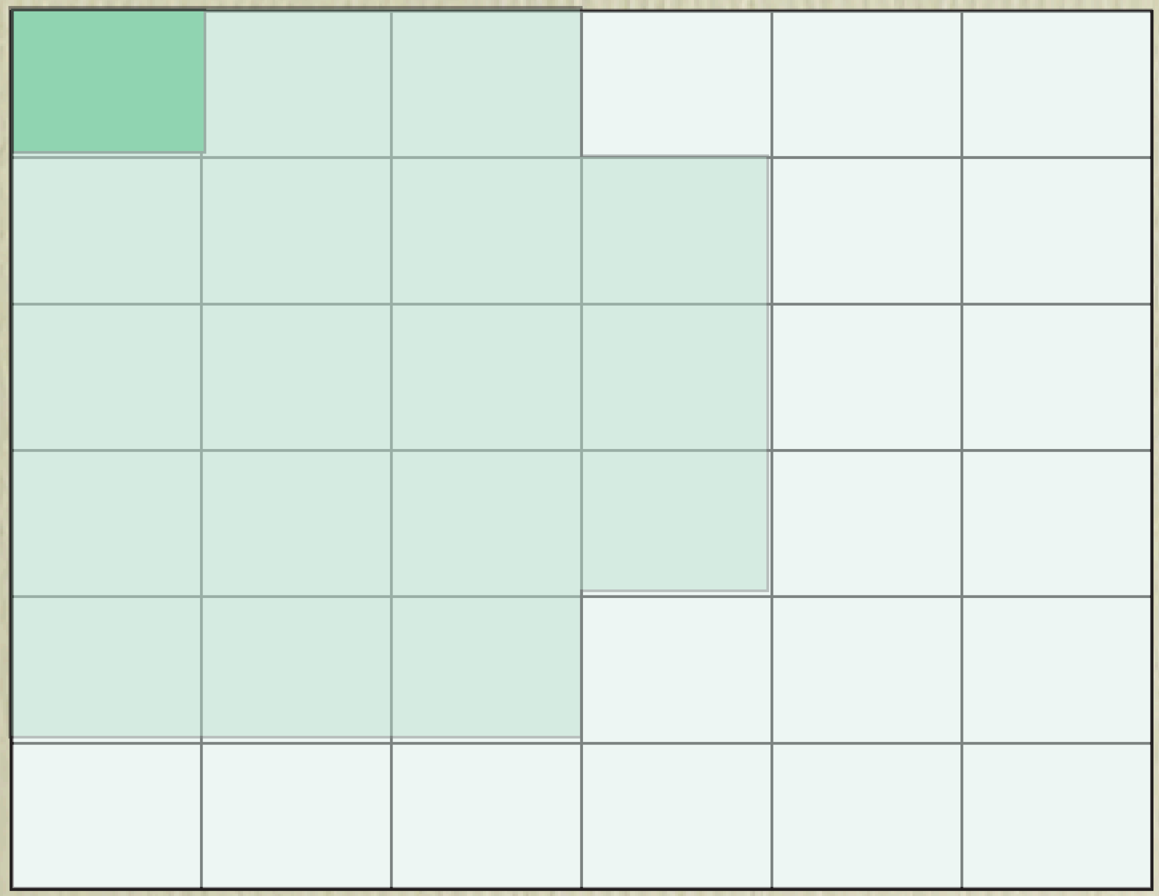

Eigenstate Projections

$$a_n = \langle E_n | \alpha \rangle \qquad p_n^\alpha = |\langle E_n | \alpha \rangle|^2$$

p_n^α measures the tendency of an eigenstate to be large in a certain region of phase space. Since

$$|\langle E_n | \alpha \rangle|^2 = |\langle E_n | \alpha(t) \rangle|^2,$$

such regions of large overlap are correlated (O'Connor, EJH).

Time averaged phase space transport

$$P(\alpha|\beta) \equiv \frac{1}{T} \int_0^{T \to \infty} |\langle \beta | \alpha(t) \rangle|^2 \, dt$$

Easily shown:

$$P(\alpha|\beta) = \sum_n p_n^\alpha p_n^\beta$$

Quantum Ergodicity:

$$P(\alpha|\beta) = P(\alpha|\gamma) = P(\beta|\delta) = \; ...$$

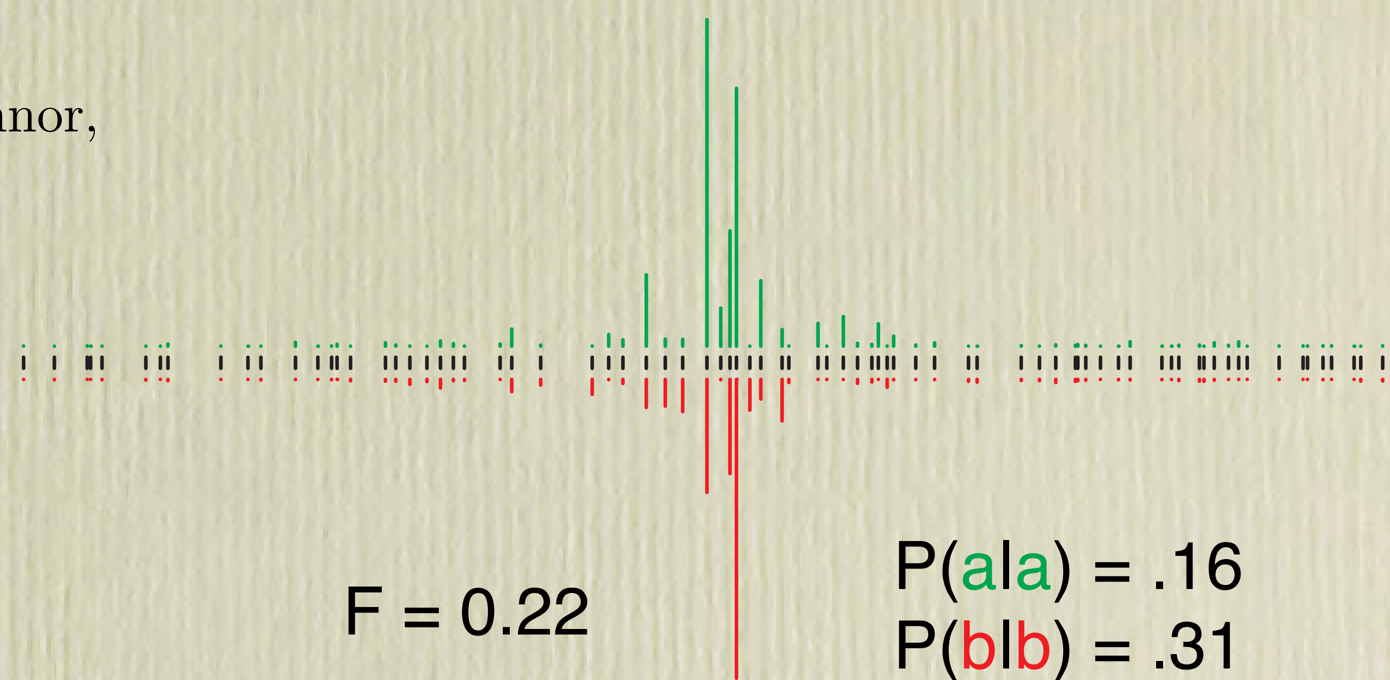

F = 0.22

P(a|a) = .16
P(b|b) = .31
P(a|b) = .16

$$\langle \phi_a | \phi_a(t) \rangle$$

$$\int_{-\infty}^{\infty} e^{i\omega t} \langle \phi_a | \phi_a(t) \rangle \, dt$$

$$P_{aa}(t) = |\langle \phi_a | \phi_a(t) \rangle|^2$$

One Photon-
Absorption Spectra

$$P(a|a) = \lim_{T \to \infty} \frac{1}{T} \int_0^T P_{aa}(t) \, dt$$

SPECTRA ⟷ DYNAMICS

Phase Space Flow

Two Photon-
Raman Spectra

$$P(b|a) = \lim_{T \to \infty} \frac{1}{T} \int_0^T P_{ba}(t) \, dt$$

$$\left| \int_0^{\infty} e^{i\omega t} \langle \phi_b | \phi_a(t) \rangle \, dt \right|^2$$

$$P_{ba}(t) = |\langle \phi_b | \phi_a(t) \rangle|^2$$

$$\langle \phi_b | \phi_a(t) \rangle$$

Another view of absorption/emission from a time dependent viewpoint

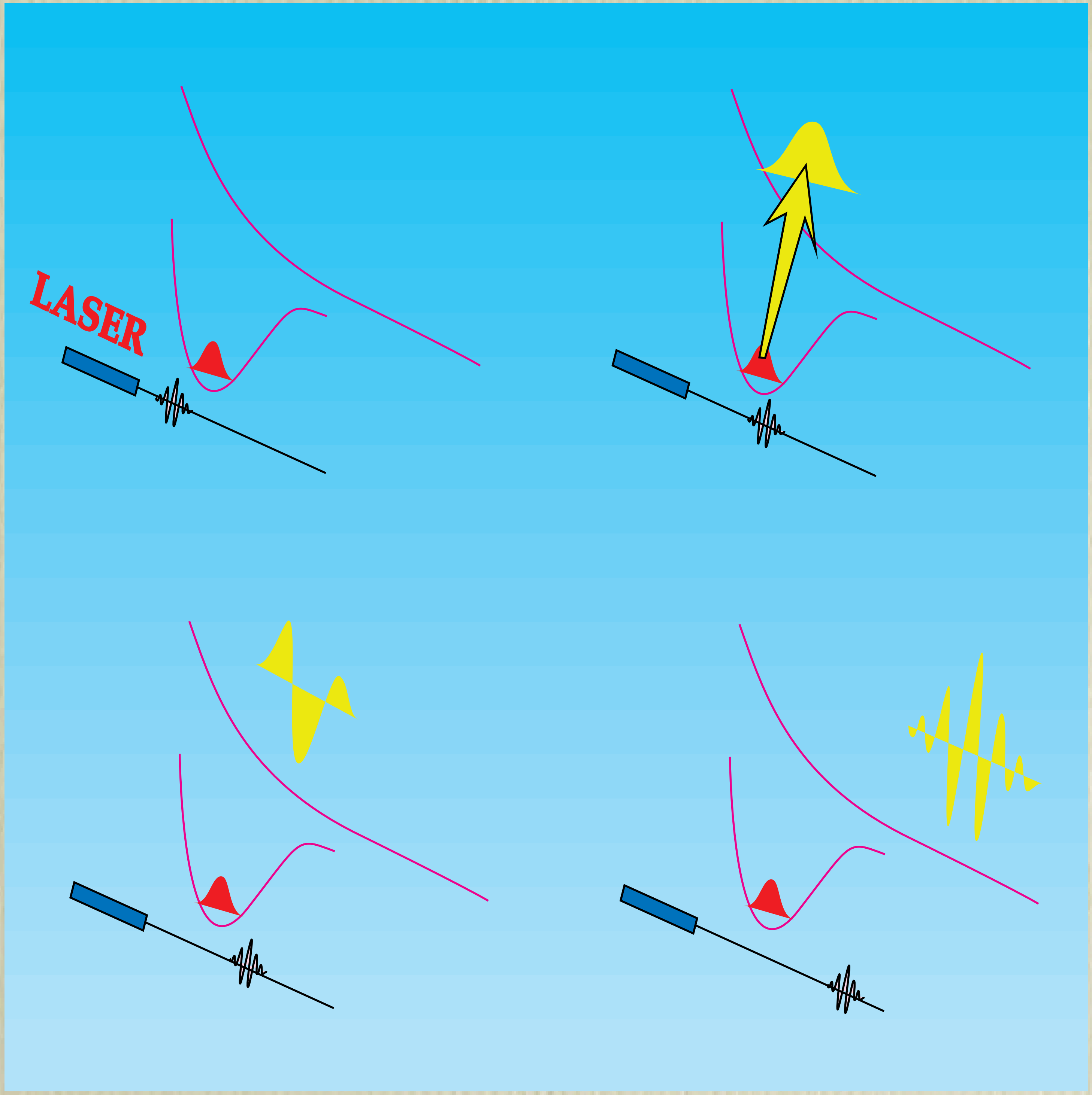

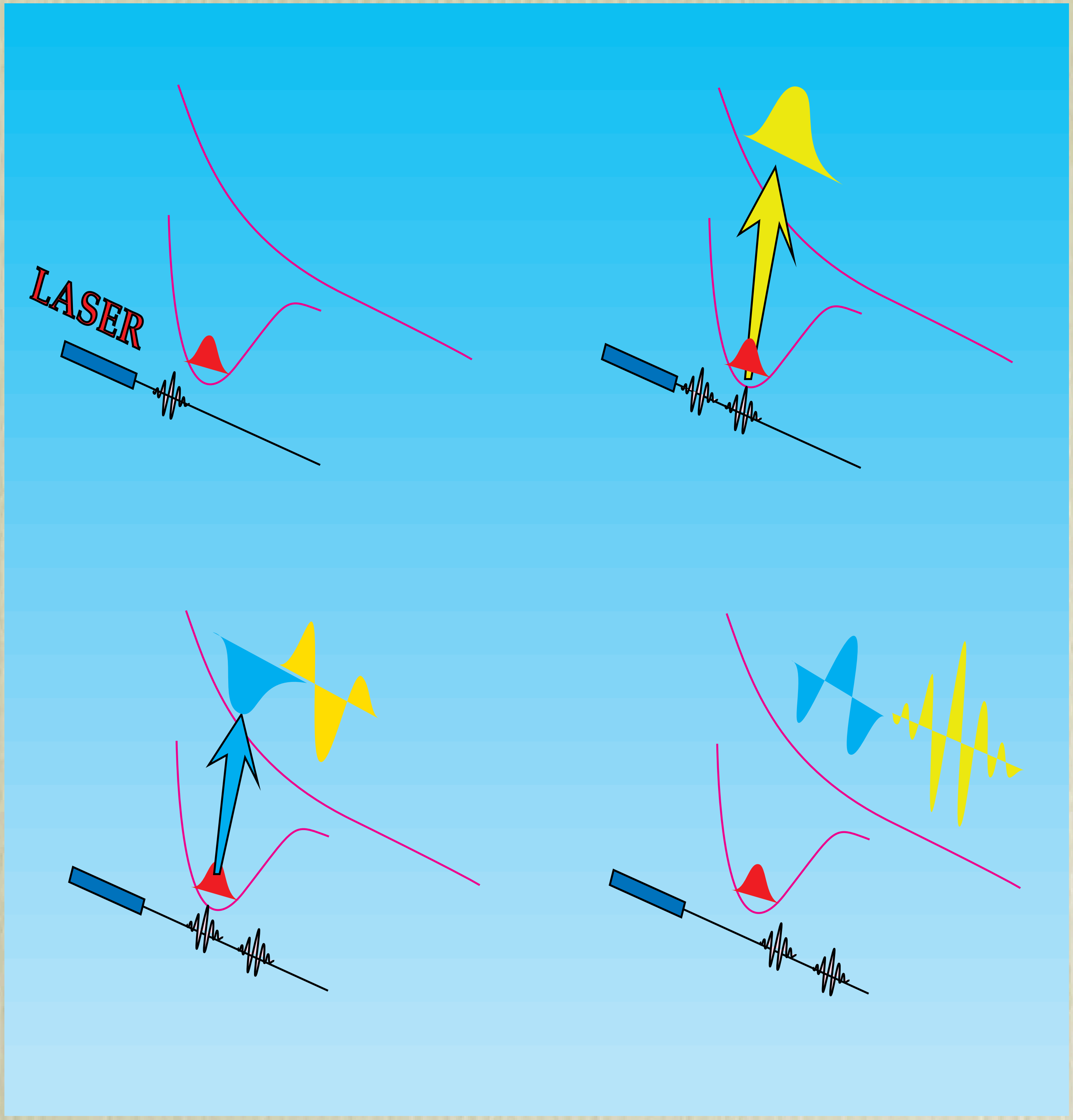
LASER

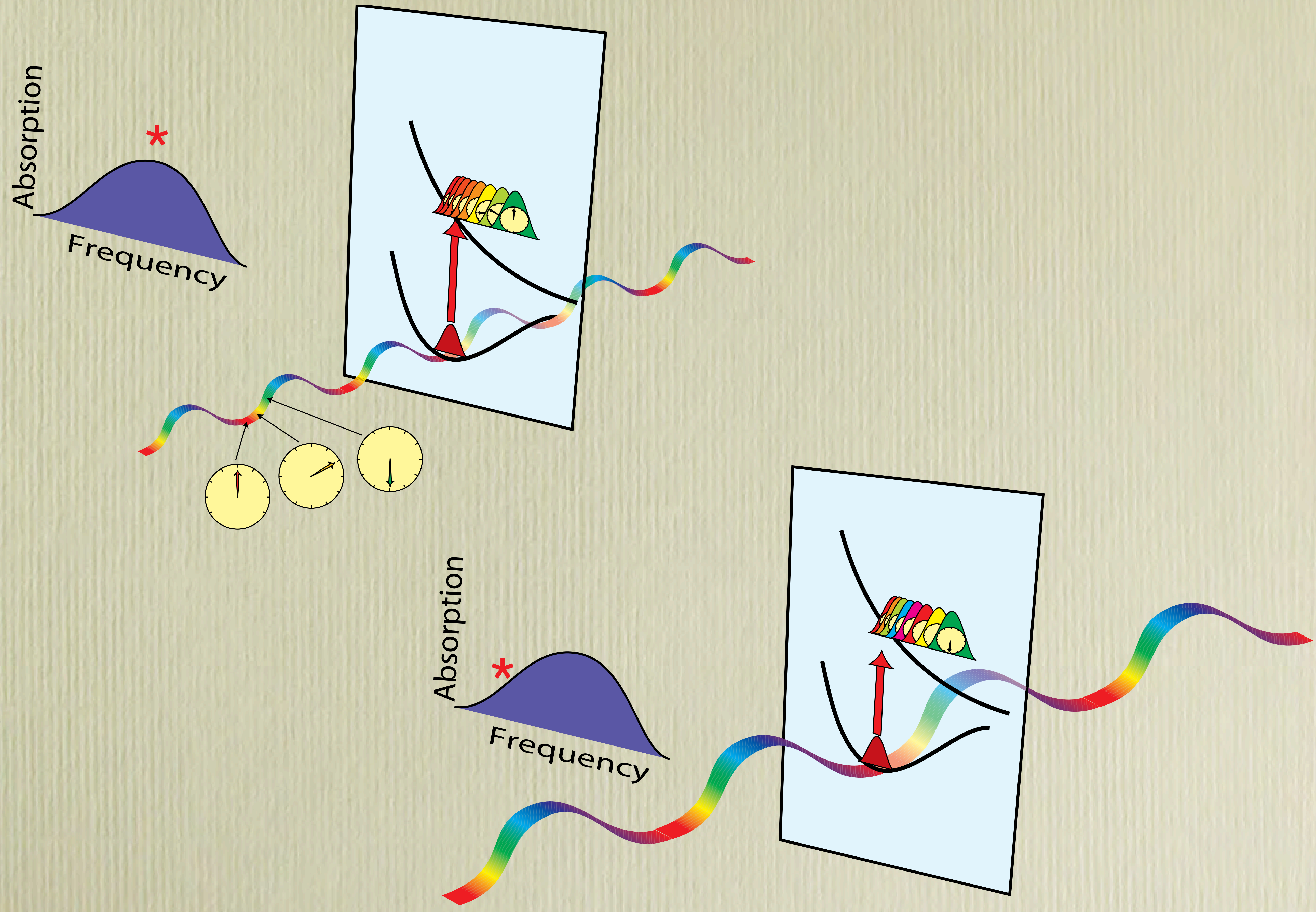
Absorption
*
Frequency
Absorption
*
Frequency

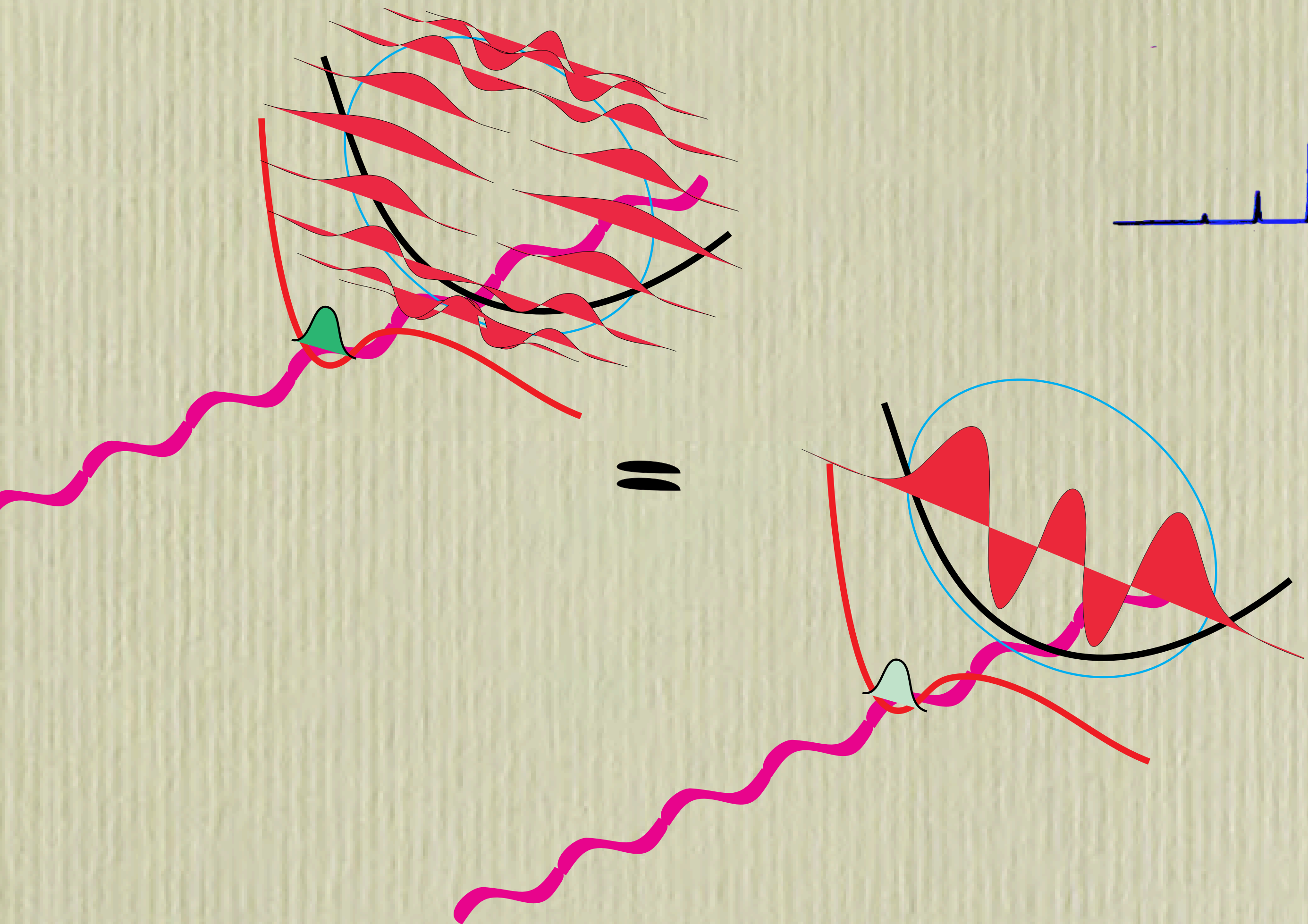

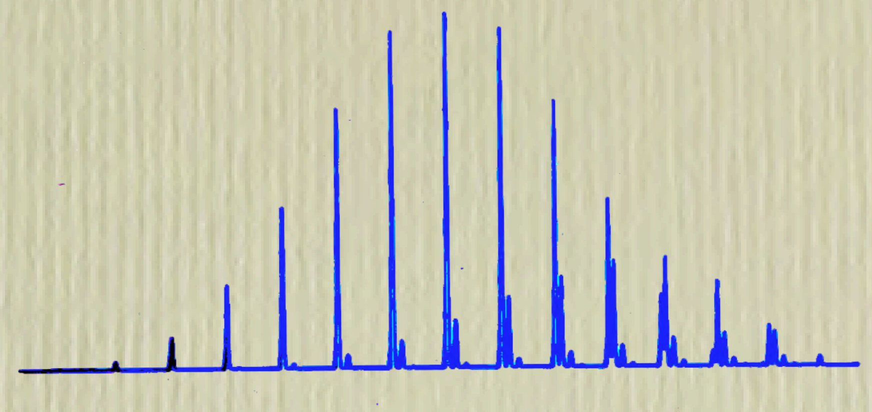

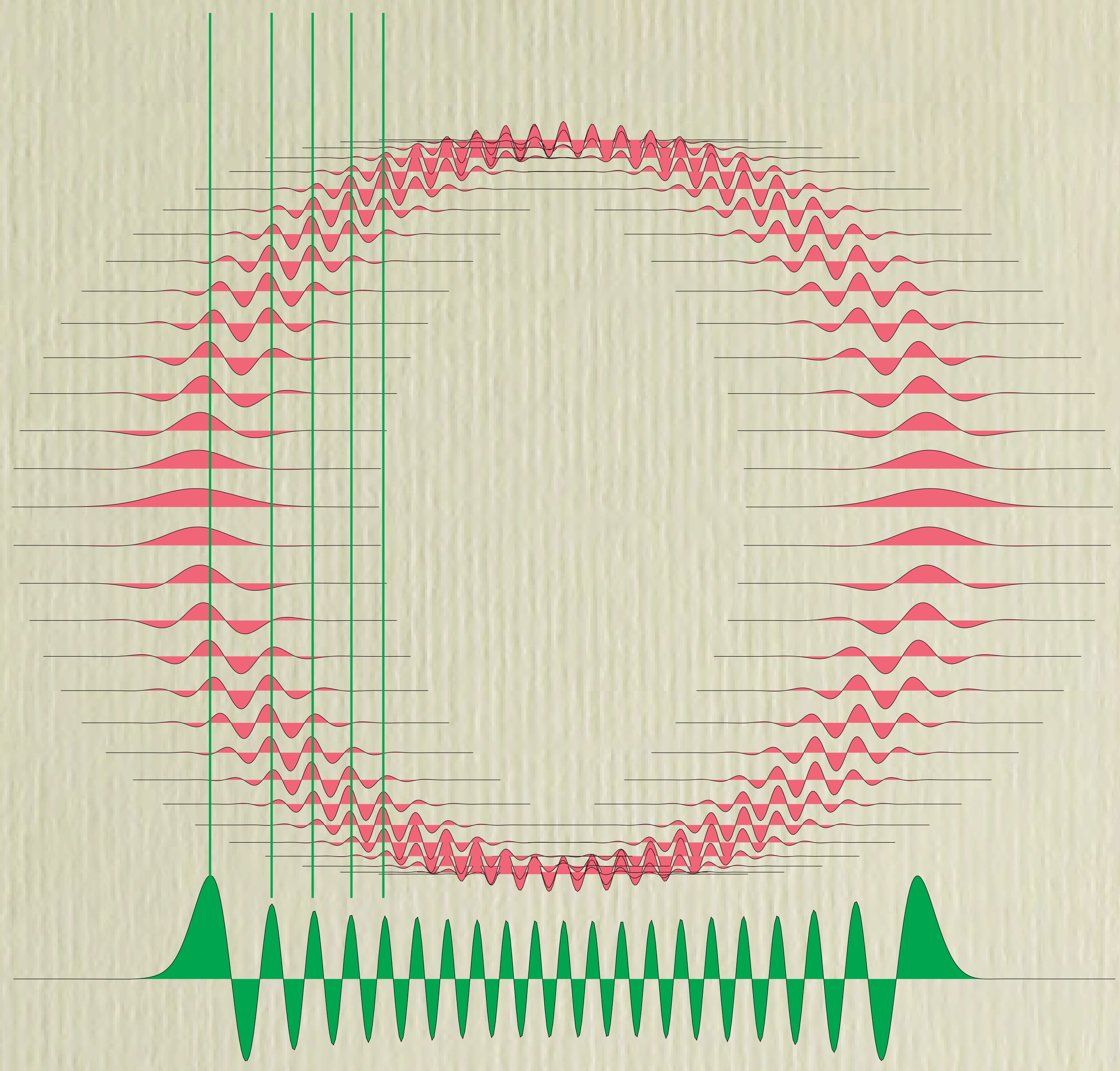

Extreme quantum control!
Using perfect phasing to build
an eigenstate.

A note on quantum control....

A c.w. laser...

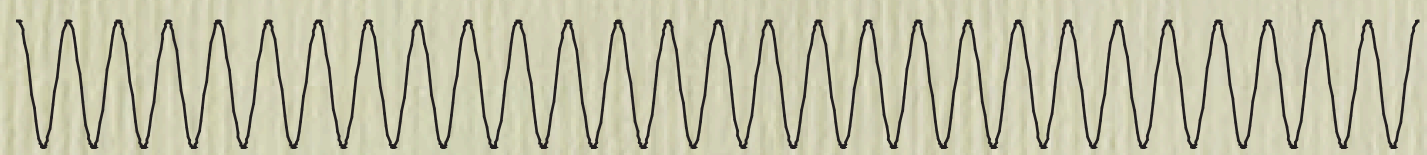

is just a pulsed femtosecond laser...

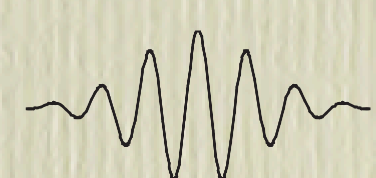

with a high repetition rate!

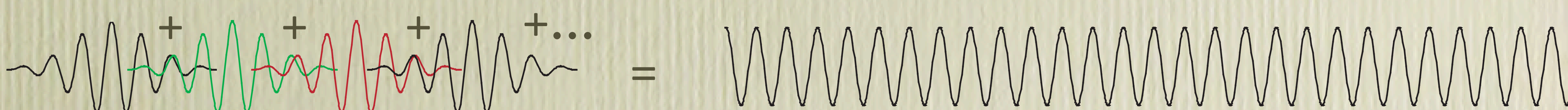

Semiclassical Methods

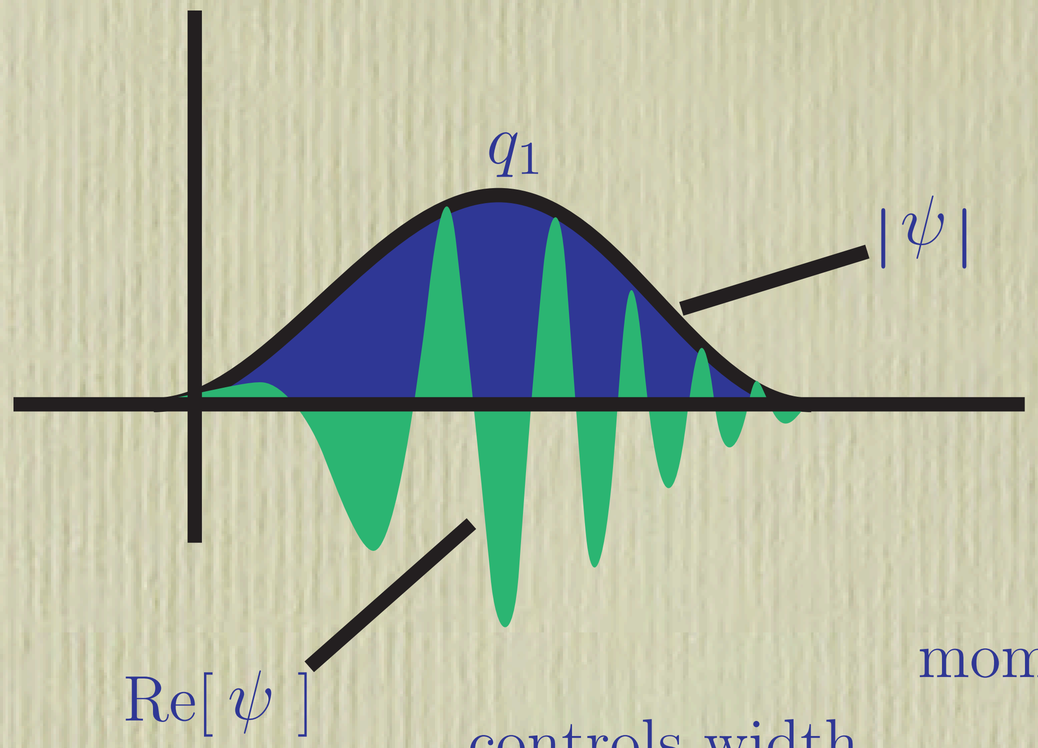

position-momentum correlation

controls width

average momentum

$$\psi_{\alpha_1}(q) \;=\; \left(\frac{2\,\mathrm{a}_1}{\pi\hbar}\right)^{1/4} \exp\left[-\frac{\mathrm{a}_1 + i\mathrm{b}_1}{\hbar}(q-q_1)^2 + \frac{i}{\hbar}p_1(q-q_1) \;+\; \frac{i}{\hbar}\,\phi_1\,\right]$$

normalization factor

average position

phase

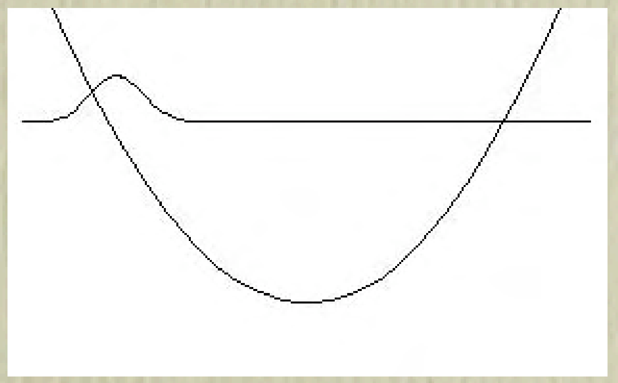

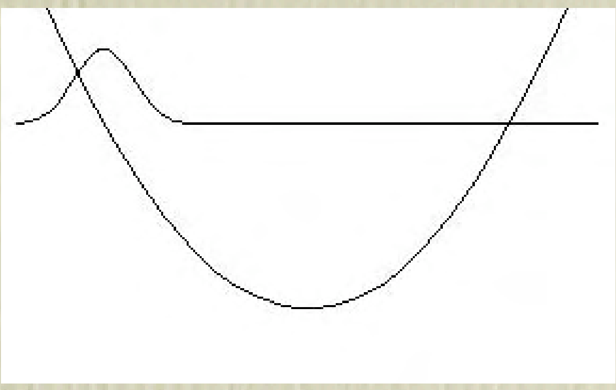

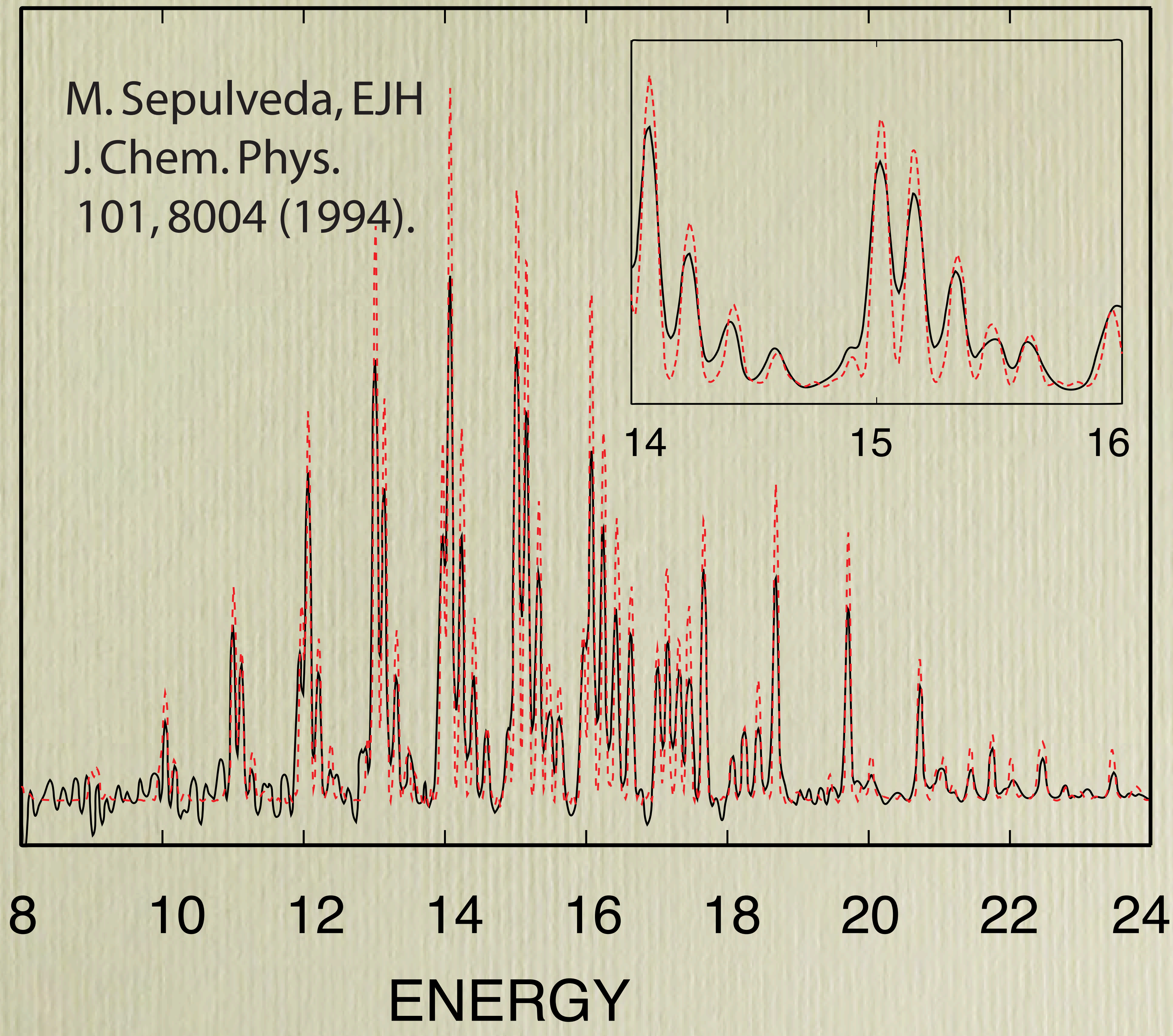
M. Sepulveda, EJH
J. Chem. Phys.
101, 8004 (1994).
14
15
16
8
10
12
14
16
18
20
22
24
ENERGY

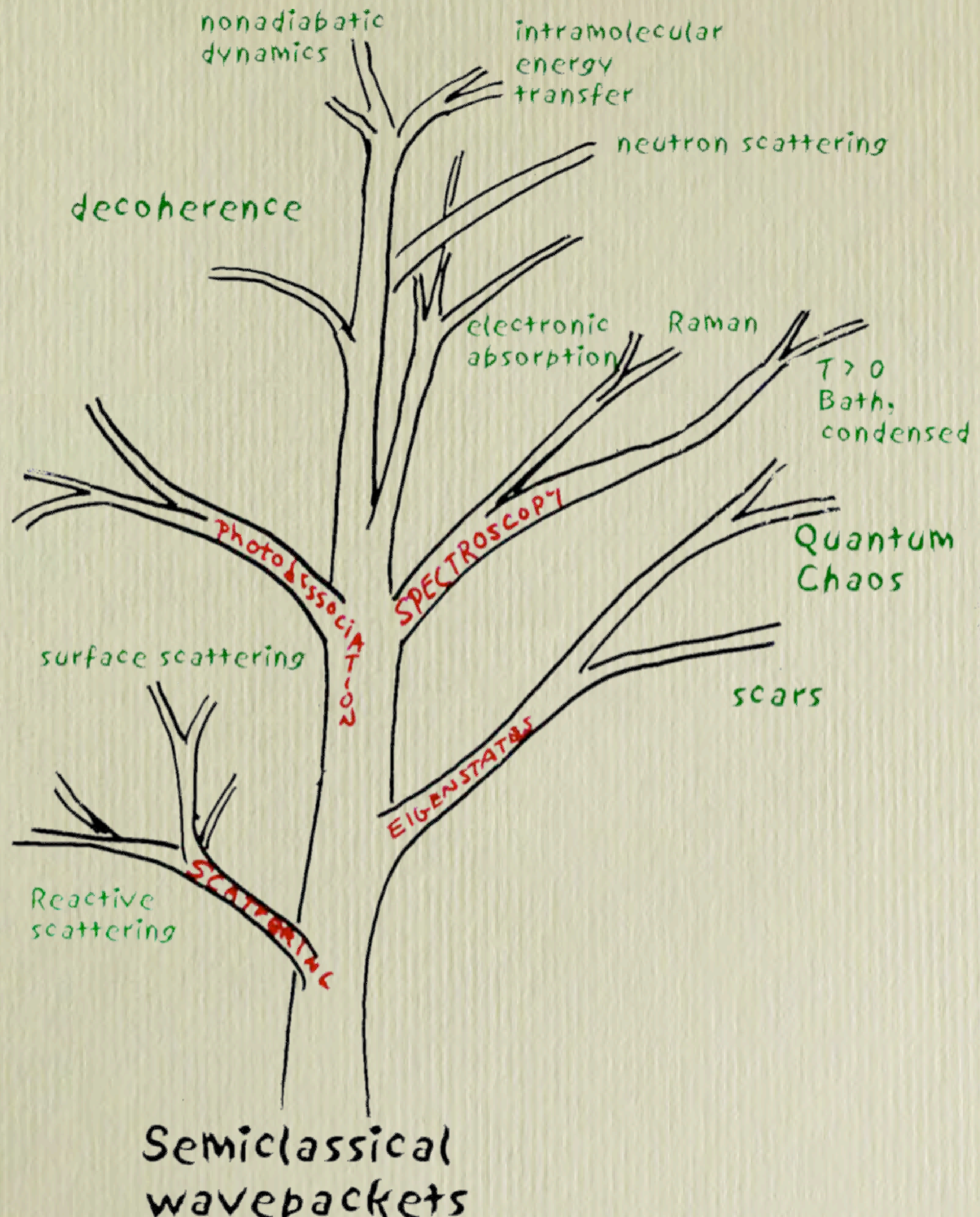

nonadiabatic dynamics
intramolecular energy transfer
neutron scattering
decoherence
electronic absorption
Raman
T > 0
Bath,
condensed
Quantum Chaos
scars
surface scattering
Reactive scattering
PHOTODISSOCIATION
SPECTROSCOPY
EIGENSTATES
SCATTERING
Semiclassical wavepackets

A note on many degrees of freedom, decoherence

MIssing Mode Effect (MIME)

- A partially resolved spectrum gives a very evenly spaced set of peaks, but the spacing is not near any normal mode frequency of the molecule

Separable Morse oscillators - local mode Hamiltonian with normal mode "pluck"

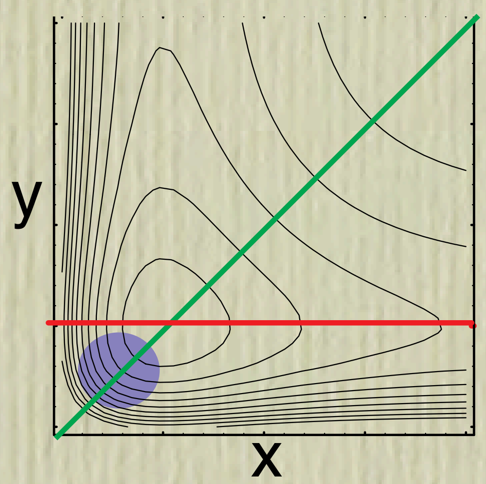

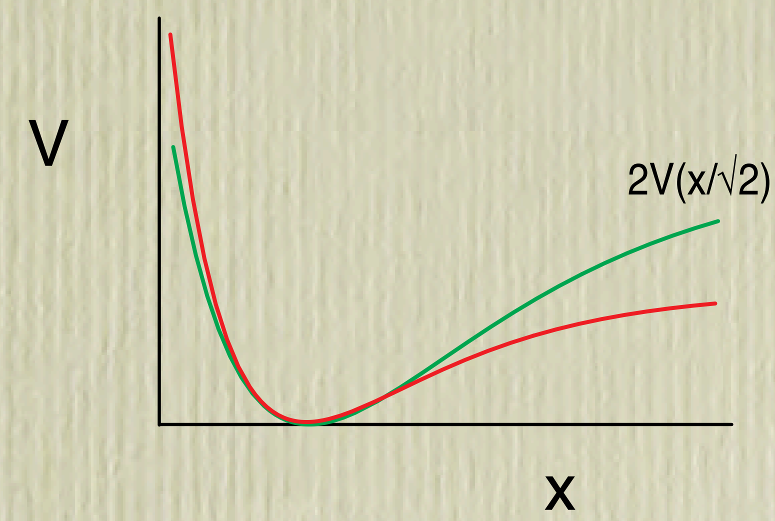

V(x,y) = V(x) + V(y)

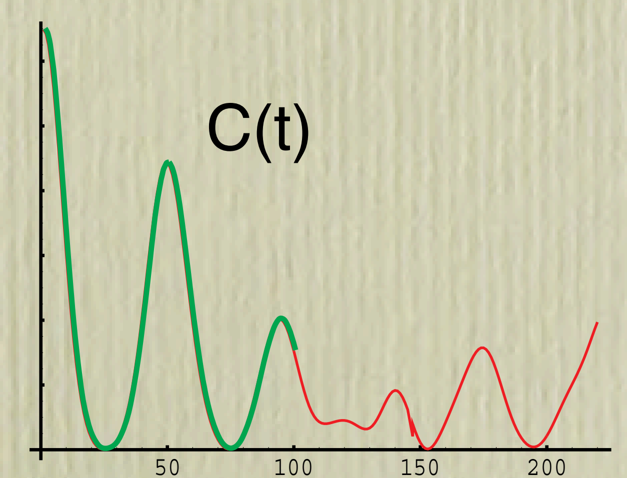

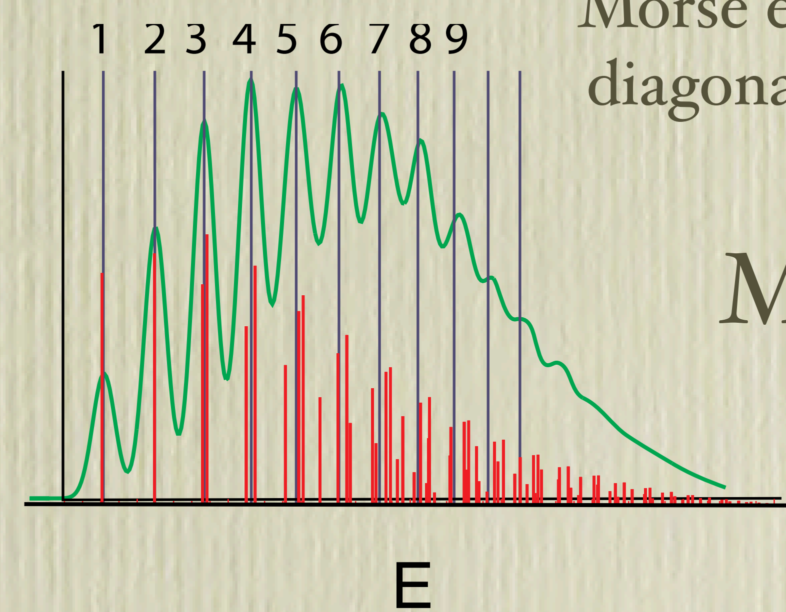

Morse energies for diagonal potential

MIME effect!

$\omega_x = 2.07, \ \omega_y = 3.0$

Initial decay

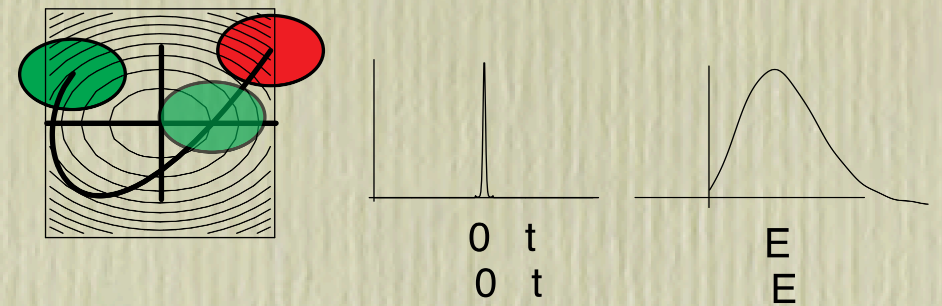

Recurrence-
compromise
time!

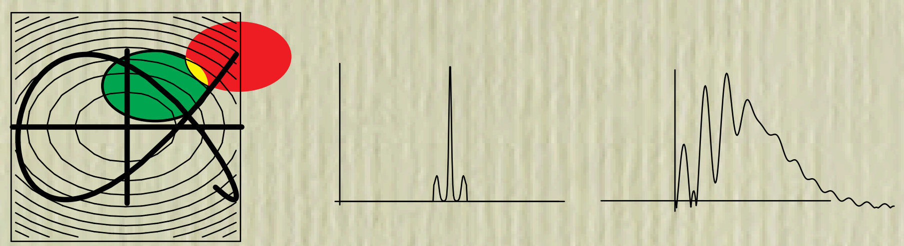

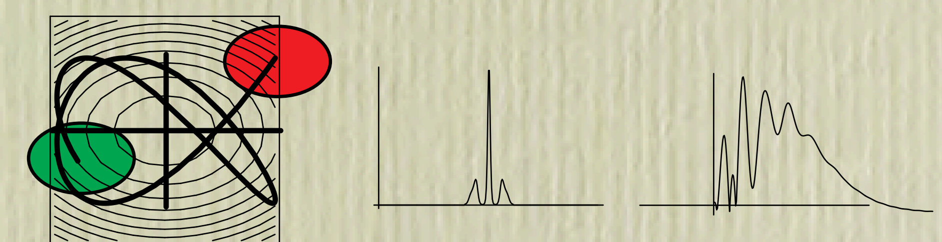

Strong
Recurrence

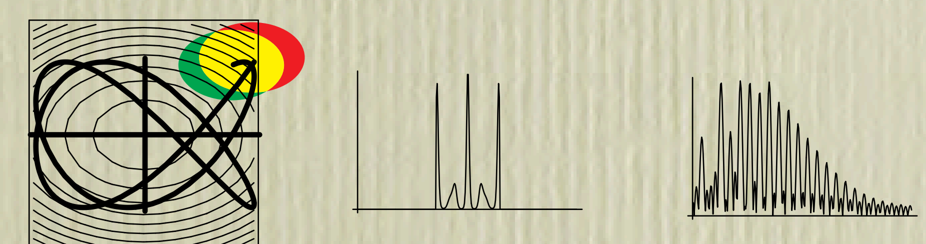

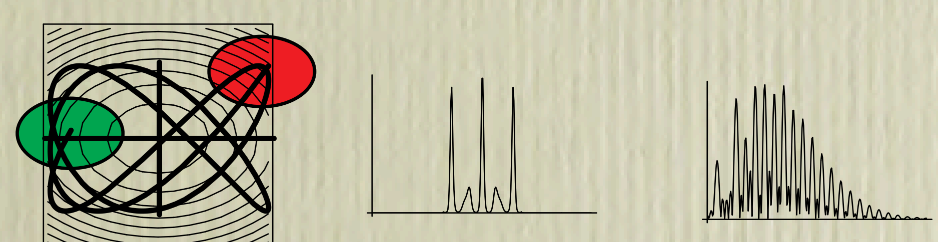

$W\text{-}(CO)_5(py)$ @ 10 K

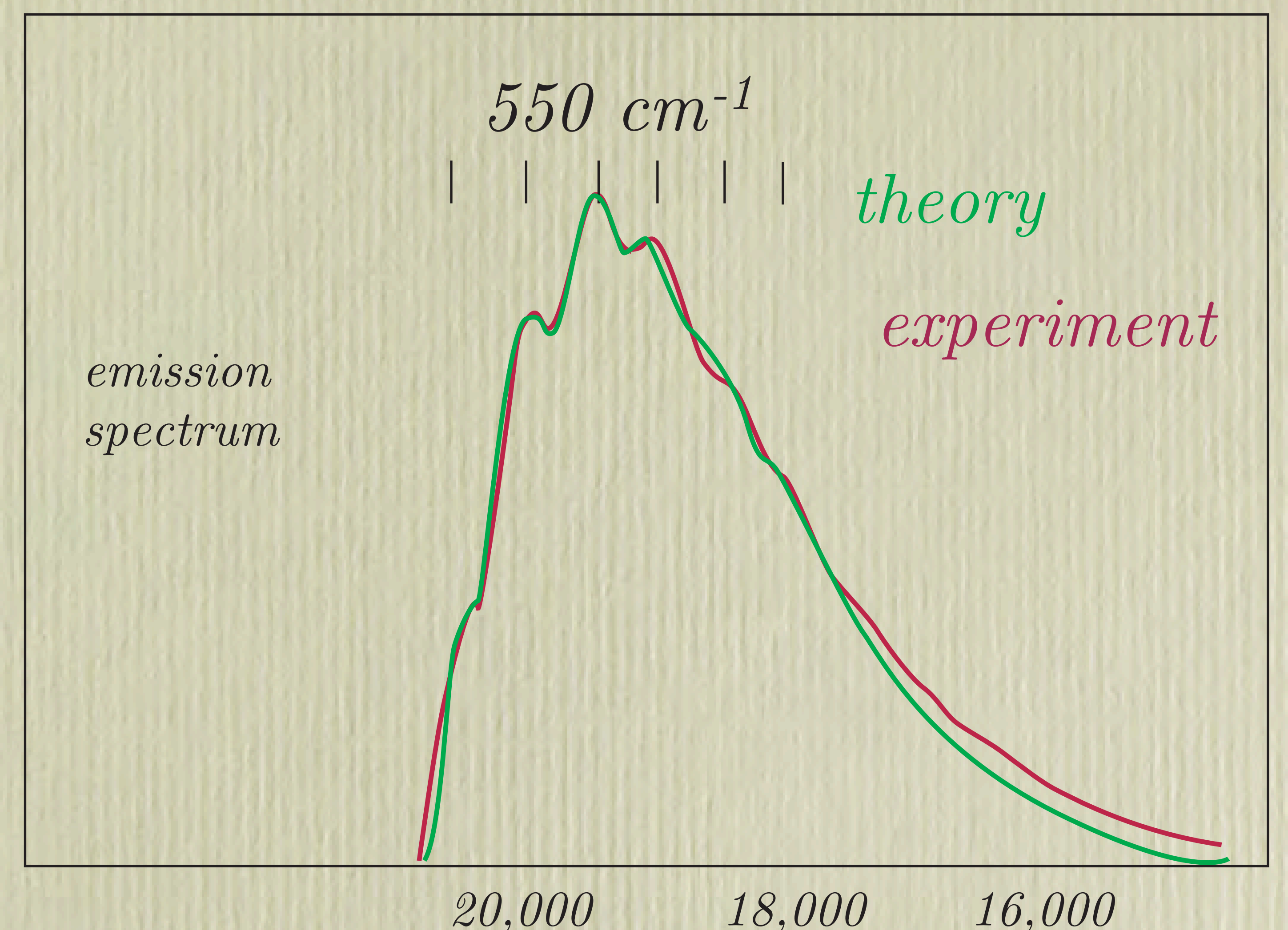

$$\omega_{MIME} = \frac{\sum_n \omega_n^2 \Delta_n^2}{\sum_n \omega_n \Delta_n^2}$$

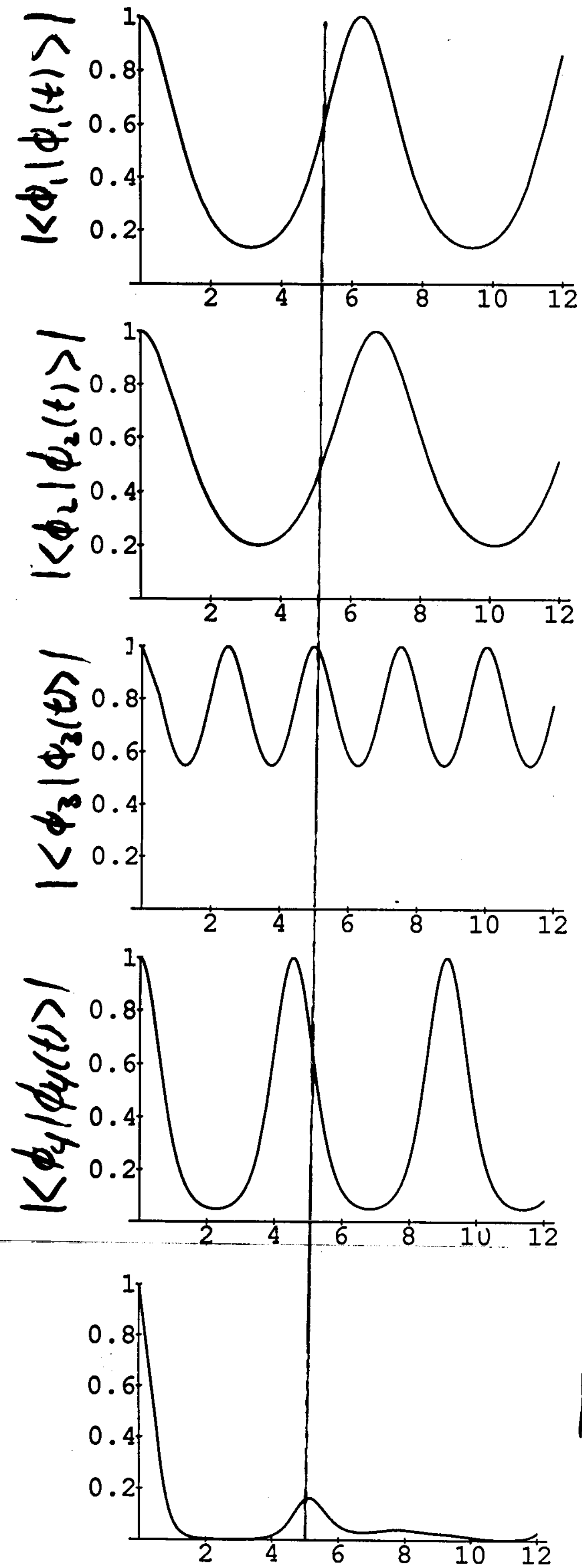

$$\omega_{MIME} = \frac{\sum_i \Delta_i^2 \omega_i^2}{\sum_i \Delta_i^2 \omega_i} = 5.11$$

$$|\langle \phi | \phi(t) \rangle| = \left| \prod_i^4 \langle \phi_i | \phi_i(t) \rangle \right|$$

MIME - W(CO)$_5$Py

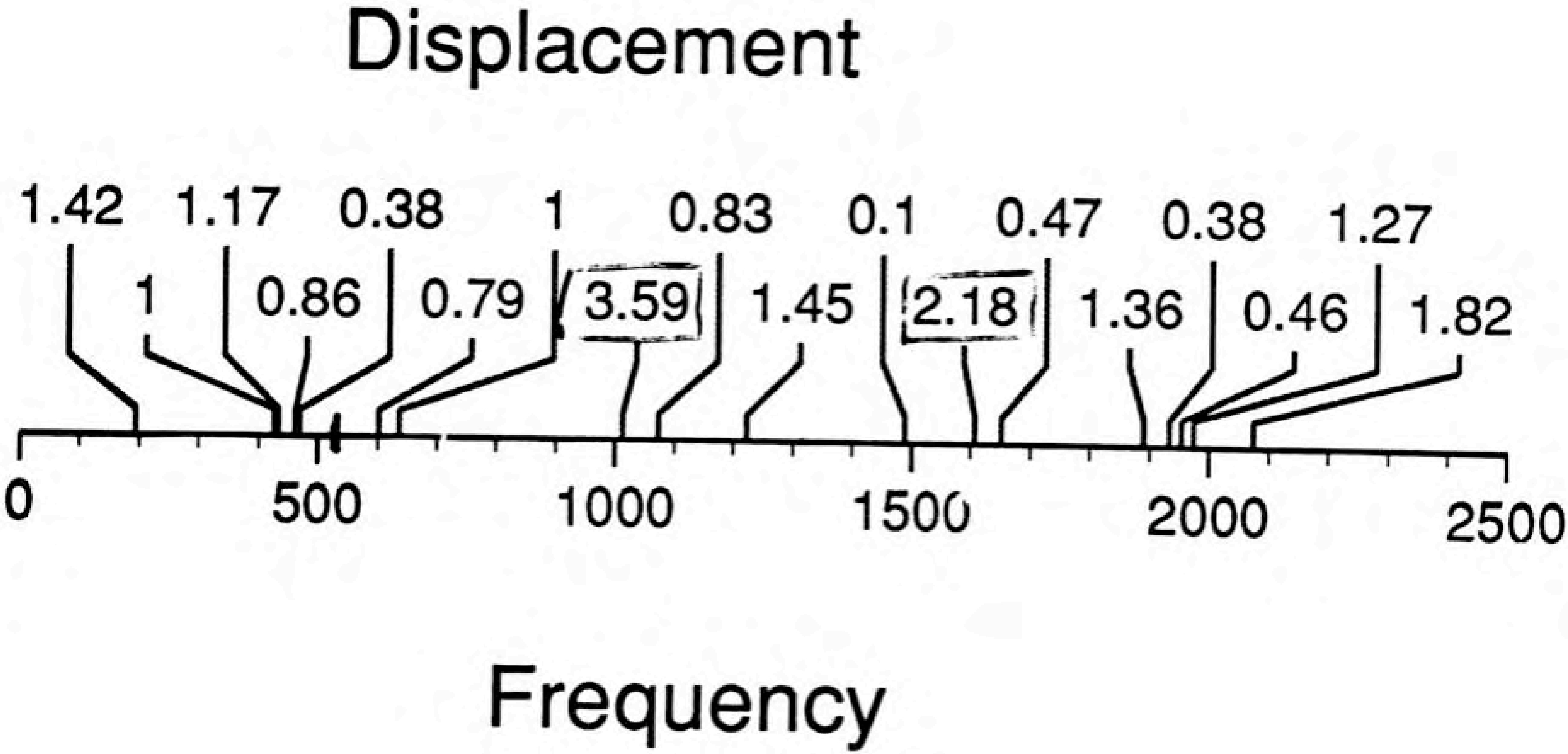

Displacement
1.42
1.17
0.38
1
0.83
0.1
0.47
0.38
1.27
1
0.86
0.79
3.59
1.45
2.18
1.36
0.46
1.82
0
500
1000
1500
2000
2500
Frequency

frequency (cm^{-1})	$\frac{I_k}{I_{636}}$ [a]	$\frac{\Delta_k}{\Delta_{636}}$ [b]	Emission Best fit [c] Δ_k
2075	1.82(0.51)	.28(.04)	0.28
1973	1.27(0.36)	.24(.03)	0.24
1953	0.46(0.13)	.15(.02)	0.15
1934	0.38(0.11)	.14(.02)	0.14
1890	1.36(0.38)	.27(.04)	0.27
1651	0.47(0.13)	.18(.03)	0.18
1607	2.18(0.61)	.39(.05)	0.39
1489	0.10(0.03)	.10(.01)	0.10
1223	1.45(0.41)	.43(.06)	0.43
1073	0.83(0.23)	.37(.05)	0.37
1012	3.59(1.01)	.81(.11)	0.81
636	1.00(0.28)	.68(.10)	0.68
602	0.79(0.22)	.64(.09)	0.64
470	0.38(0.11)	.56(.08)	0.56
462	0.86(0.24)	.87(.12)	0.87
434	1.17(0.32)	.08(.15)	1.08
427	1.00(0.28)	.01(.14)	1.01
195	0.41(0.12)	.42(.20)	1.42

a) Calculated by integrating the Raman peaks obtained at 476.5 nm excitation.

b) Relative displacement determined from the Raman intensities and scaled by 0.68 to make them comparable to the absolute displacements shown in the right hand column and used in eq. 6.

c) The values used in eq. 6 were $\Gamma = 72\ cm^{-1}$, $E = 20500\ cm^{-1}$ and the Δ_k's and ω's shown in this table.

Case study: benzophenone

$$V(x,y) = \frac{1}{2}\omega_x^2 x^2 + \frac{1}{2}\omega_y^2 y^2 + \lambda x^2 y$$

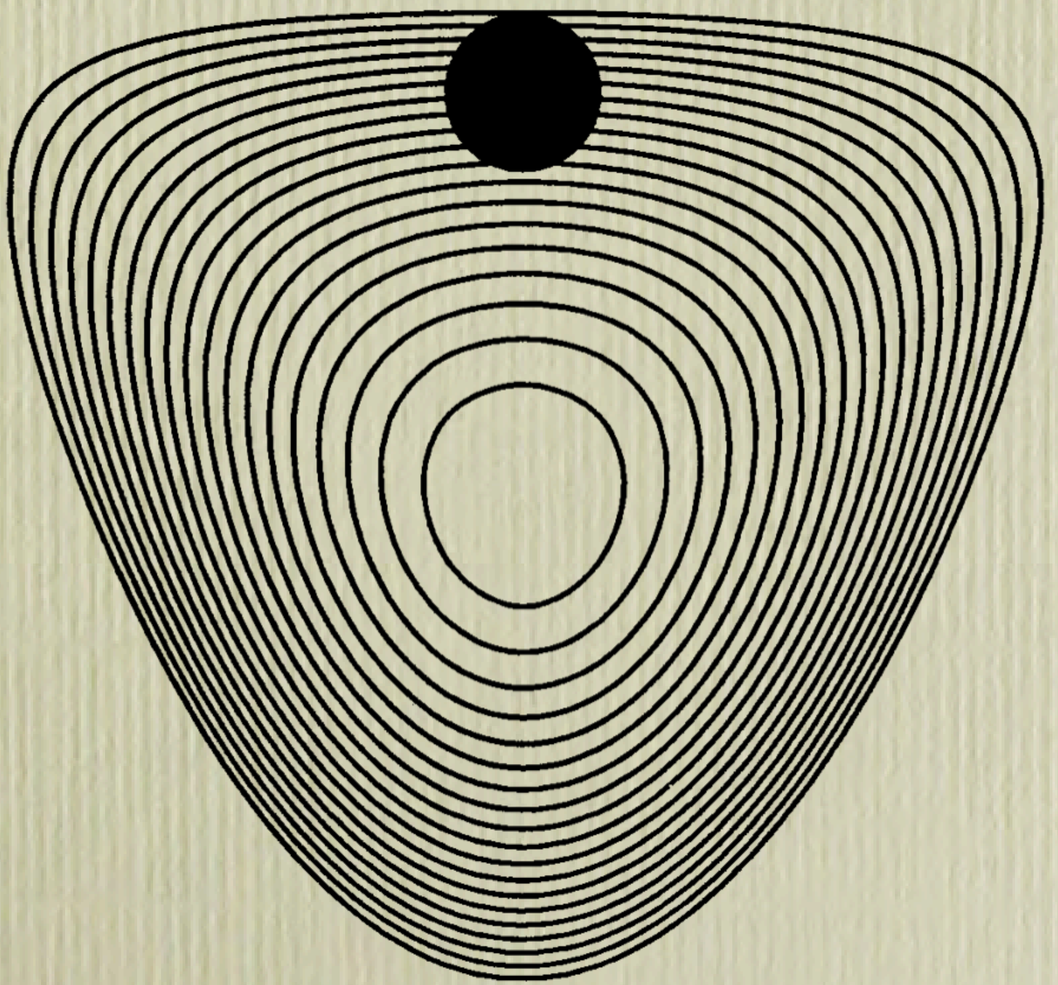

$$\omega_x = 1$$

$$\omega_y = 1.1$$

$$\lambda = 0.11$$

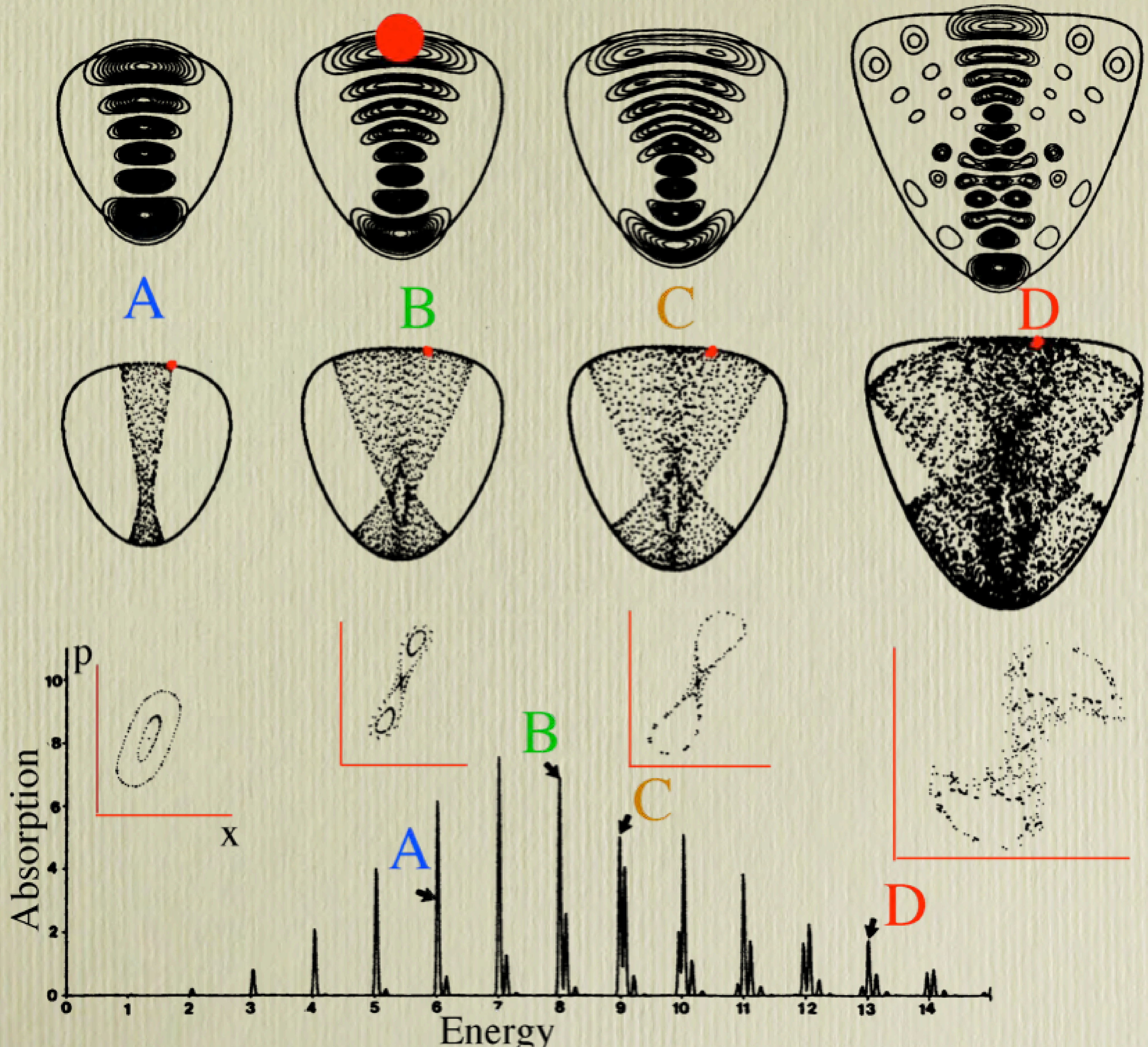

A
B
C
D
p
x
Absorption
Energy
0
1
2
3
4
5
6
7
8
9
10
11
12
13
14
0
2
4
6
8
10
A
B
C
D

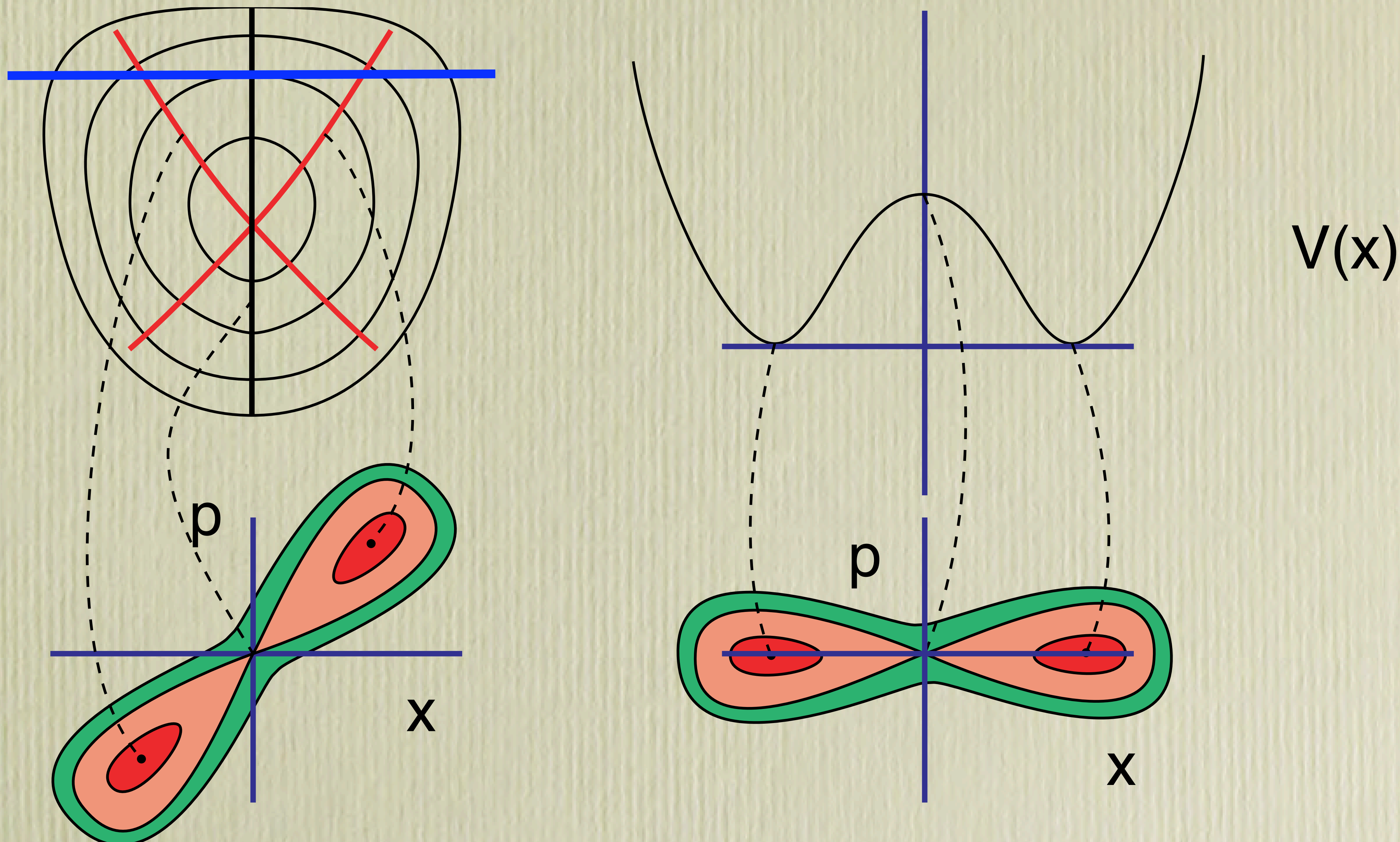
p
x
p
x
V(x)

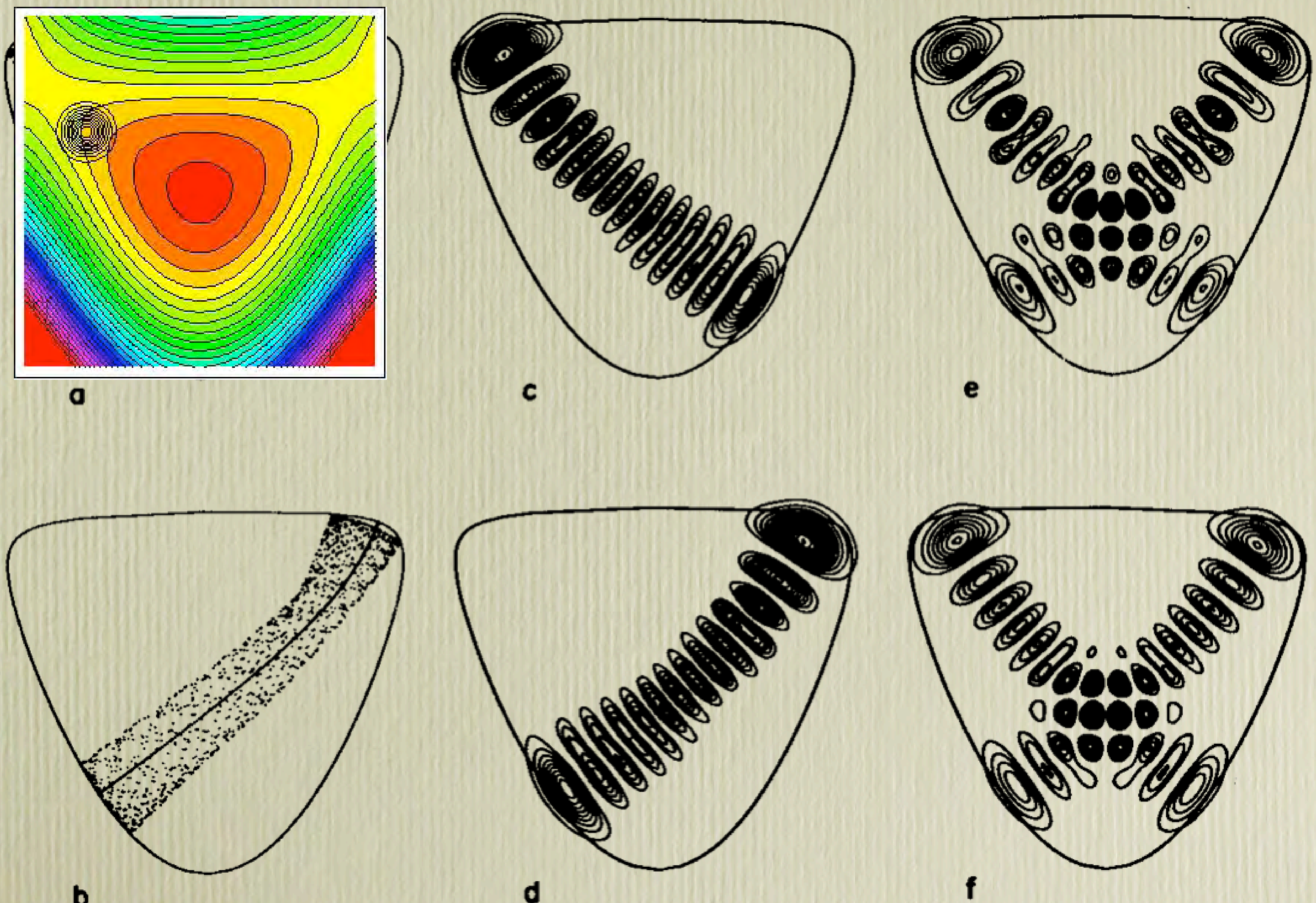
a
b
c
d
e
f

$$V(x,y) = \frac{1}{2}\omega_x^2 x^2 + \frac{1}{2}\omega_y^2 y^2 + \lambda x^2 y$$

$$V^{eff}(x,t) = \frac{1}{2}(\omega_x^2 + \lambda y_0 \cos(\omega_y t))x^2 + \frac{1}{2}\omega_{y_0}^2 \cos^2(\omega_y t)$$

Mathieu stability

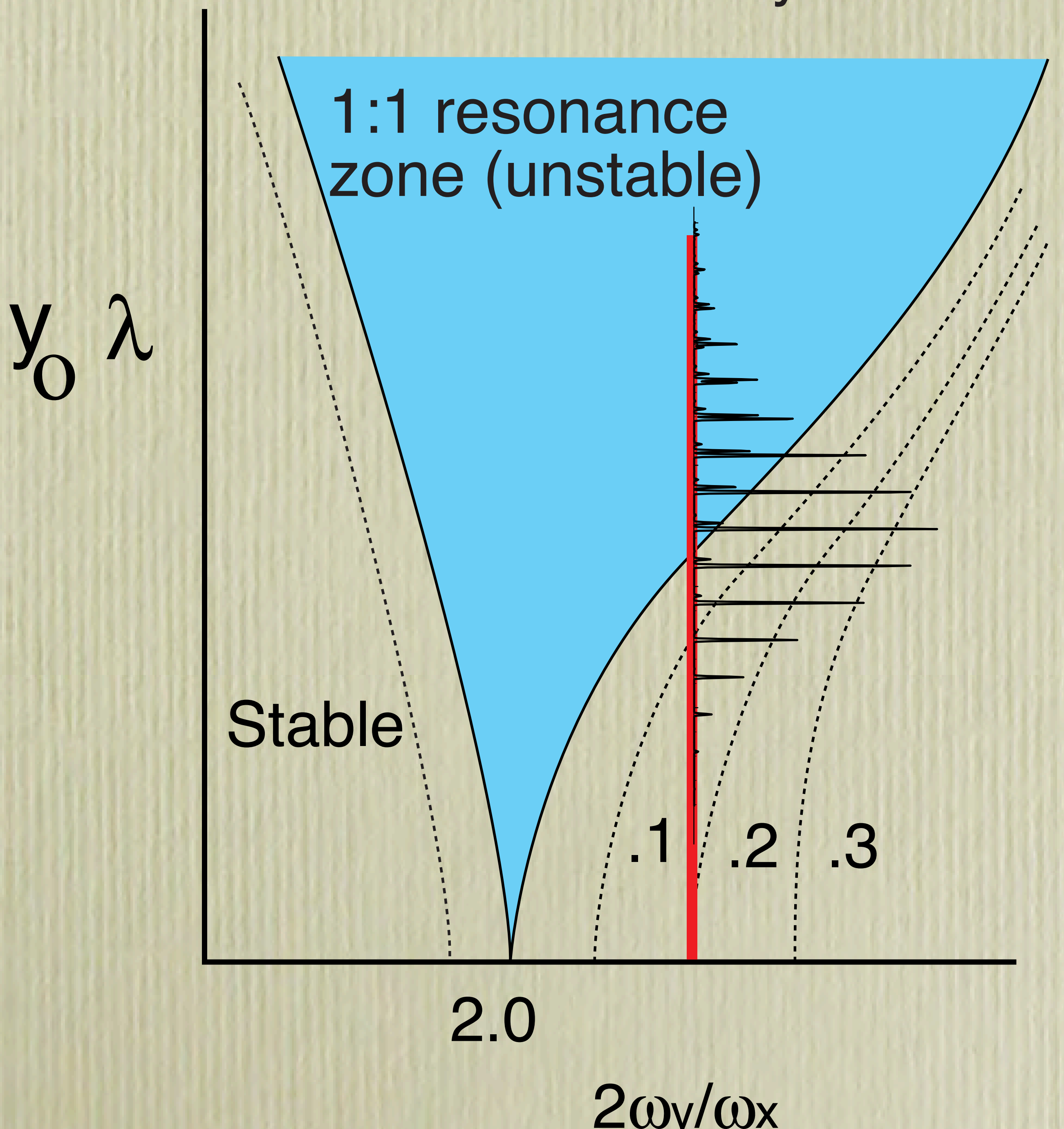

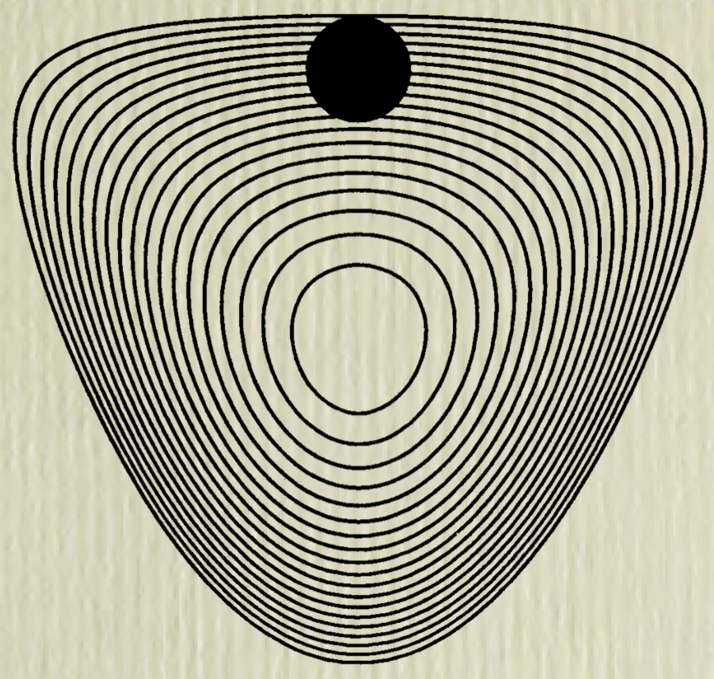

Pre-Resonant Level Attraction

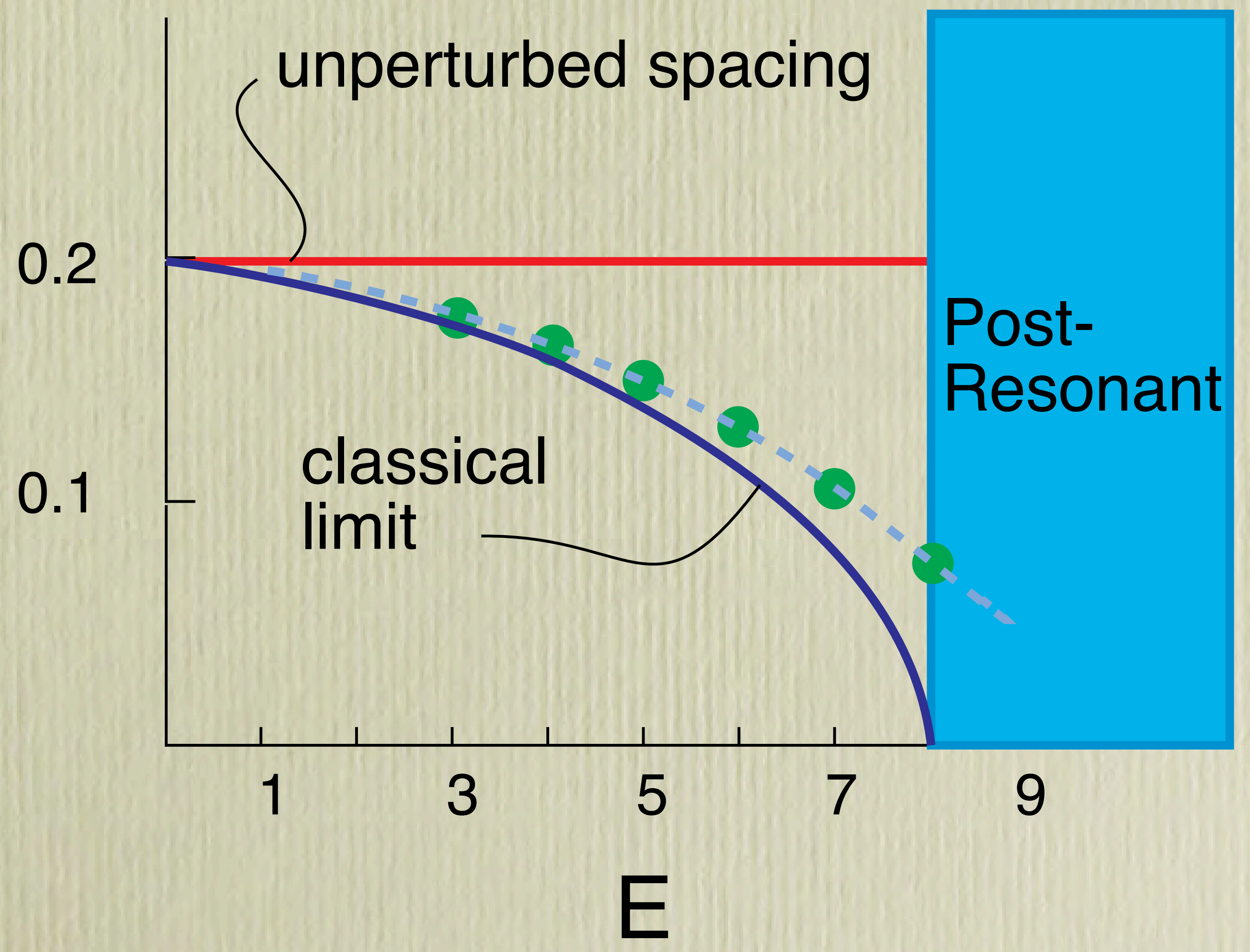

Prominent, and restricted, vibrational state mixing in the fluorescence excitation spectrum of benzophenone

Karl W. Holtzclaw and David W. Pratt[a)]
Department of Chemistry, University of Pittsburgh, Pittsburgh, Pennsylvania 15260

(Received 4 February 1986; accepted 14 February 1986)

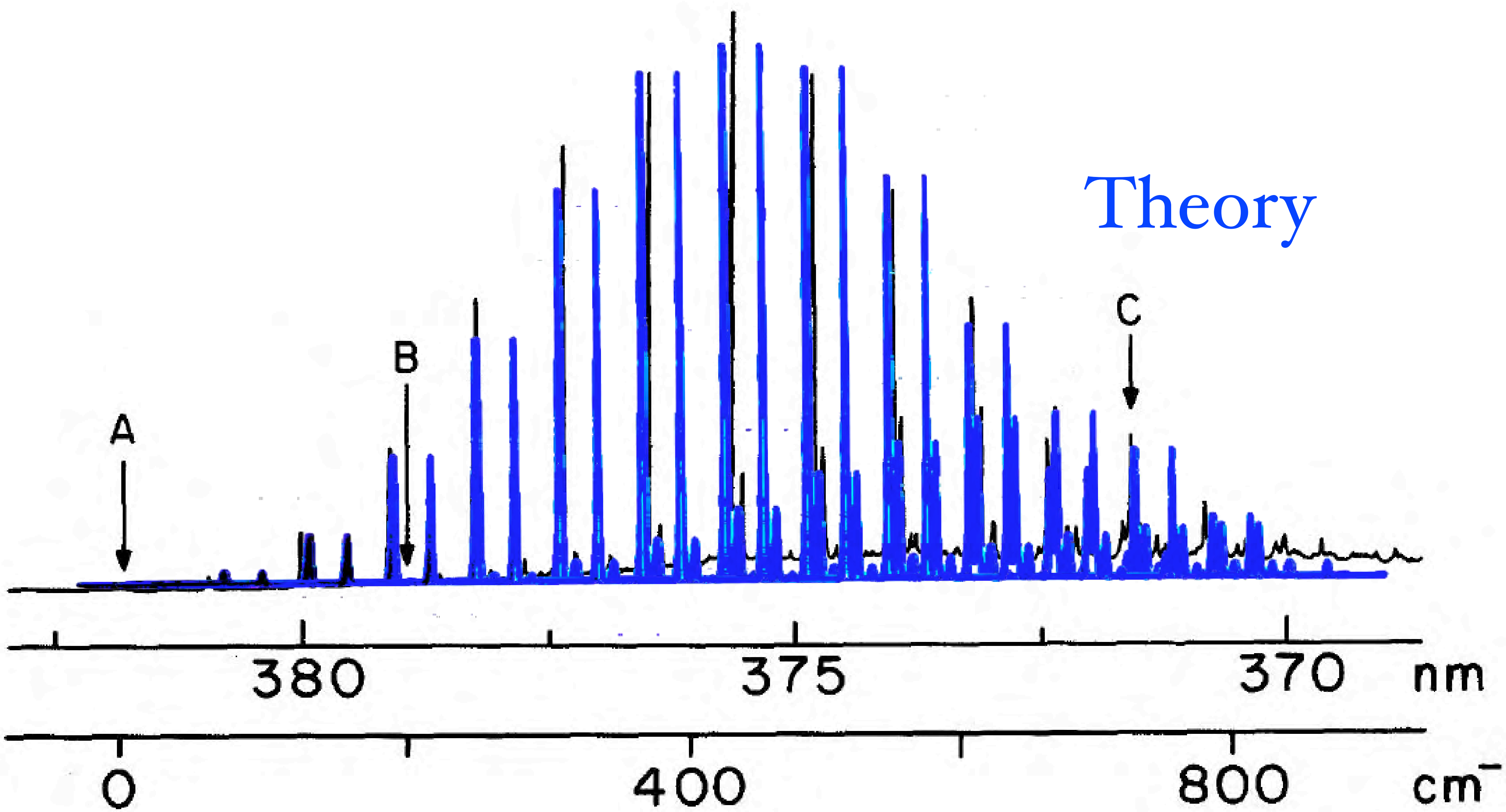

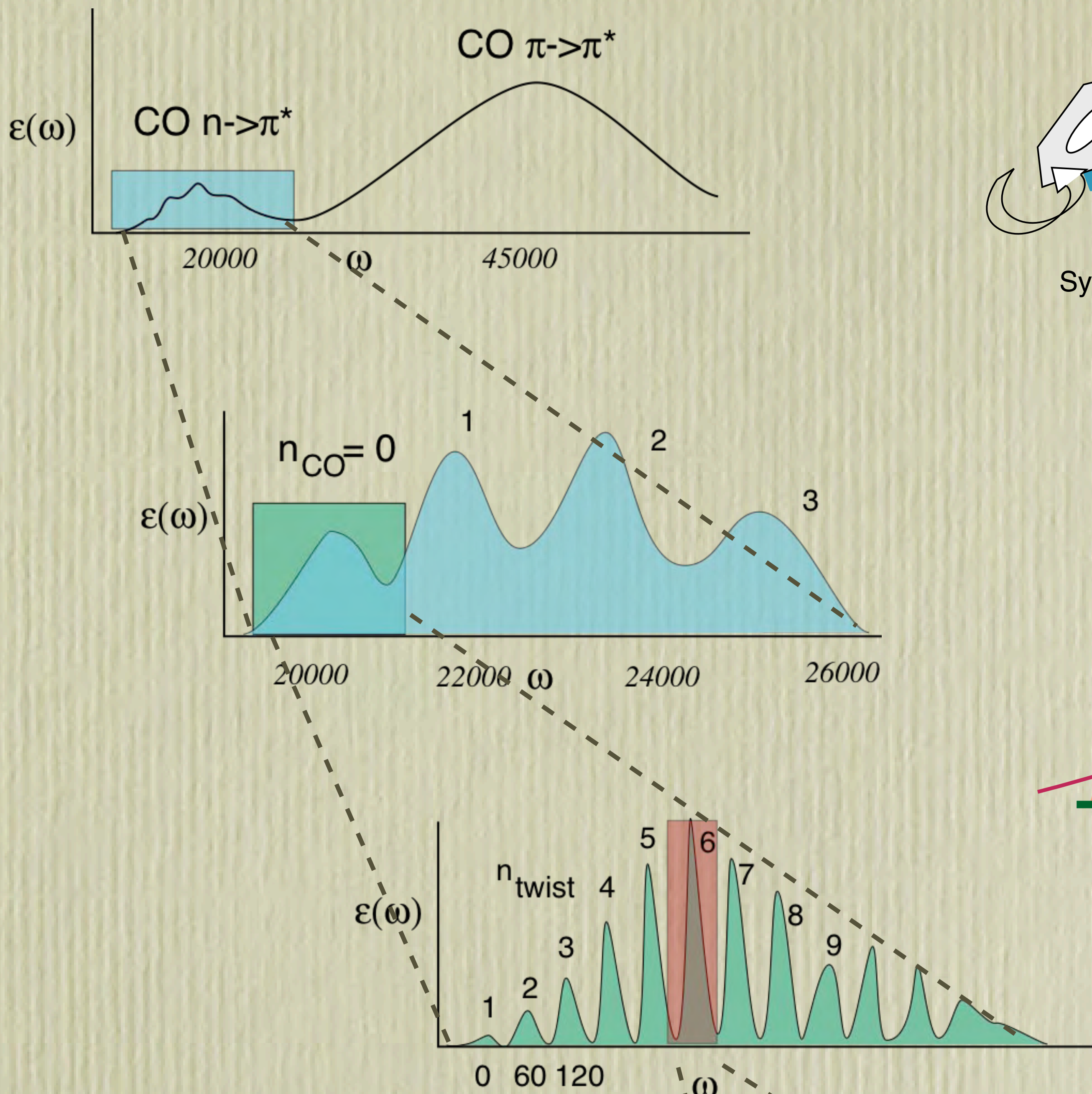

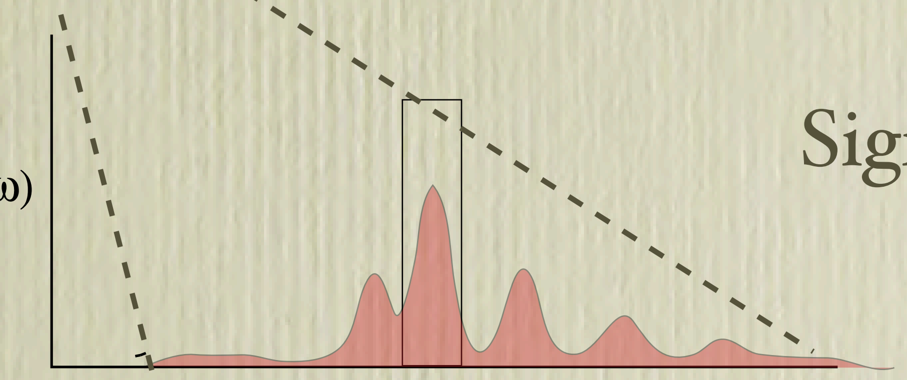

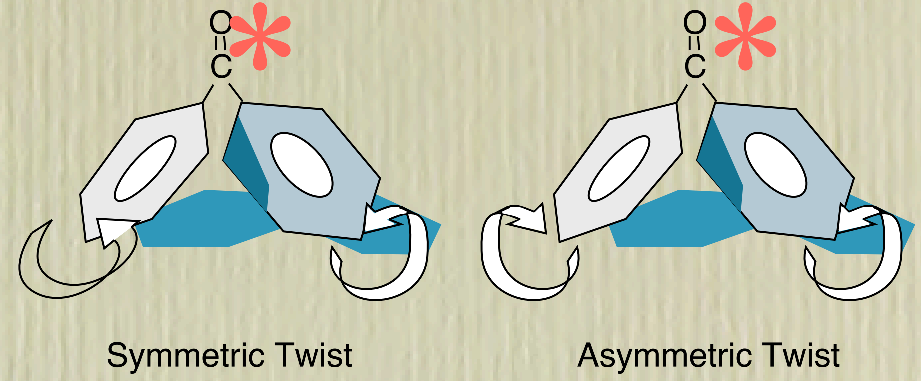

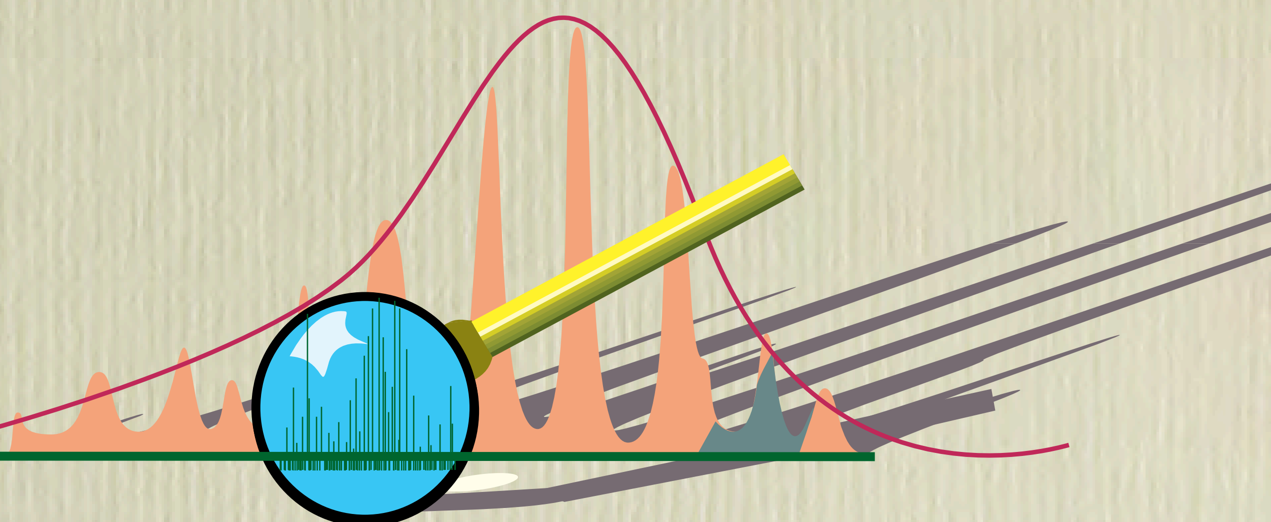

Spectral Hierarchy

Signature of twist-twist coupling

Benzophenone Twist Modes

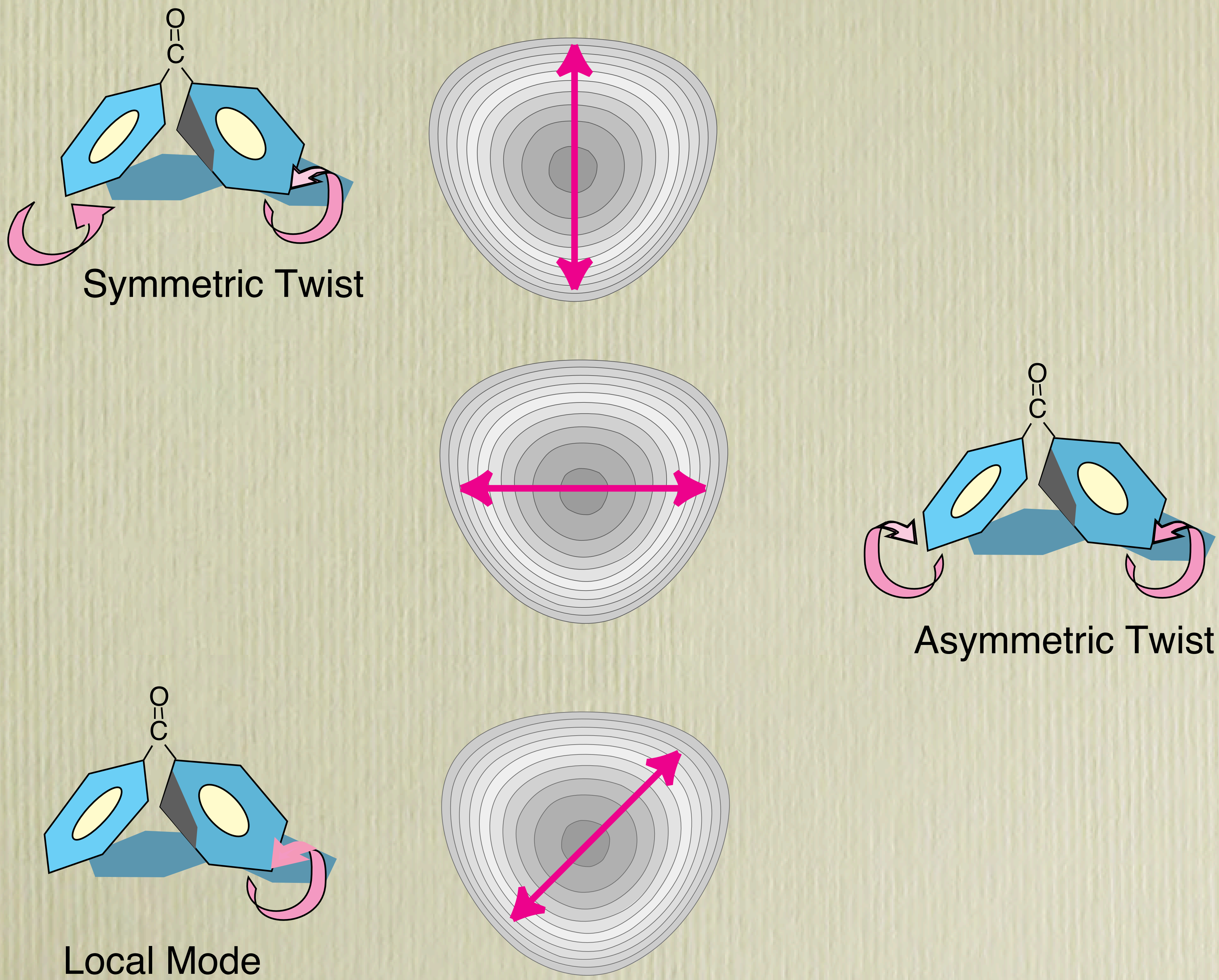

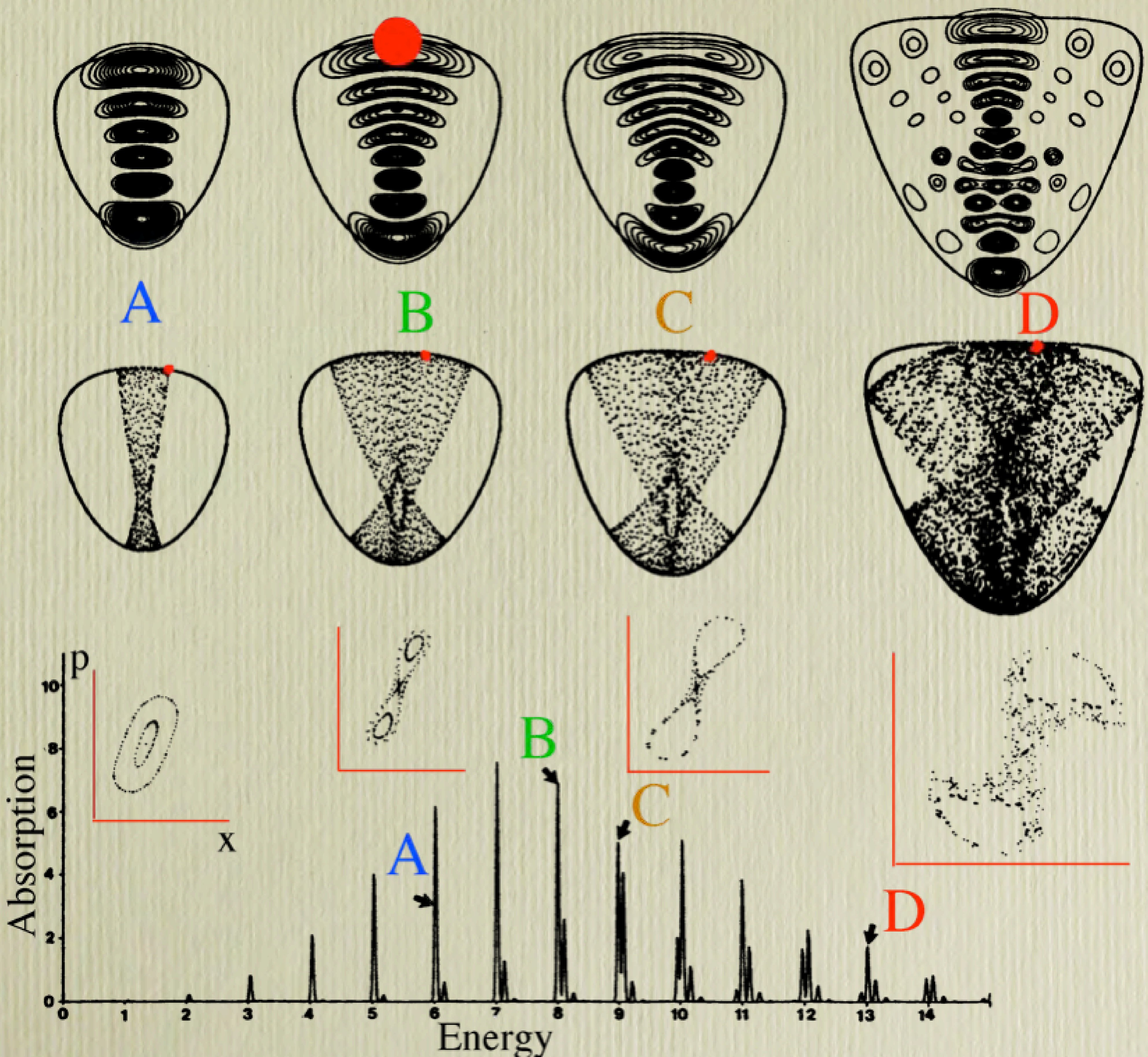

A
B
C
D
p
x
Absorption
Energy
0
2
4
6
8
10
0
1
2
3
4
5
6
7
8
9
10
11
12
13
14

Reduced dimensionality

High energy needed to excite some high frequency degrees of freedom can lock them out

Examples: Benzophenone

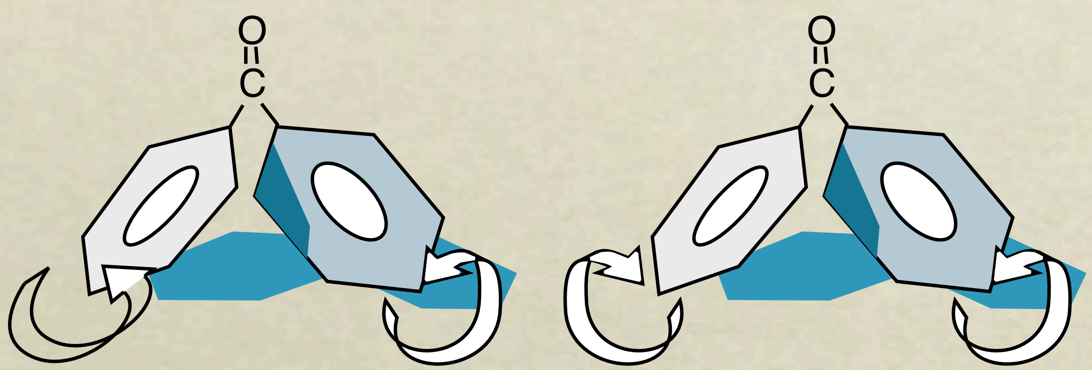

Symmetric Twist   Asymmetric Twist

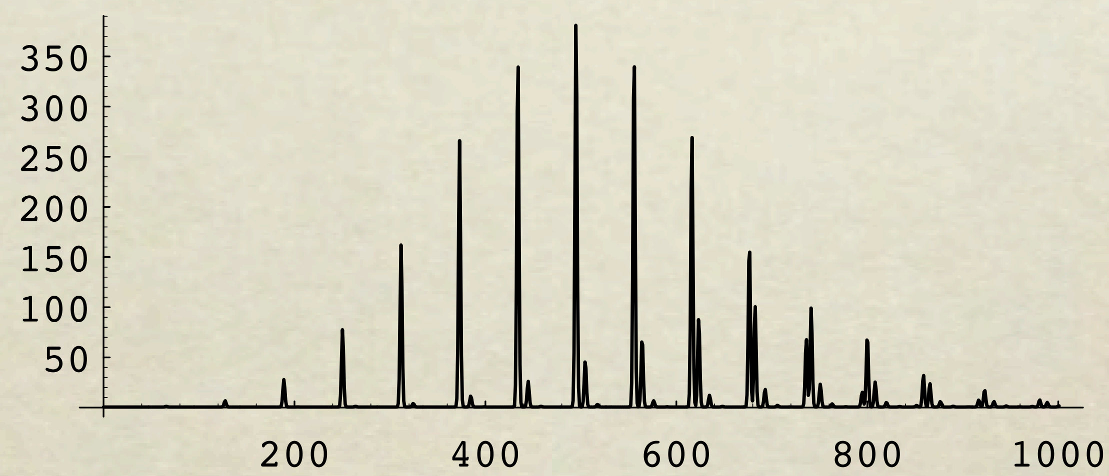

String theory:Living in 4 dimensions instead of 11!!

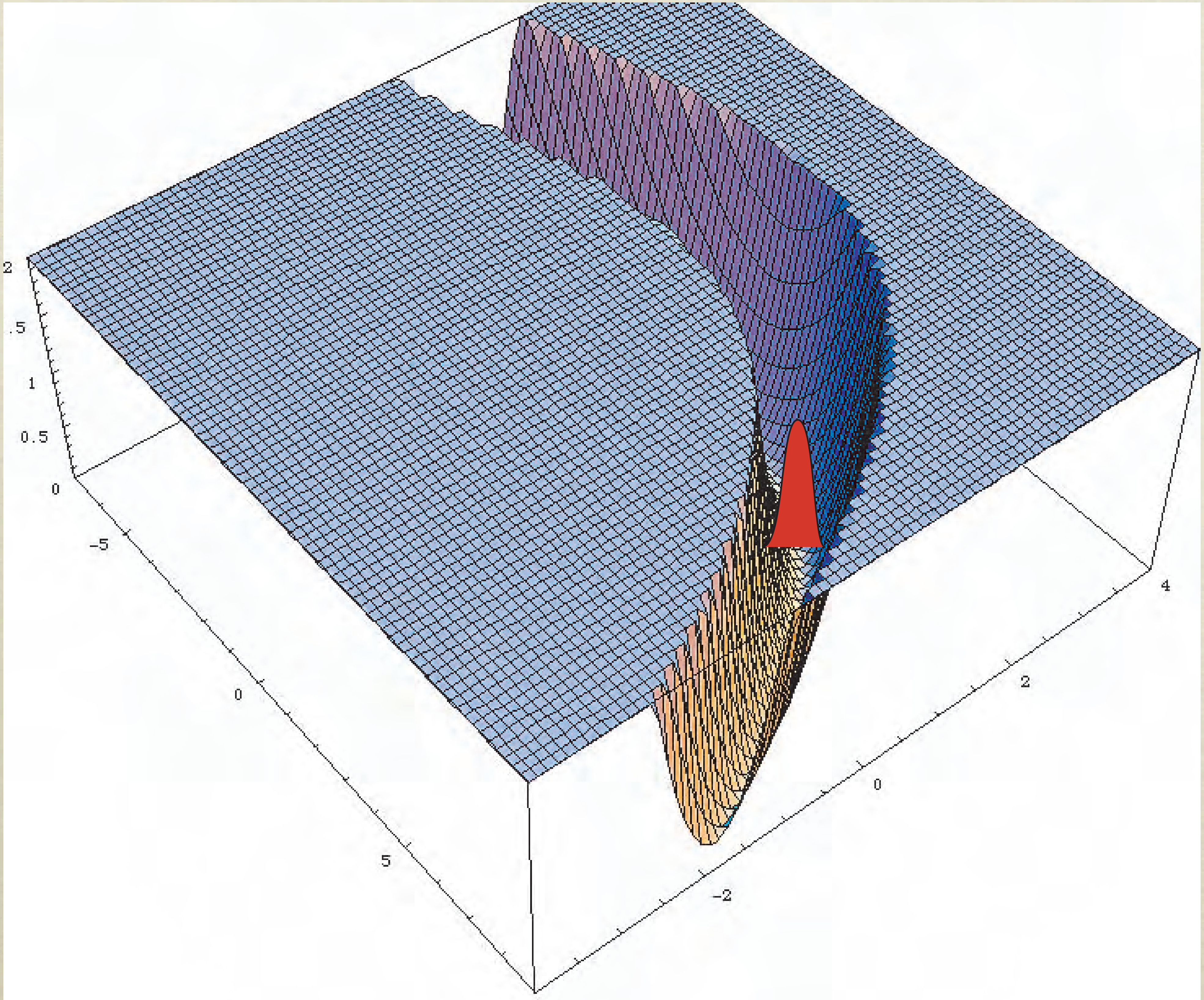

2
.5
1
0.5
0
-5
0
5
4
2
0
-2


Raman
Scattering

What determines Raman spectral intensities?

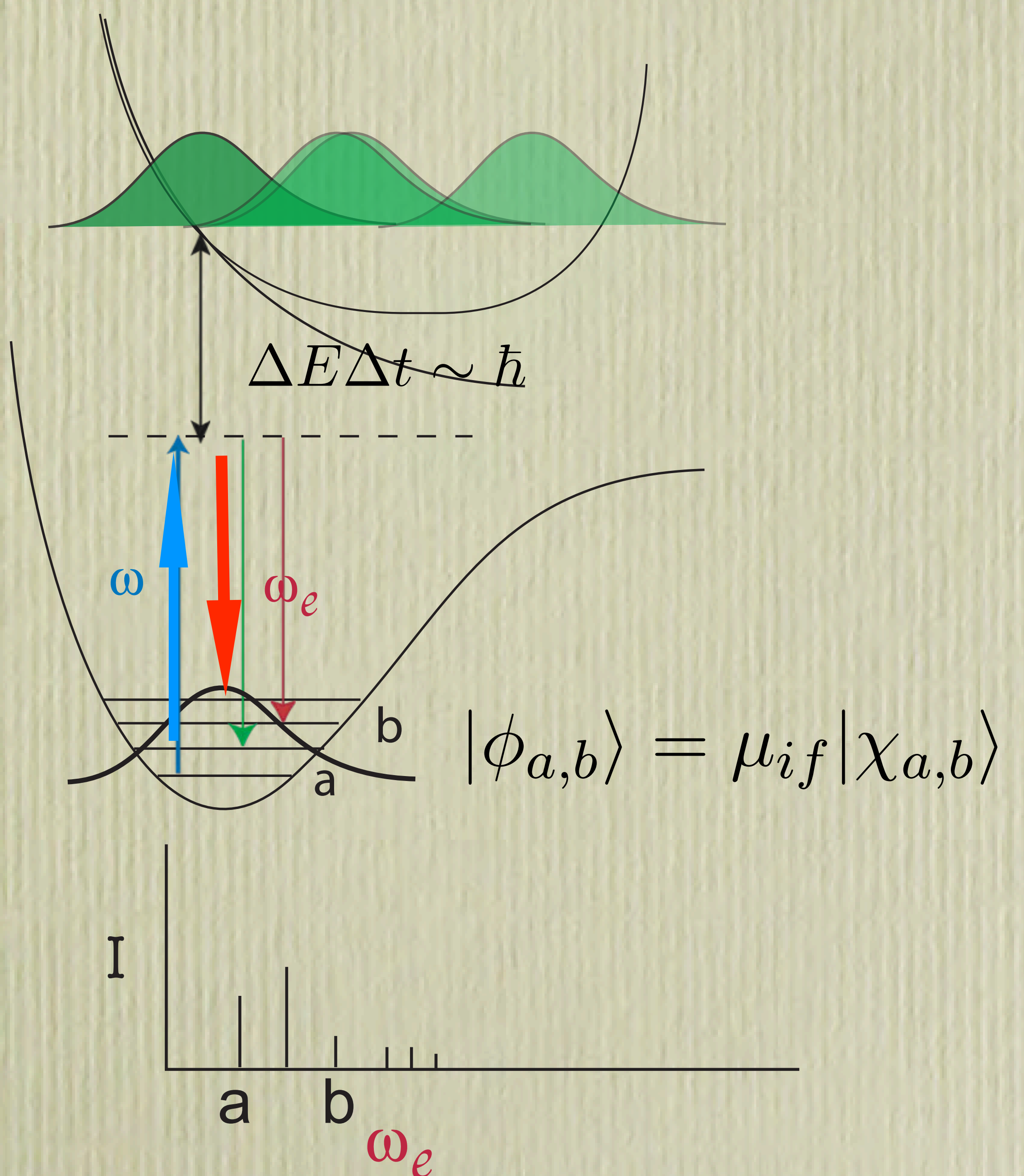

- Kramers-Heisenberg-Dirac

$$I_{ab}(\omega) = \left| \sum_{\mathbf{m}}^{\infty} \frac{\langle \phi_b | \mathbf{m} \rangle \langle \mathbf{m} | \phi_a \rangle}{E_a + \hbar\omega - E_{\mathbf{m}} + i\epsilon} \right|^2$$

Good luck: 10^(18) states **m** to sum over!

Instead: run wavepacket for a short time!

$$I_{ab}(\omega) = \left| \int_0^{\infty} e^{i\omega t} \langle \phi_b | \phi_a(t) \rangle \, dt \right|^2$$

Soo-Y. Lee and Eric J. Heller, “Time Dependent Theory of Raman Scattering”, *J. Chem. Phys.* **71**, 4777-88 (1979).

What determines Raman spectral intensities?

If the wave packet does not return, for whatever reason, (dissociation, decoherence, lost in a big phase space, etc.) then the short time propagation gives the Raman intensities of individual lines even on resonance.

$$I_{ab}(\omega) = \left| \int_0^\infty e^{i\omega t} \langle \phi_b | \phi_a(t) \rangle \, dt \right|^2$$

A separate projection onto another final state for each line strength.

$$|R_\omega^a\rangle = \int_0^\infty e^{i\omega t} |\phi_a(t)\rangle \, dt$$

"Raman wave function"

$$I_{ab}(\omega) = |\langle \phi_b | R_\omega^a \rangle|^2$$

What determines Raman spectral intensities? (polyatomics)

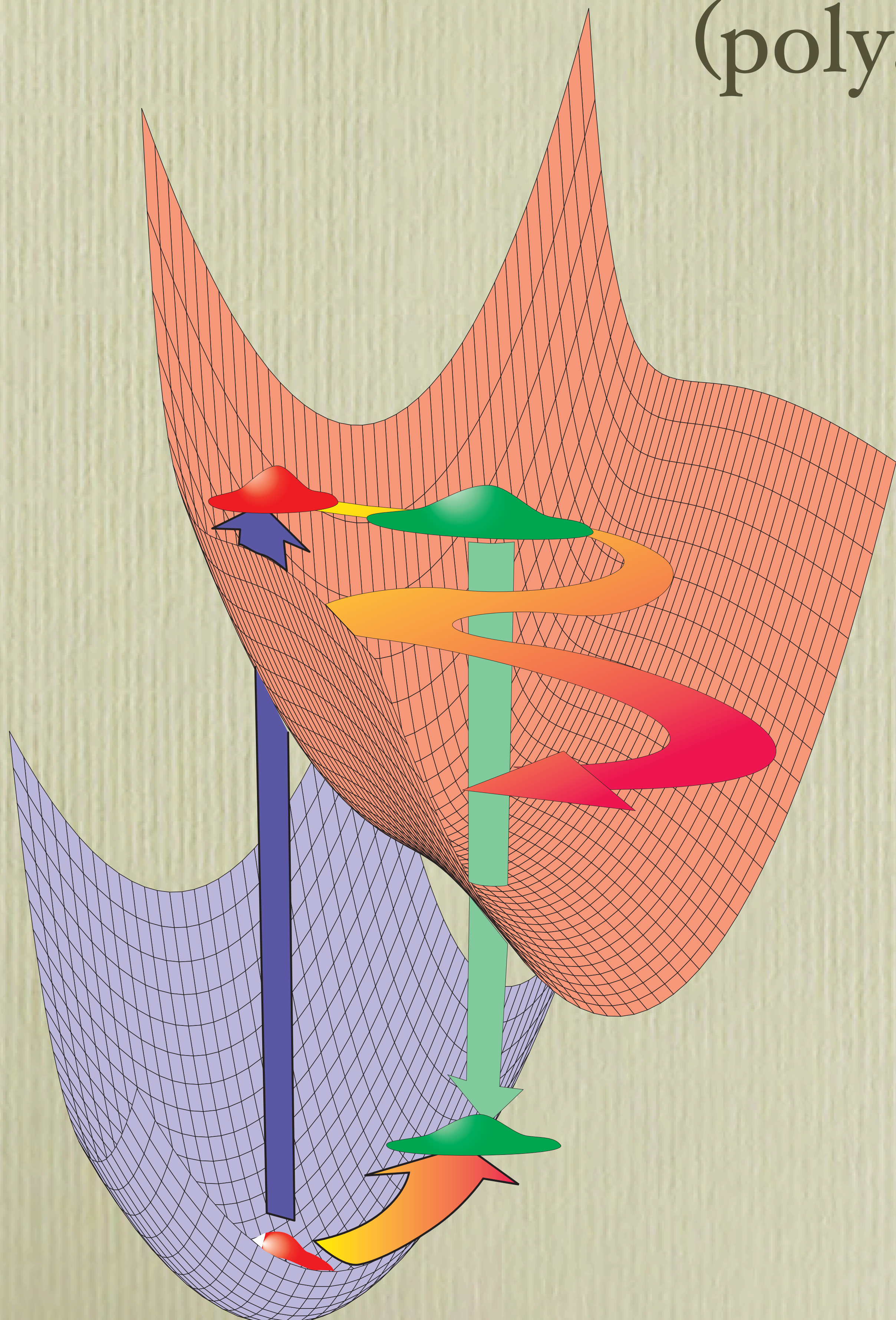

The story is more interesting for polyatomics-the direction of initial motion clearly determines what states the Raman wavefunction will overlap

Ratio of line intensities of two modes:

$$\frac{I_n}{I_m} = \frac{\omega_m}{\omega_n} \left(\frac{\partial V / \partial x_n}{\partial V / \partial x_m} \right)^2$$

Time dependent Semiclassical:

van Vleck Green's function; vV, Morette, 1940's

$$
\begin{aligned}
G(\mathbf{q},\mathbf{q}_0;t) &\approx G_{sc}(\mathbf{q},\mathbf{q}_0;t) \\
&= \left(\frac{1}{2\pi i\hbar}\right)^{d/2} \sum_j \left|\mathrm{Det}\left(\frac{\partial^2 S_j(\mathbf{q},\mathbf{q}_0;t)}{\partial\mathbf{q}\partial\mathbf{q}_0}\right)\right|^{1/2} \\
&\quad \times \exp\left(iS_j(\mathbf{q},\mathbf{q}_0;t)/\hbar - \frac{i\pi\nu_j}{2}\right)
\end{aligned}
$$

first full Van Vleck implementation - early 90's!

Re[ψ]

quantum semiclassical

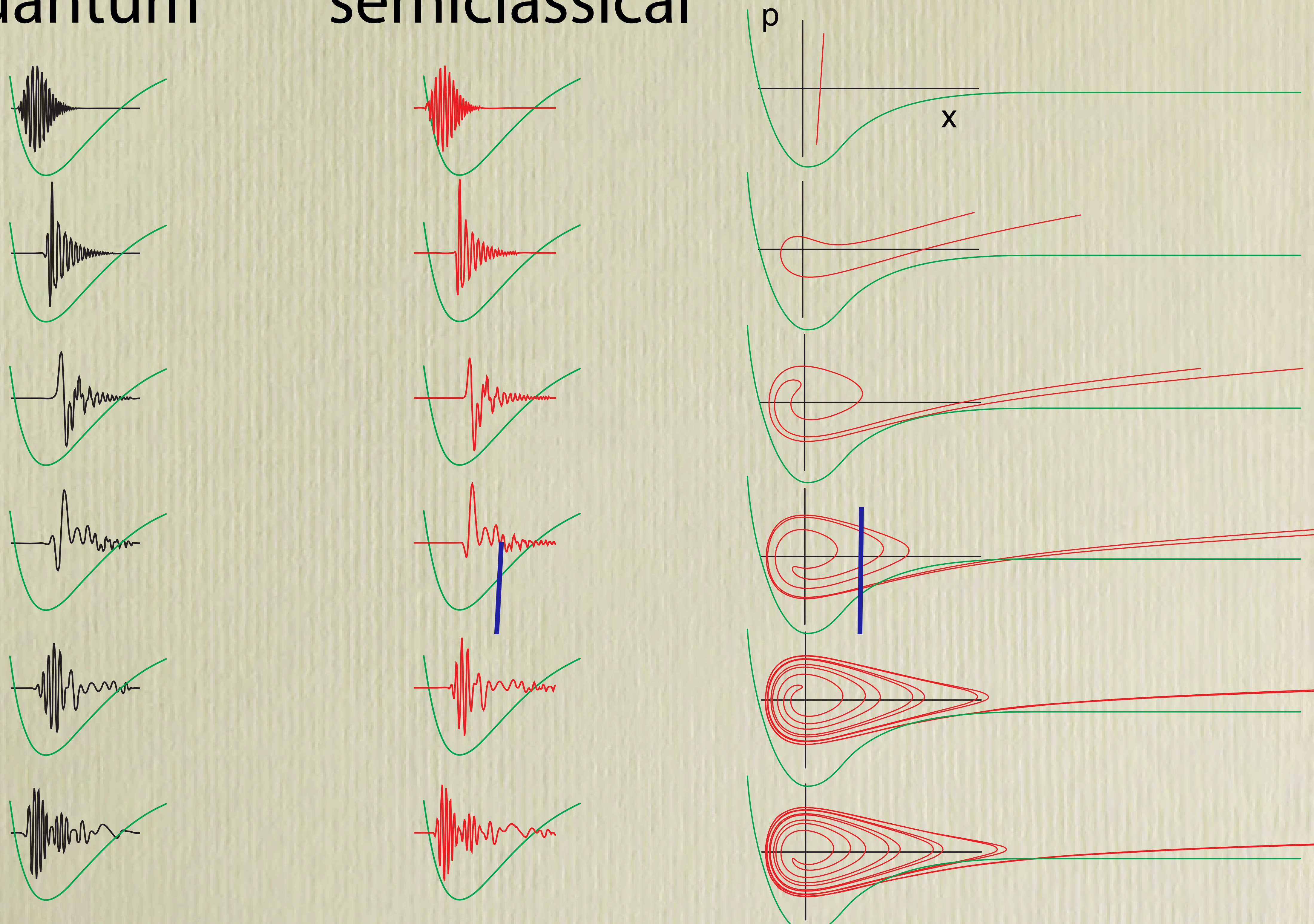

Off-center guided thawed Gaussians

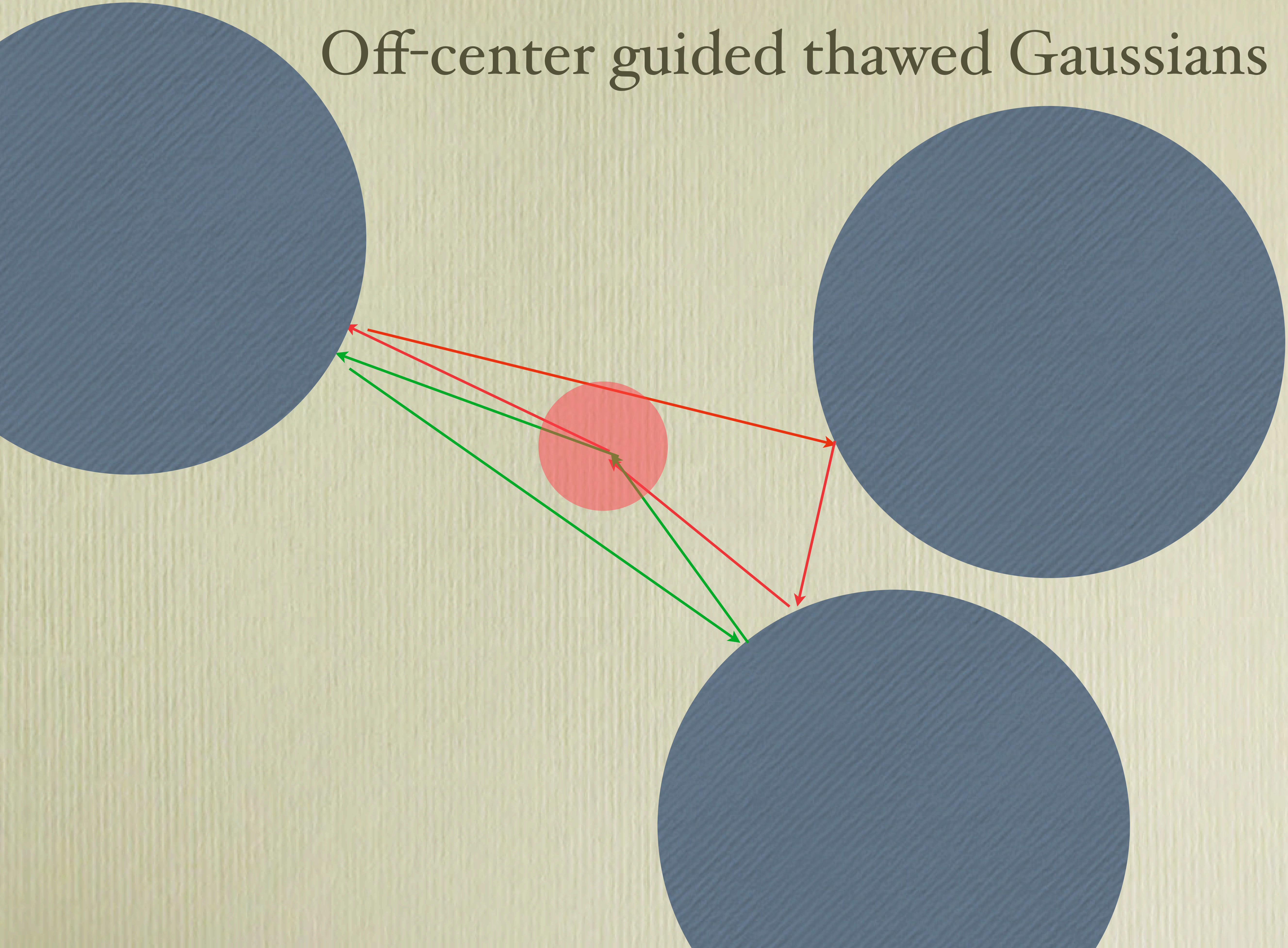

Idea: Instead of

$$\psi(\vec{x},t) = \sum_n a_n(t) g_n(\vec{x},t)$$

use a sum over *thawed gaussian propagators*

$$\psi(\vec{x},t) = \sum_n G_n^{TGA}(t)\psi(\vec{x},0)$$

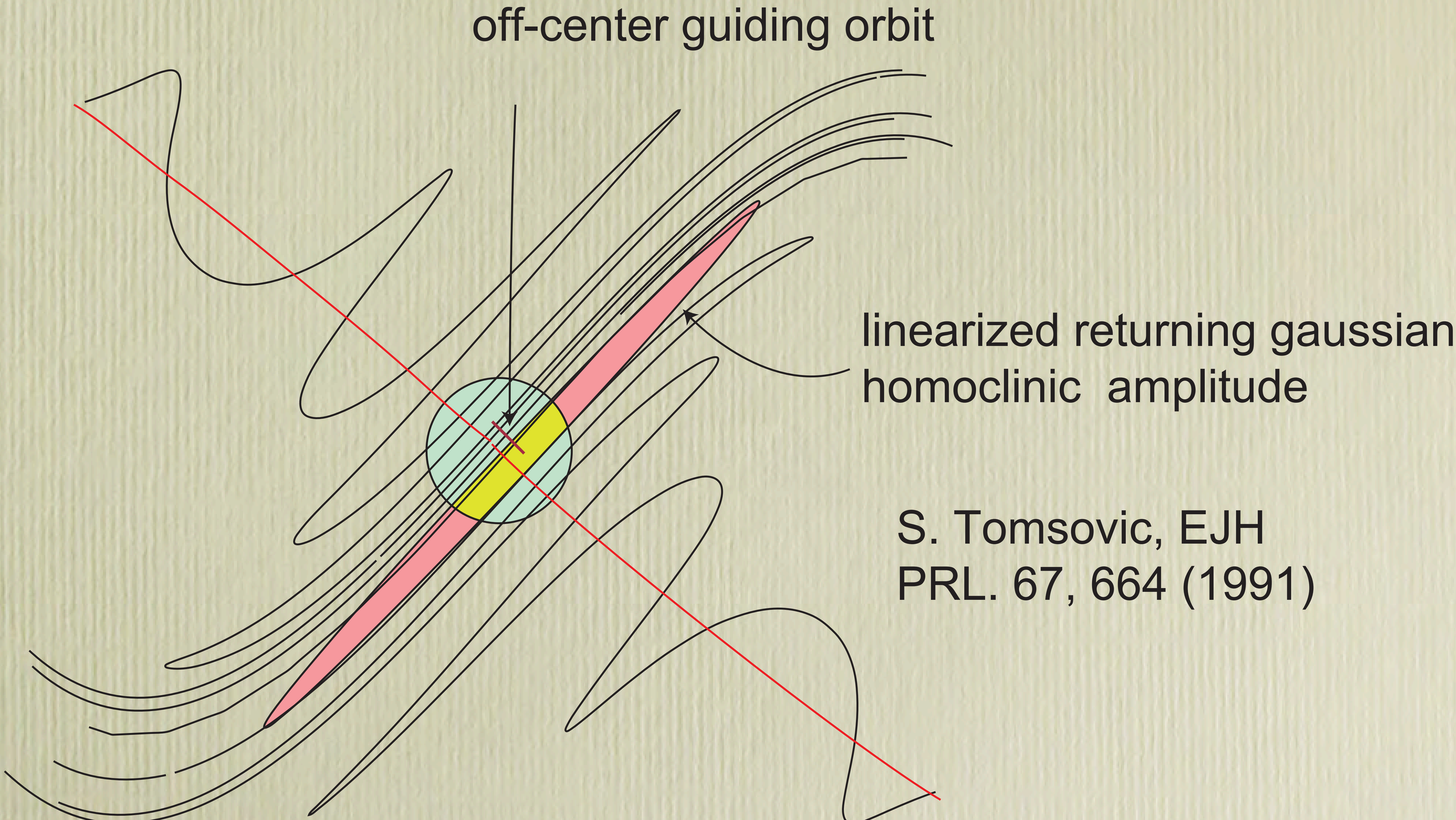

S. Tomsovic, EJH
PRL. 67, 664 (1991)

Homoclinic orbits

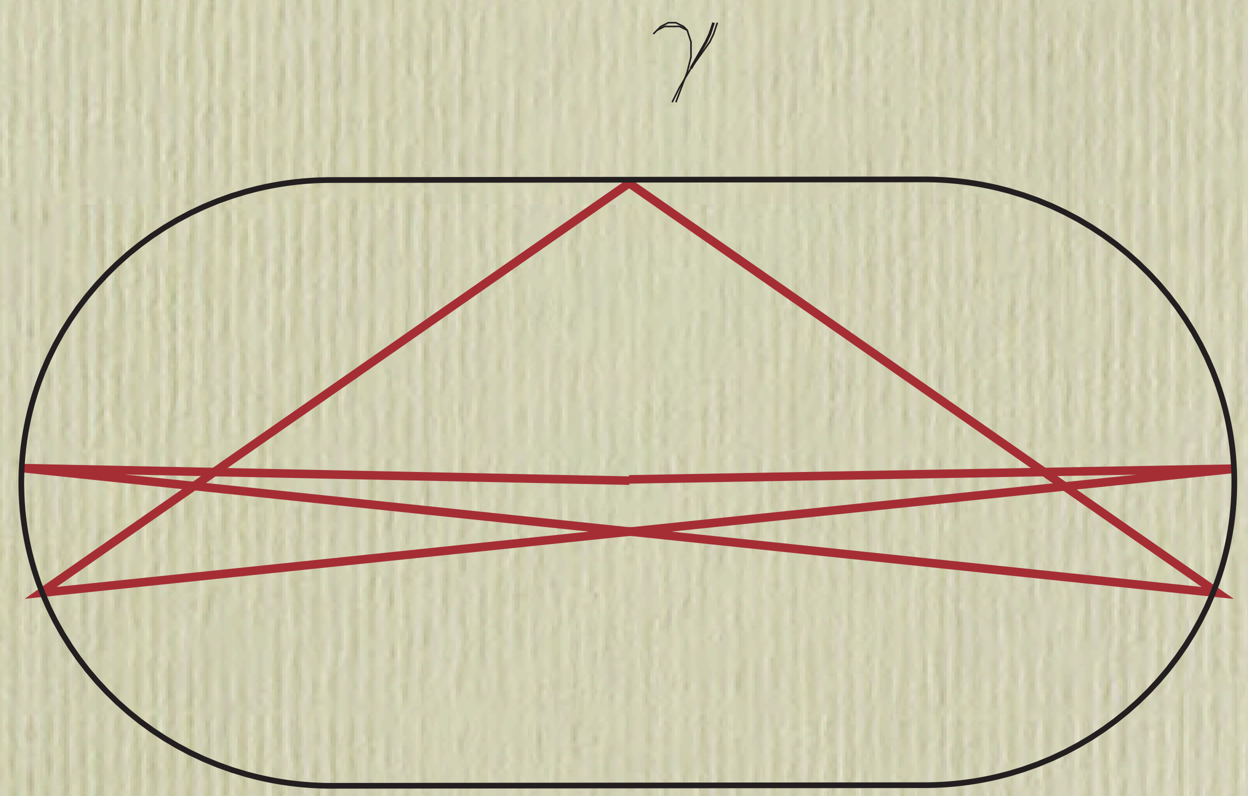

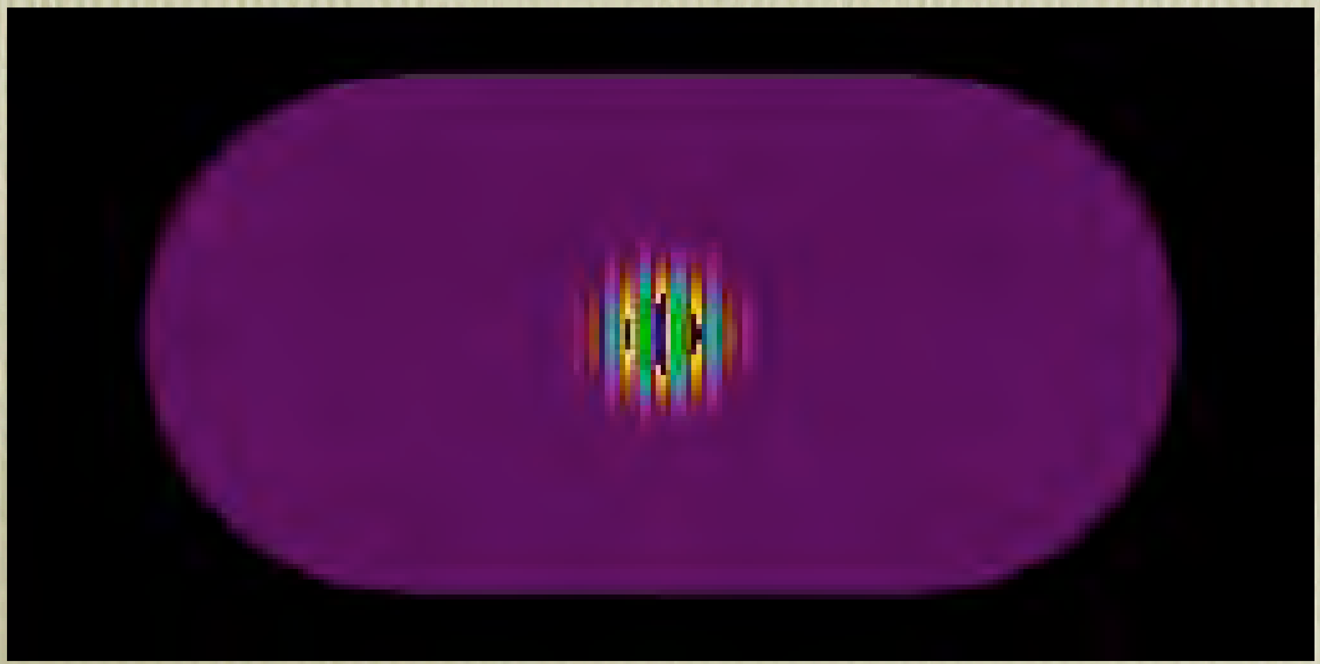

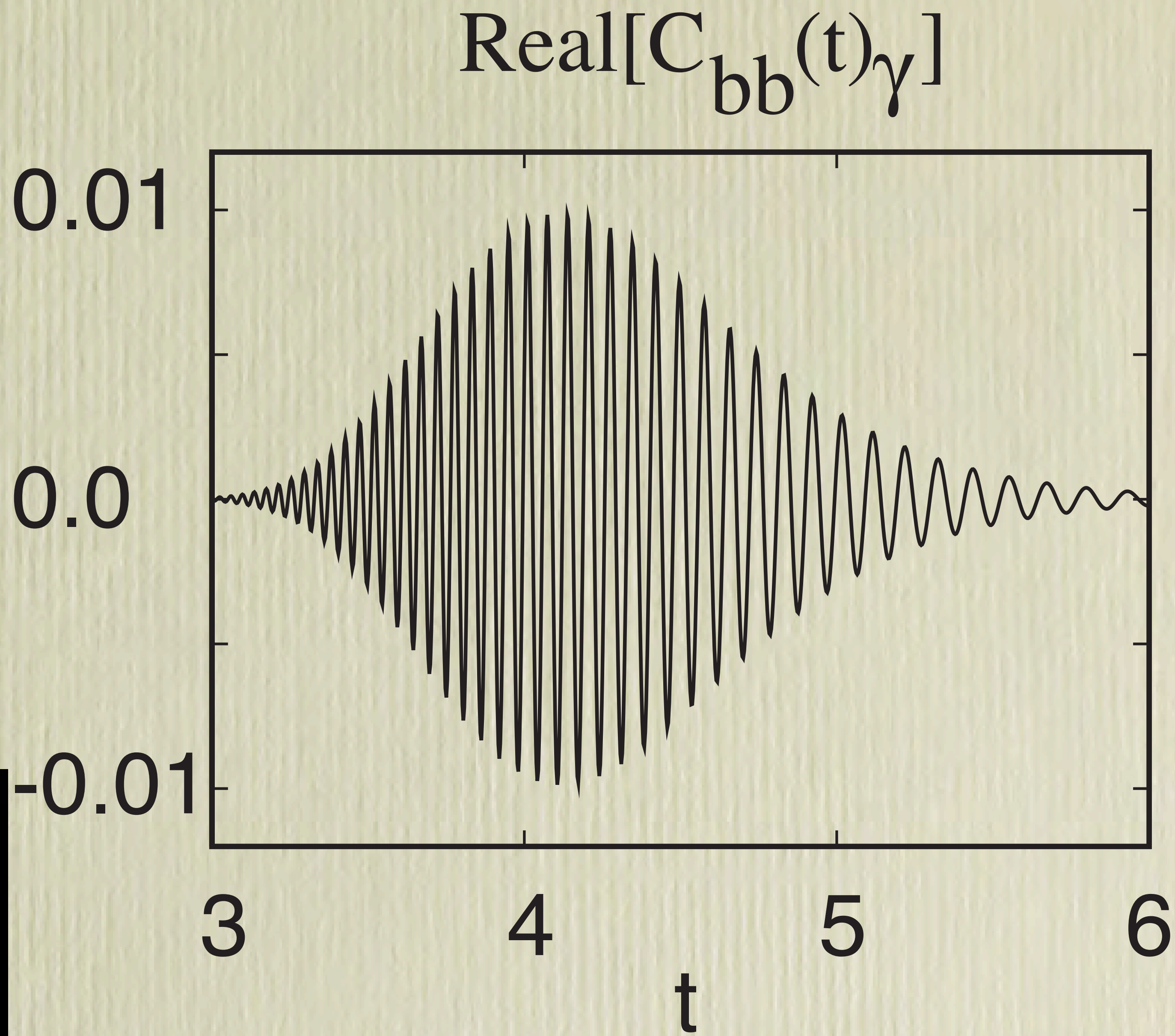

Stadium Correlation Function

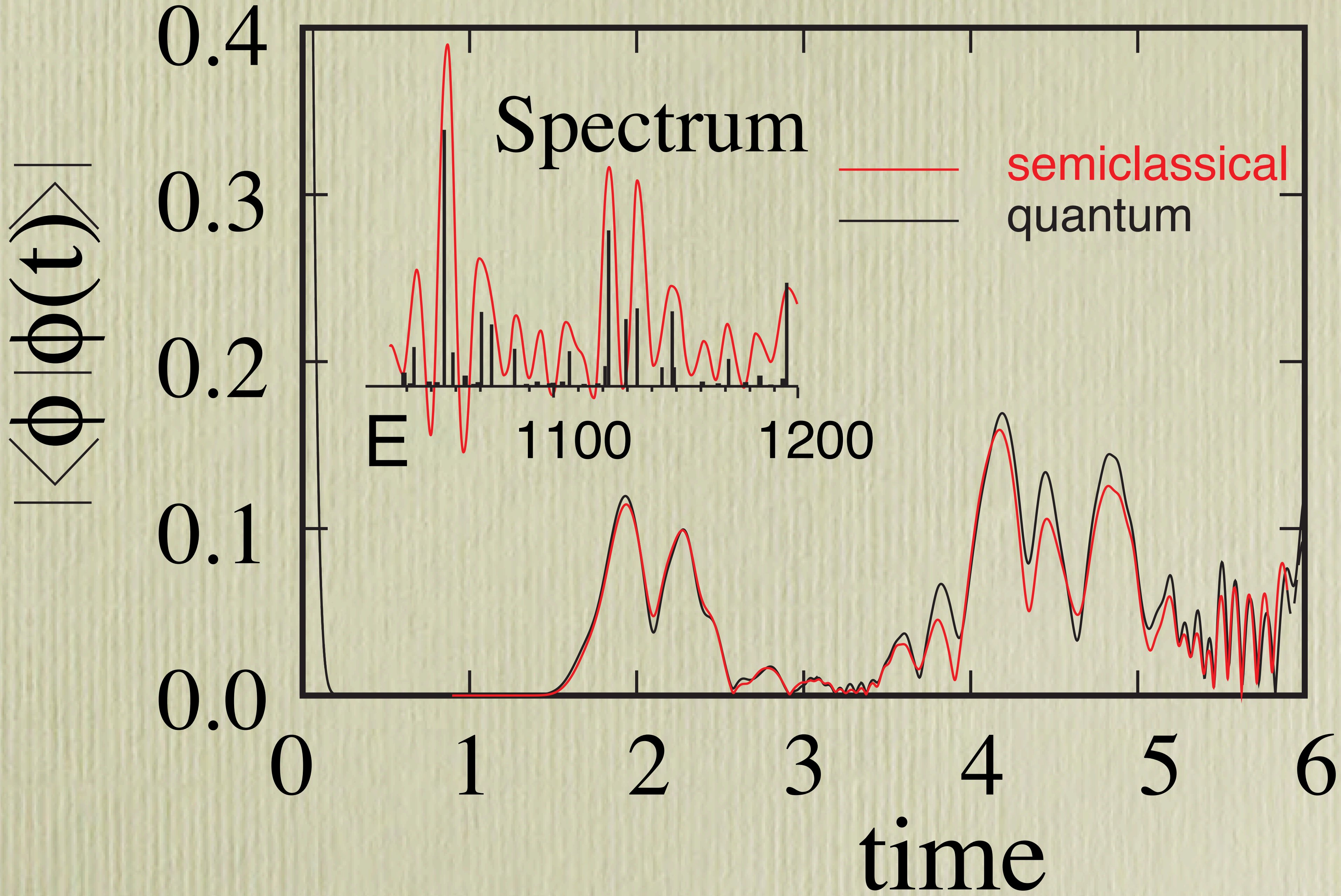

Tomsovic, EJH
PRL 1991

64,000 off center guided
w.p.

Getting the whole emission spectrum

$$I(\omega_s) = \frac{\omega_I \omega_S^3}{2\pi} \int_{-\infty}^{\infty} e^{i\omega' t} \langle R^a(\omega) | R^a(\omega, t) \rangle \; dt$$

Raman wavefunction propagated
on the *initial* surface

"Simple Aspects of Raman Scattering"

Example: On resonance quantum yield of fluorescent (Raman) photons in Iodine photodissociation about the same as typical pre- resonant yield in polyatomics

Incoherent neutron scattering e.g. molecules in solution

$$Y_{jj}(k,t) =$$

$$\frac{1}{Q}\int \frac{d^{2N}}{\pi^N}\langle z|e^{-\beta H/2}e^{-i\vec{k}\cdot\vec{q}_j}e^{iHt/\hbar}e^{i\vec{k}\cdot\vec{q}_j}e^{-iHt/\hbar}e^{-\beta H/2}|z\rangle$$

$$= \frac{1}{Q}\int \frac{d^{2N}}{\pi^N}\langle z_\beta|e^{-i\vec{k}\cdot\vec{q}_j}e^{iHt/\hbar}e^{i\vec{k}\cdot\vec{q}_j}e^{-iHt/\hbar}|z_\beta\rangle$$

boost propagate boost propagate

PHYSICAL REVIEW A VOLUME 36, NUMBER 6 SEPTEMBER 15, 1987

Classical and semiclassical approximations for incoherent neutron scattering

E. J. Heller
Departments of Chemistry and Physics, University of Washington, Seattle, Washington 98195

Jeffrey R. Reimers*
Department of Chemistry, B014 University of California San Diego, La Jolla, California 92093

Gerhard Drolshagen
Max-Planck-Institut für Stromungforschung Bunsenstrasse 10, D-3400 Göttingen, West Germany
(Received 2 October 1986)

Recent experience with semiclassical approximations with wave packets make possible a new intuitive basis and new computational tools for incoherent neutron scattering. We review our approach in the context of others which have been proposed for neutron scattering, and we find it advantageous to launch semiclassical approximations from the Schrödinger picture rather than the Heisenberg picture of quantum mechanics. An application to a model for crystalline HCN is given.

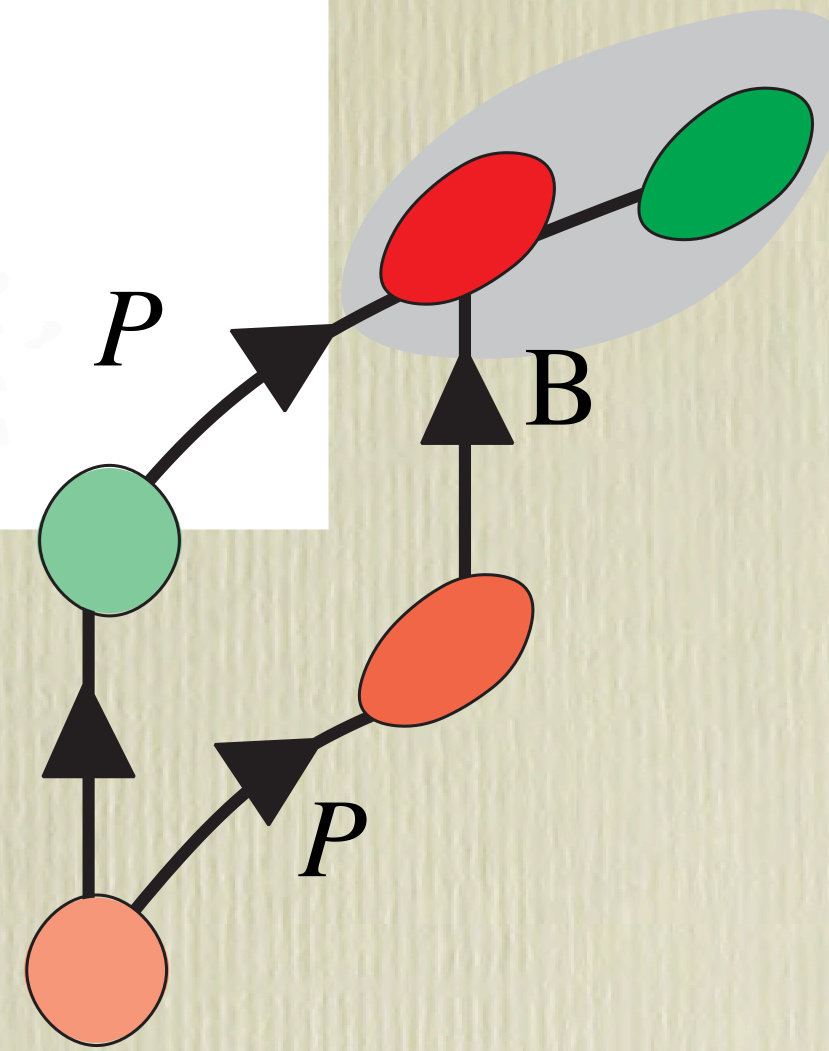

$$= \frac{1}{Q} \int \frac{d^{2N}}{\pi^N} \langle z_\beta | e^{-i\vec{k}\cdot\vec{q}_j} e^{iHt/\hbar} e^{i\vec{k}\cdot\vec{q}_j} e^{-iHt/\hbar} | z_\beta \rangle$$

Thus far we have learned...

- Time dependent theory is driven by the requirements of condensed phase systems and large molecules, whether the experiment is time dependent or not.
- Ironically, the very shortest time information about chemical dynamics is often best obtained from the frequency domain

Perspectives on Quantum Tunneling

- Decoherence and tunneling
- tunneling when you least expect it
  - dynamical tunneling
  - molecular spectra and tunneling

Barrier penetration: role of coherence

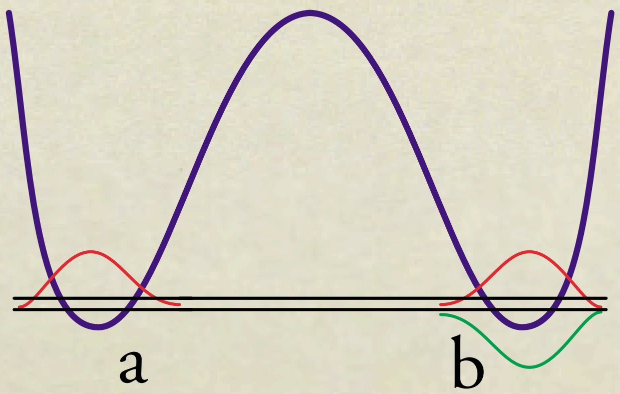

$$\Delta E \sim e^{-\int_a^b |p(x)|\ dx/\hbar}$$

A

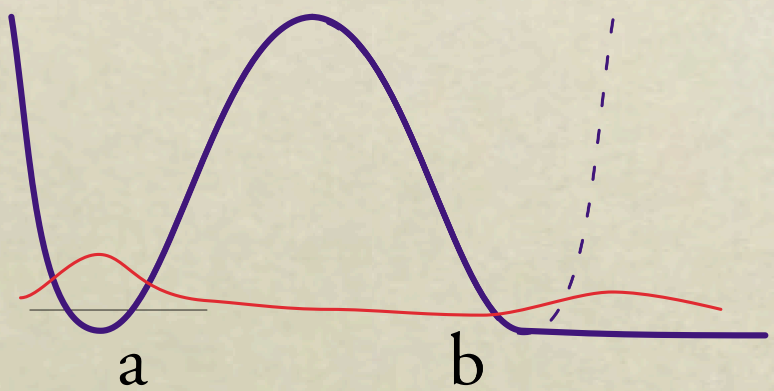

$$\Gamma \sim\ e^{-2\int_a^b |p(x)|\ dx/\hbar}$$

B

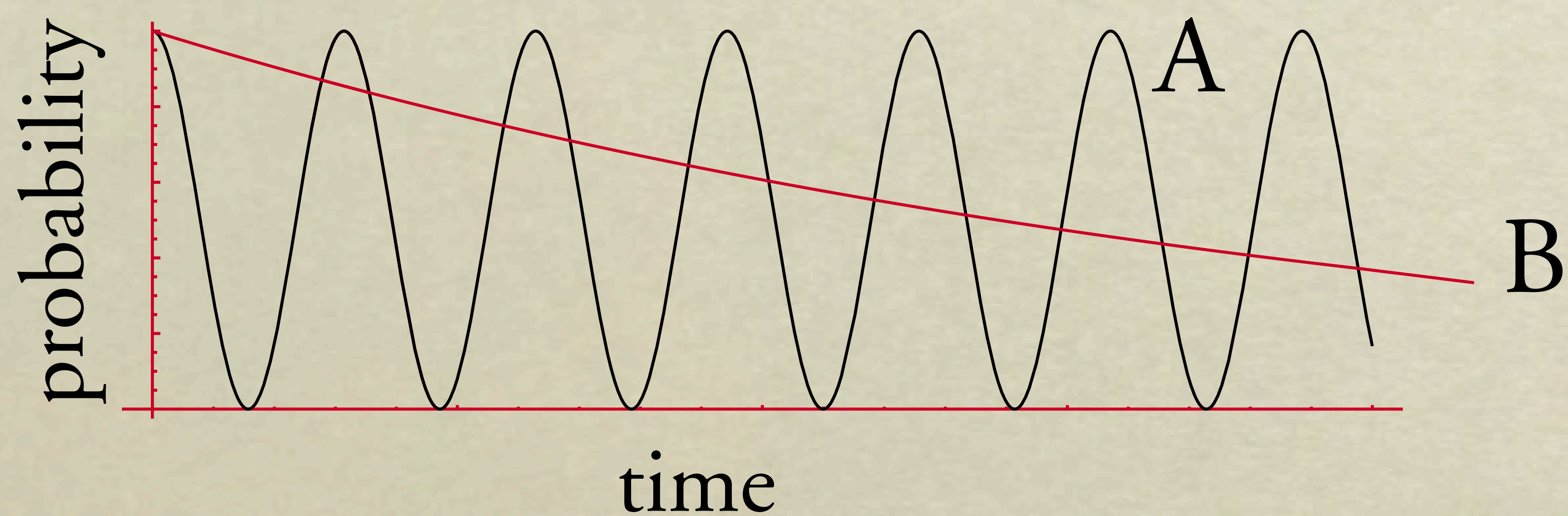

Quadratic vs. Linear buildup

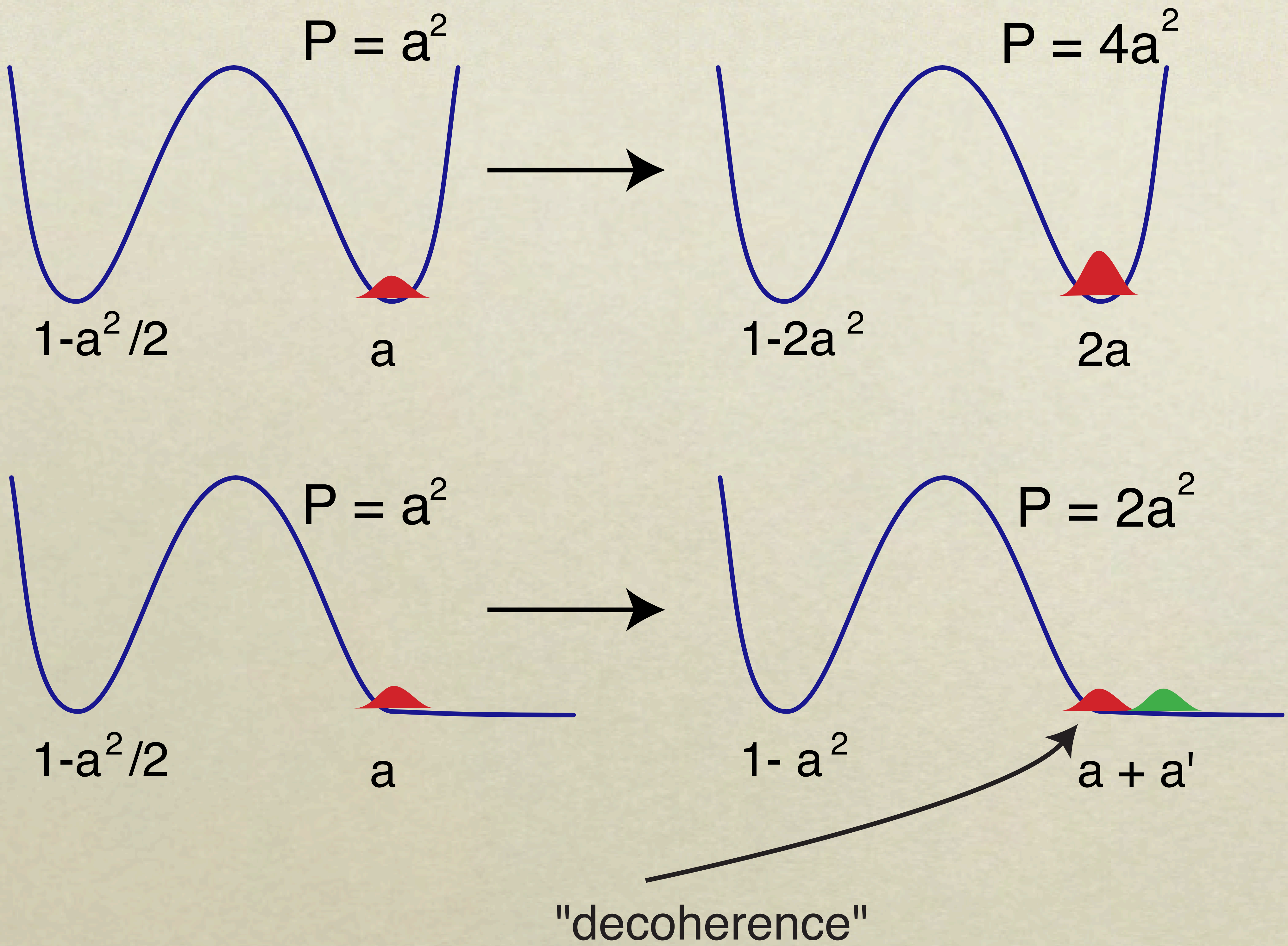

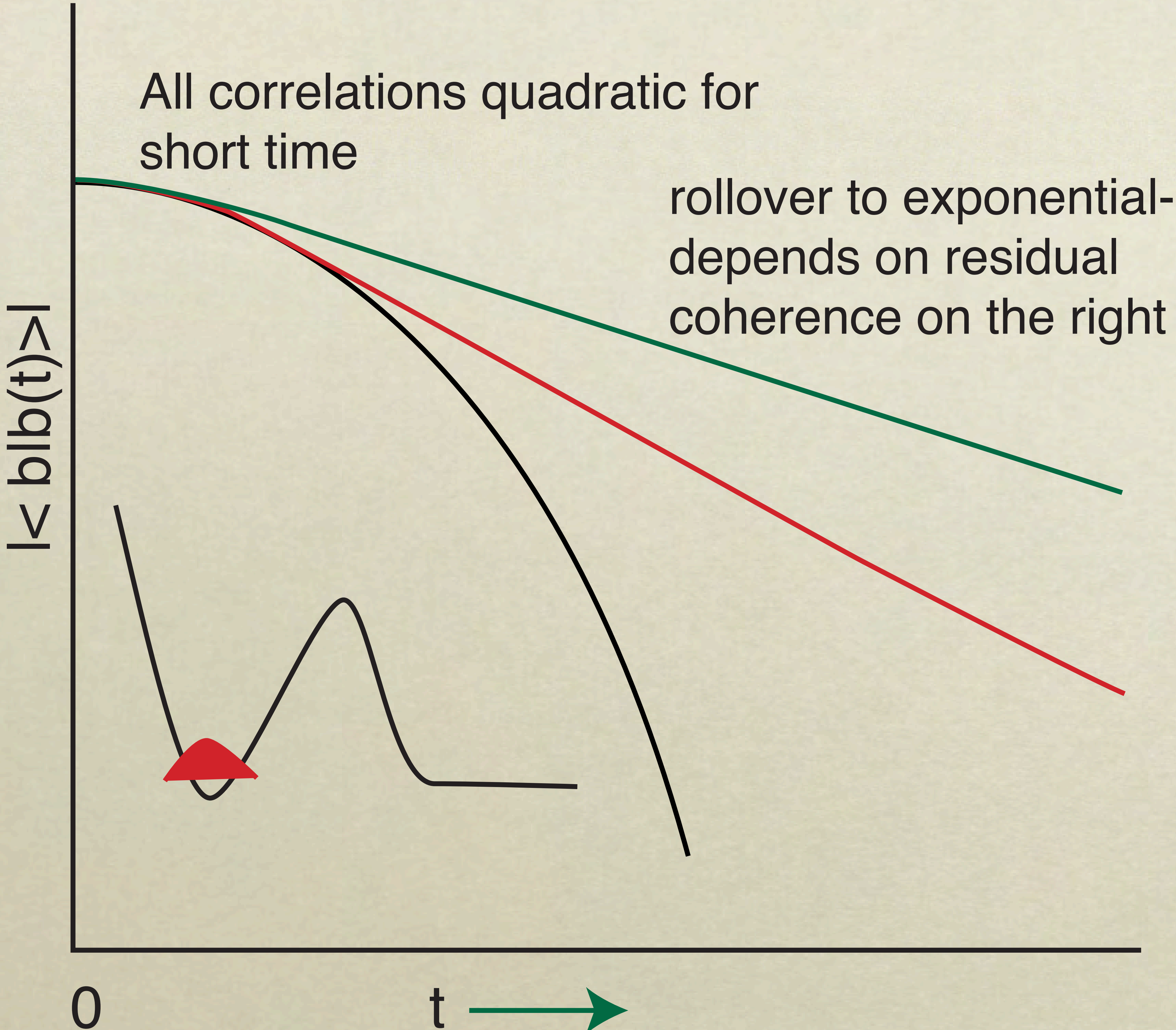
All correlations quadratic for
short time
rollover to exponential-
depends on residual
coherence on the right
|< b|b(t)>|
0
t

Finite temperatures and decoherence do not eliminate tunneling; rather, they eliminate coherent enhancement of tunneling.

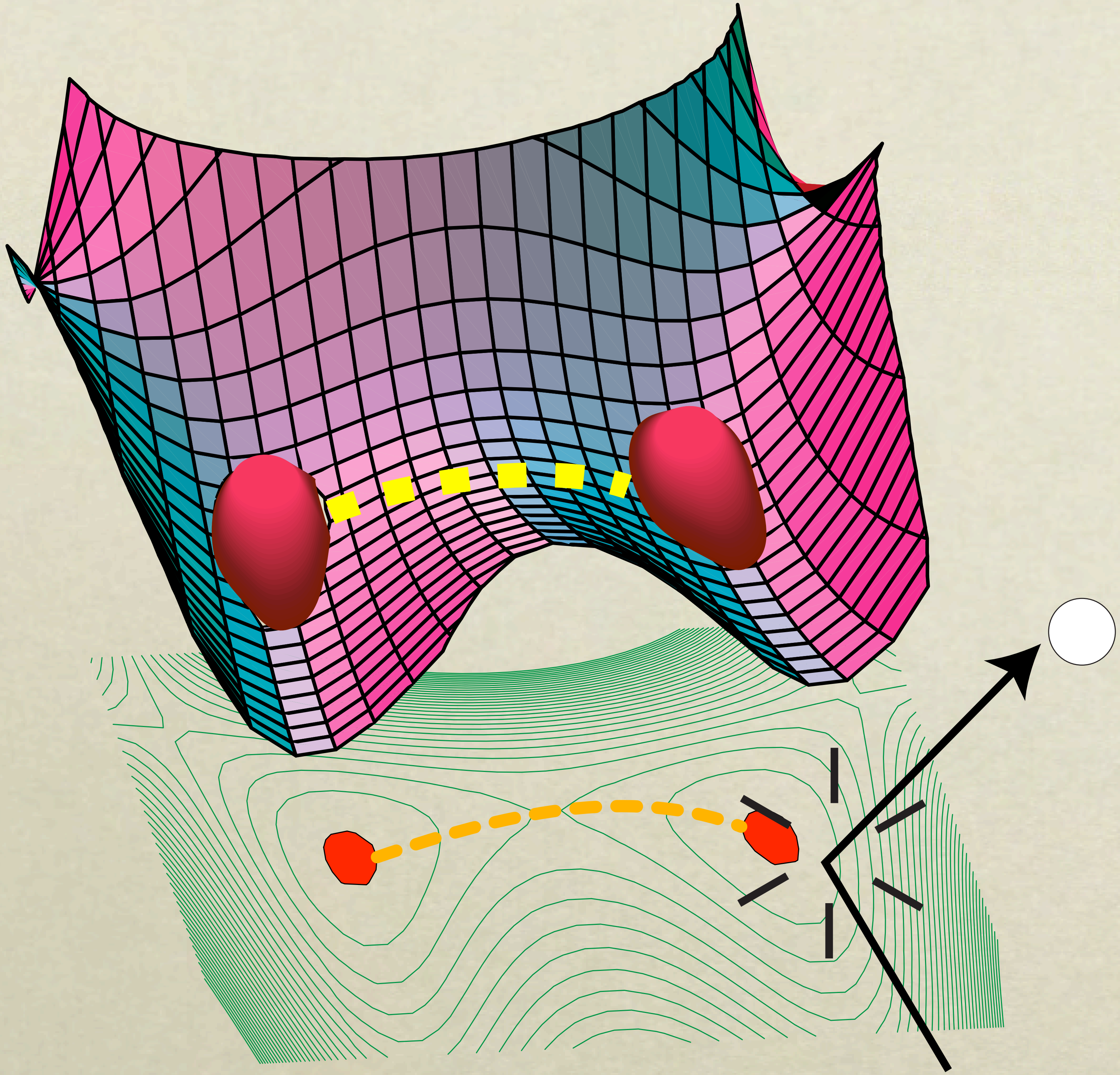

Symmetric tunneling made to behave like bound →free tunneling by decoherence

1. Comment on coherence and tunneling
2. Standard and nonstandard examples of tunneling
3. Surface jumping (not hopping)
   (with B. Segev, S. Kallush, A. Sergeev)
4. Ultracold sticking (A. Mody, J. Doyle)

Two Kinds of "Ordinary" Tunneling

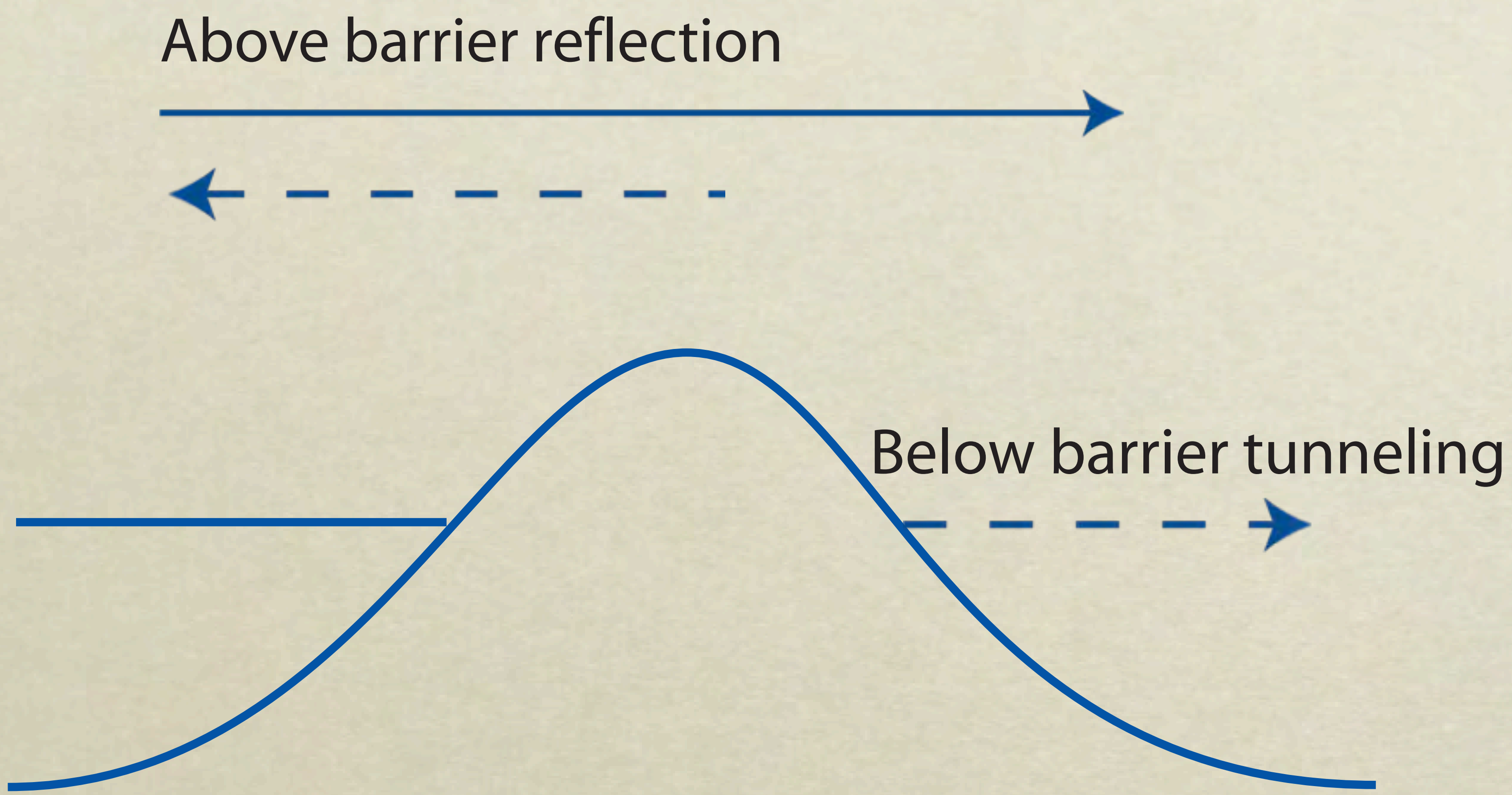

Both have analogs in "Dynamical Tunneling"

Penetration/reflection-use WKB?

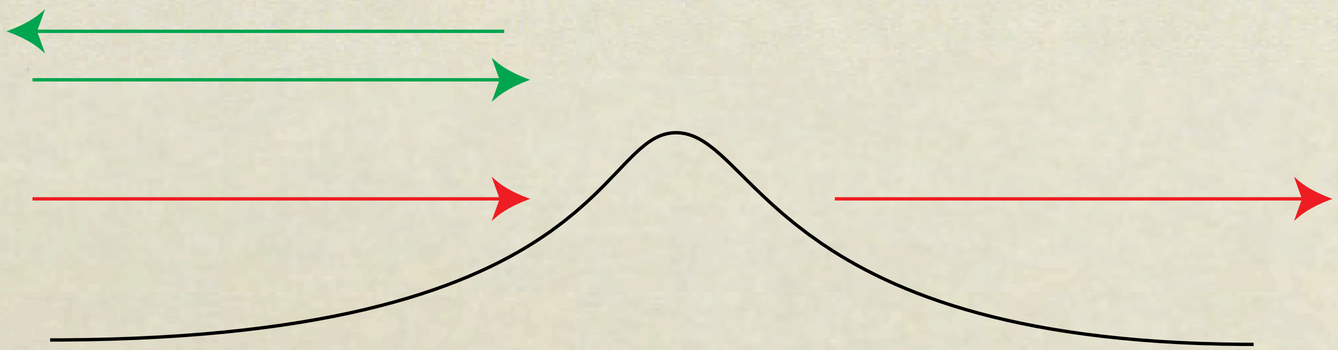

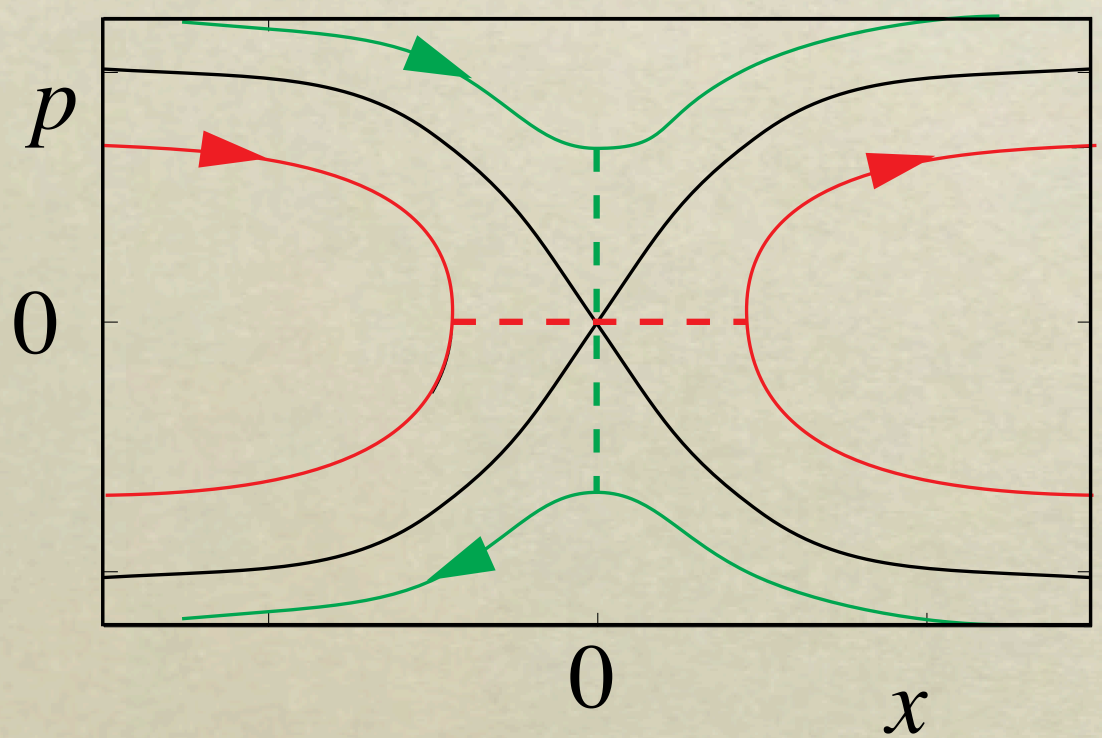

$$e^{-\int_{p_+}^{p_-} |x(p)|\, dp / \hbar}$$

$$e^{-\int_{a}^{b} |p(x)|\, dx / \hbar}$$

Low Barrier

Causes problems for both barrier tunneling and reflection. Cannot use semiclassical action-too small!

Solution: use perturbation theory

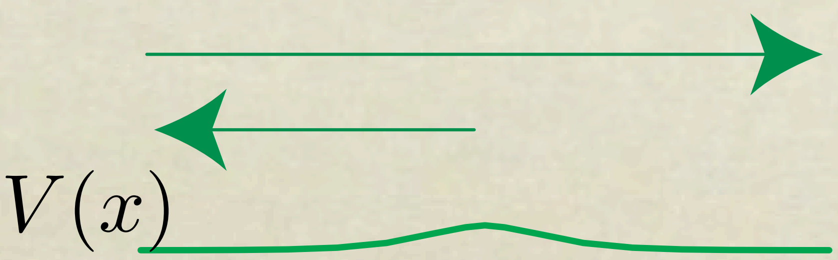

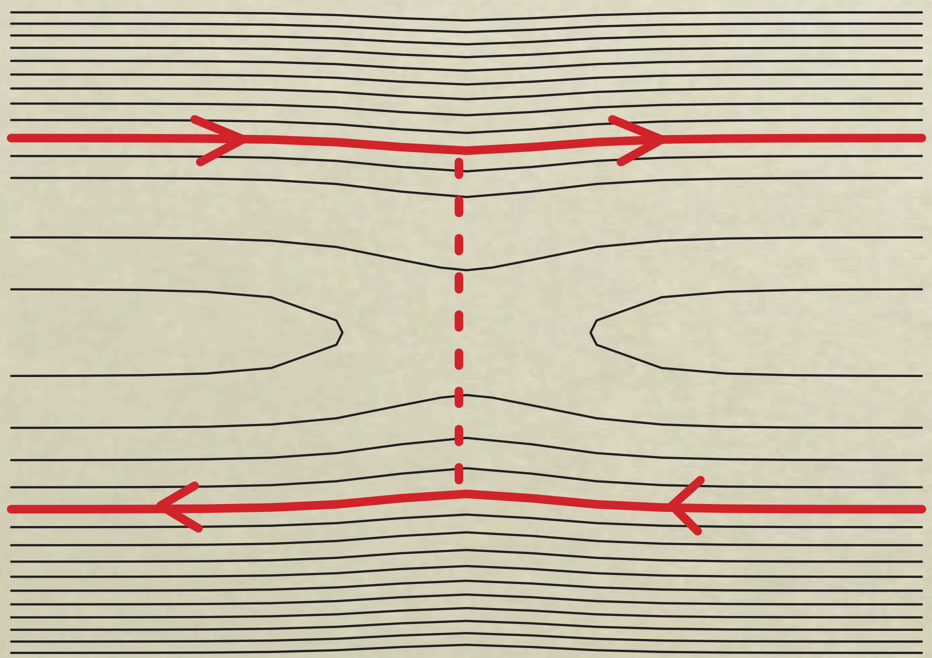

$$r = \int e^{ipx/h}\; V(x)\; \left(e^{-ipx/h}\right)^{*} dx$$

$$= \int e^{2ipx/h}\, V(x)\, dx$$

WKB Perturbation Theory

(1) what potential $V^{WKB}(x)$ makes ψ^{WKB} exact?

(2) Do perturbation theory on $[V(x) - V^{WKB}(x)]$

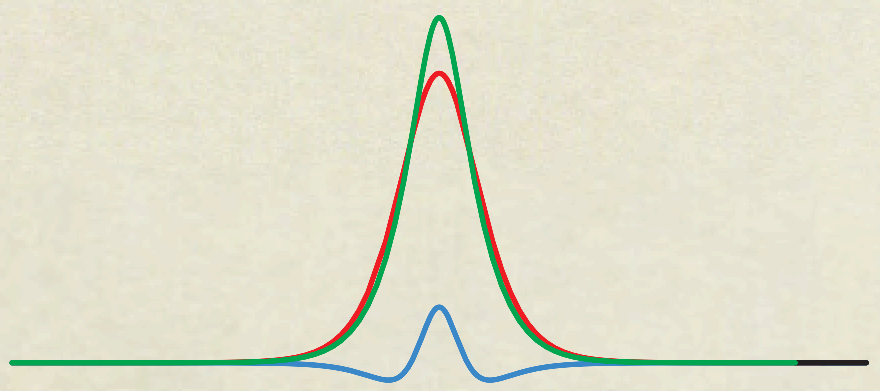

$$\left(\frac{-\hbar^2}{2m}\frac{\partial^2}{\partial x^2} + V^{WKB}(x)\right)\psi^{WKB}(x) = E\,\psi^{WKB}(x)$$

$$V^{WKB}(x) = \frac{\hbar^2\left(-5\,V'(x)^2 - 4\,E\,V''(x) + 4\,V(x)\,V''(x)\right)}{32\,(-E+V(x))^2}$$

$$R \approx \int \psi^{WKB*}(x)\,[V(x) - V^{WKB}(x)]\,\psi^{WKB}(x)\,dx$$

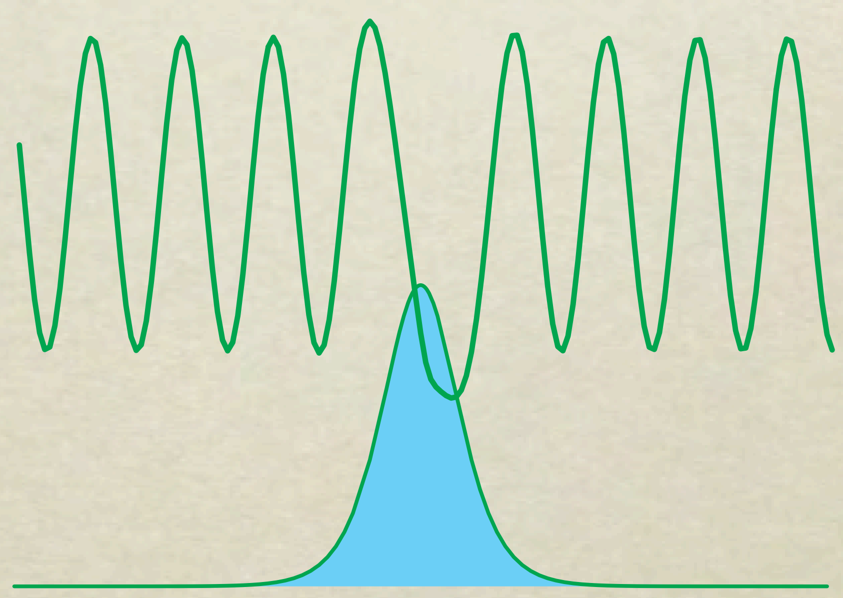

$E = 1.9$

$V(x) = V_o \,\mathrm{Sech}^2(x)$

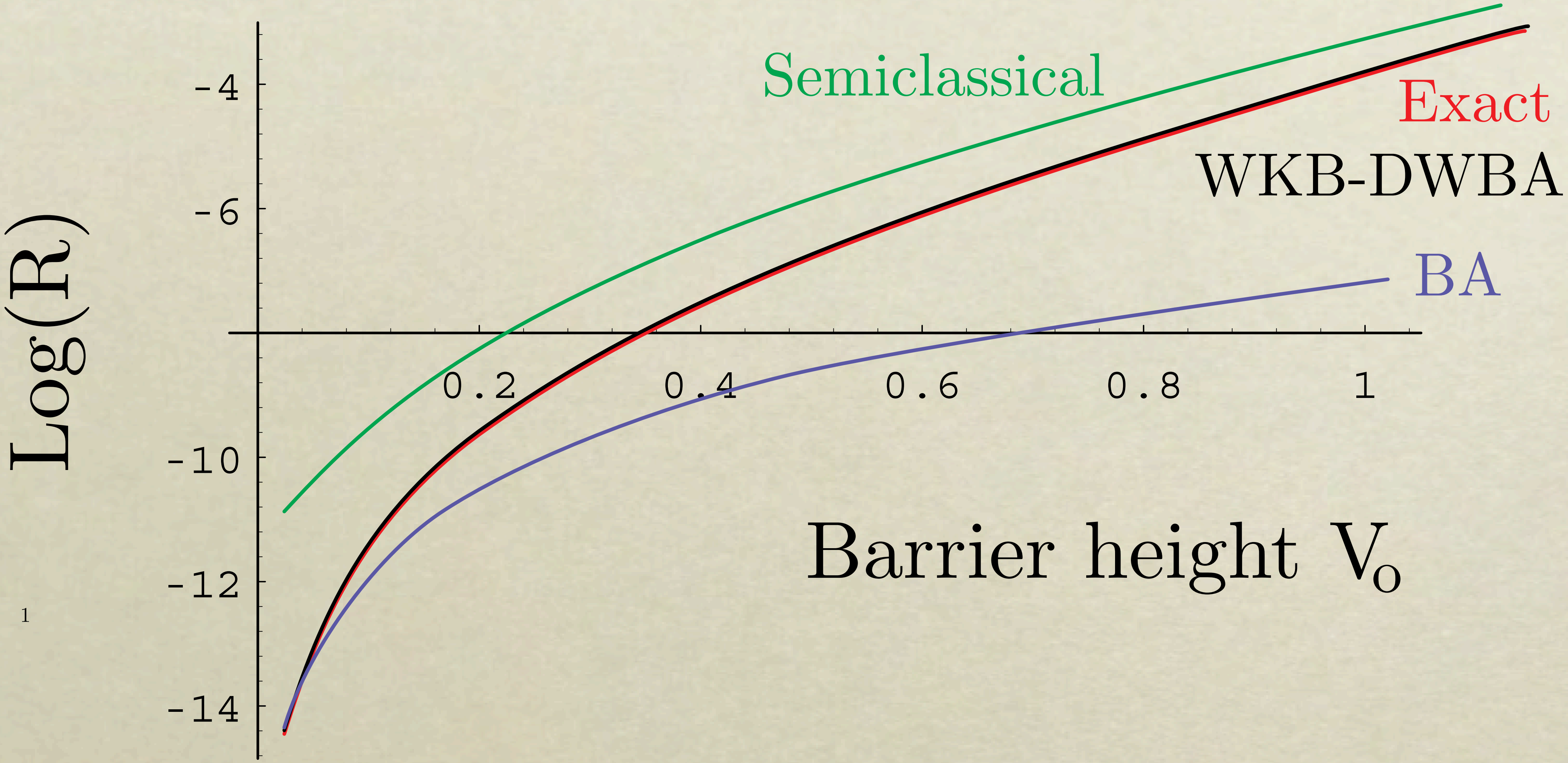

1

- N.T.Maitra and E.J.Heller, "Semiclassical perturbation approach to quantum reflection " *Phys. Rev.* A, **54**, 4763 (1997).

Dynamical Tunneling Examples

van der Waals dissociation

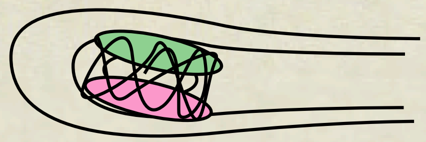

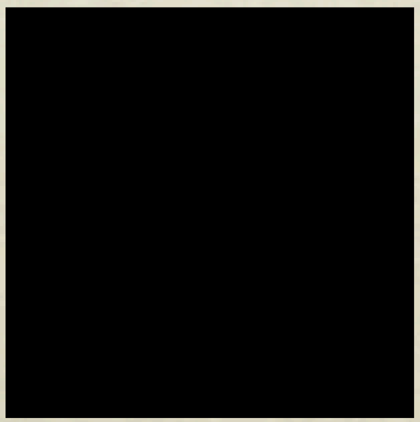

Overtone

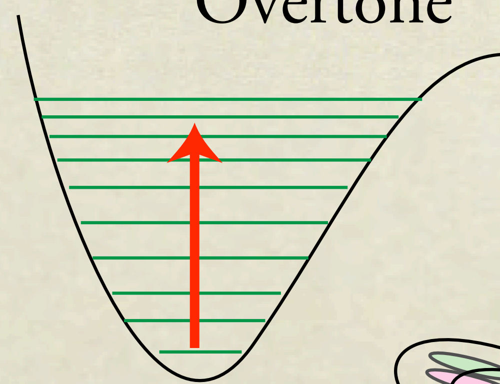

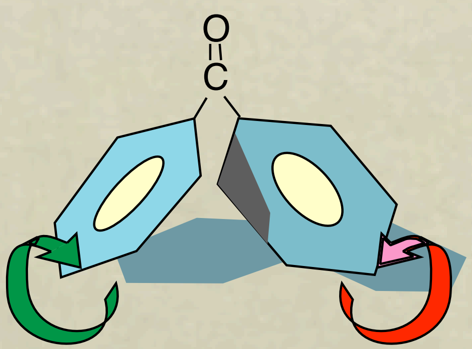

Local Mode

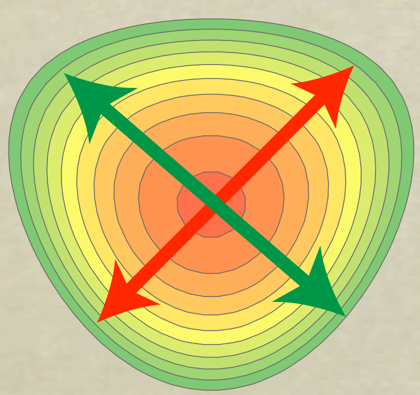

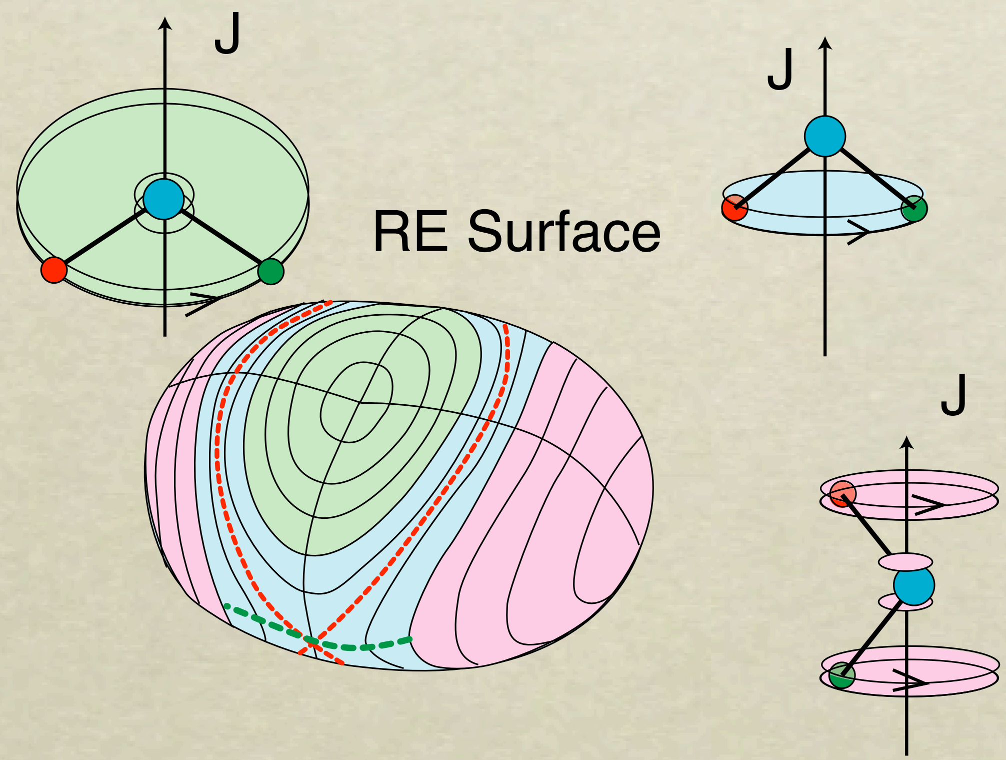

Pink- above barrier tunneling
Green- below barrier tunneling

Overtone transition: dynamical tunneling

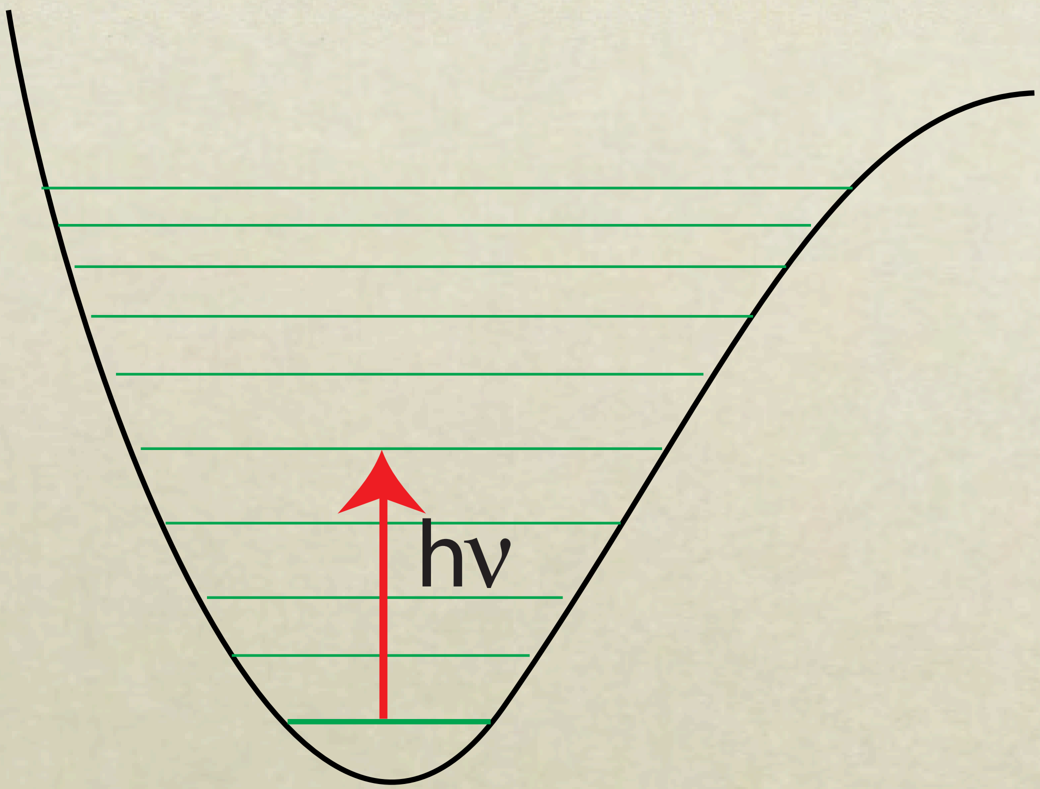

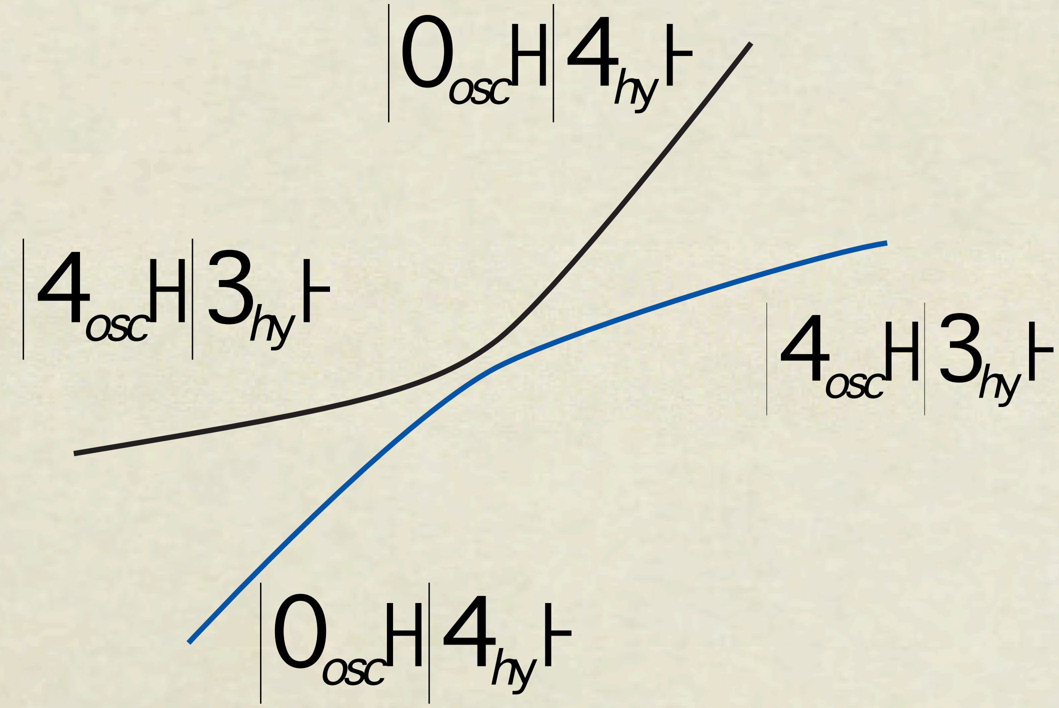

On resonance: Rabi cycling

$$\} \ (t) = |0_{osc} H|4_{hy} H \cos(\sim_{Rabi} t) + |4_{osc} H|3_{hy} H \sin(\sim_{Rabi} t)$$

Quantize the field mode: Morse + harmonic + linear coupling. Classically forbidden

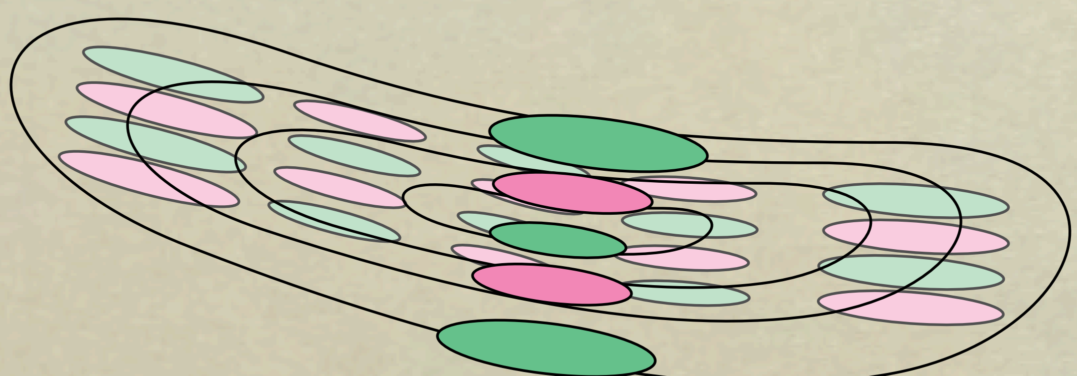

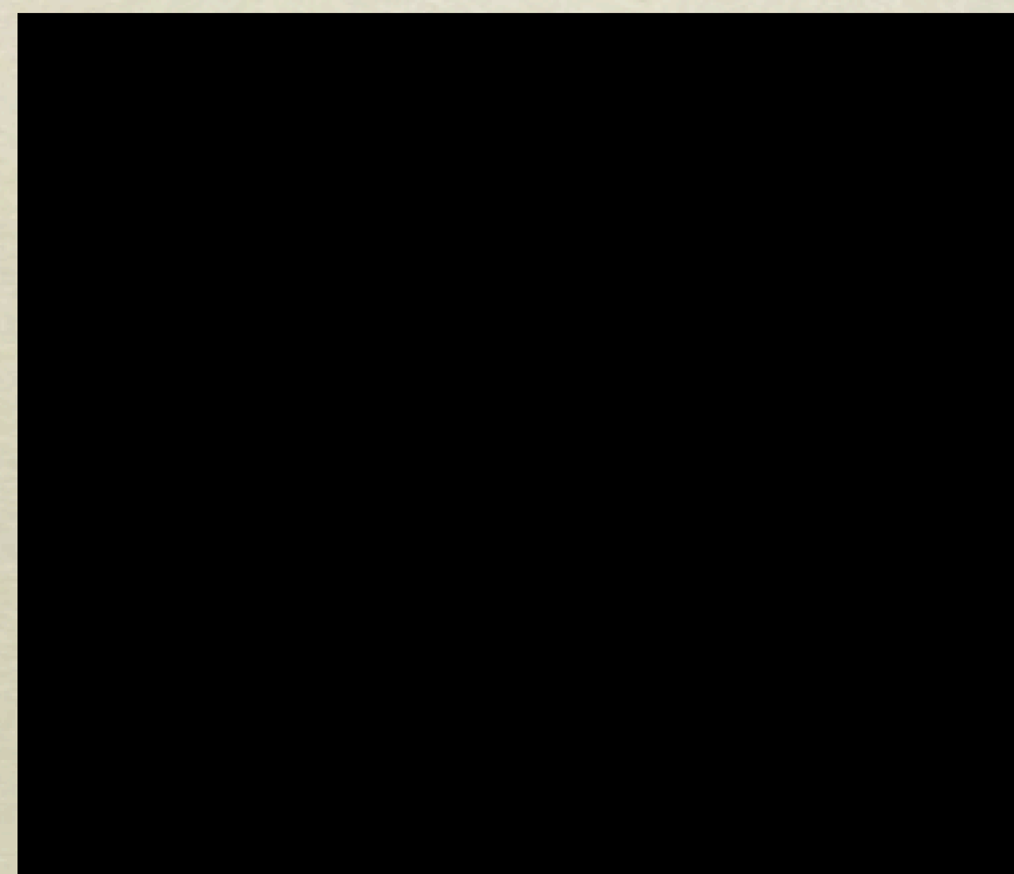

Dynamical Tunneling Examples

van der Waals
dissociation

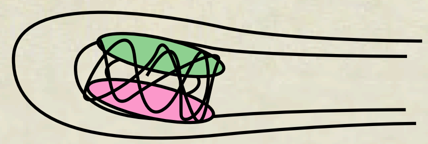

Overtone

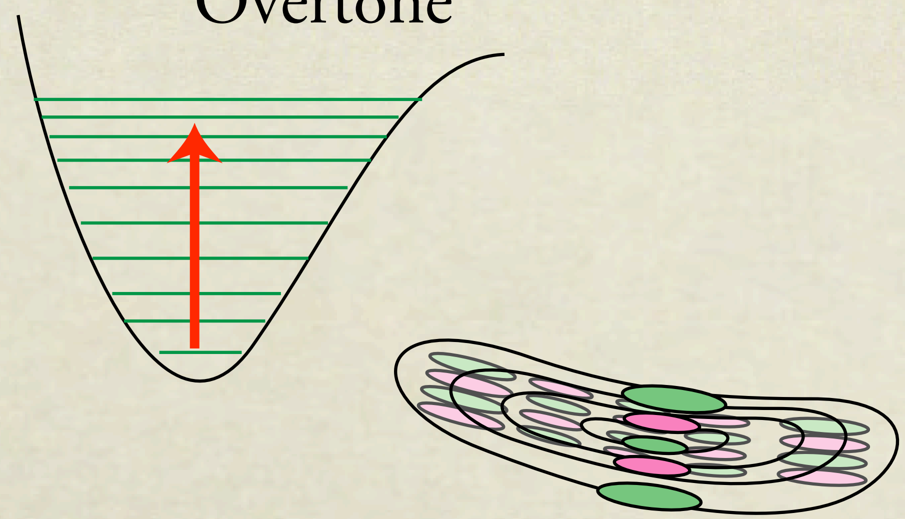

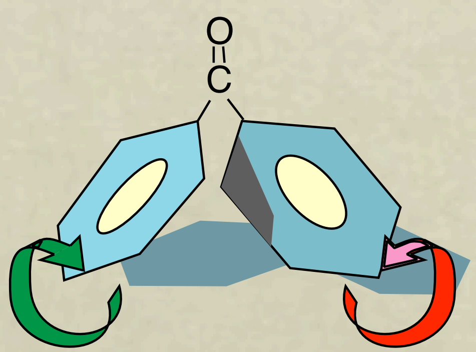

Local Mode

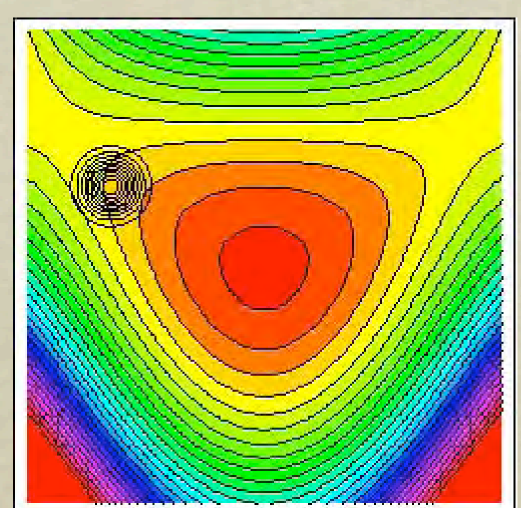

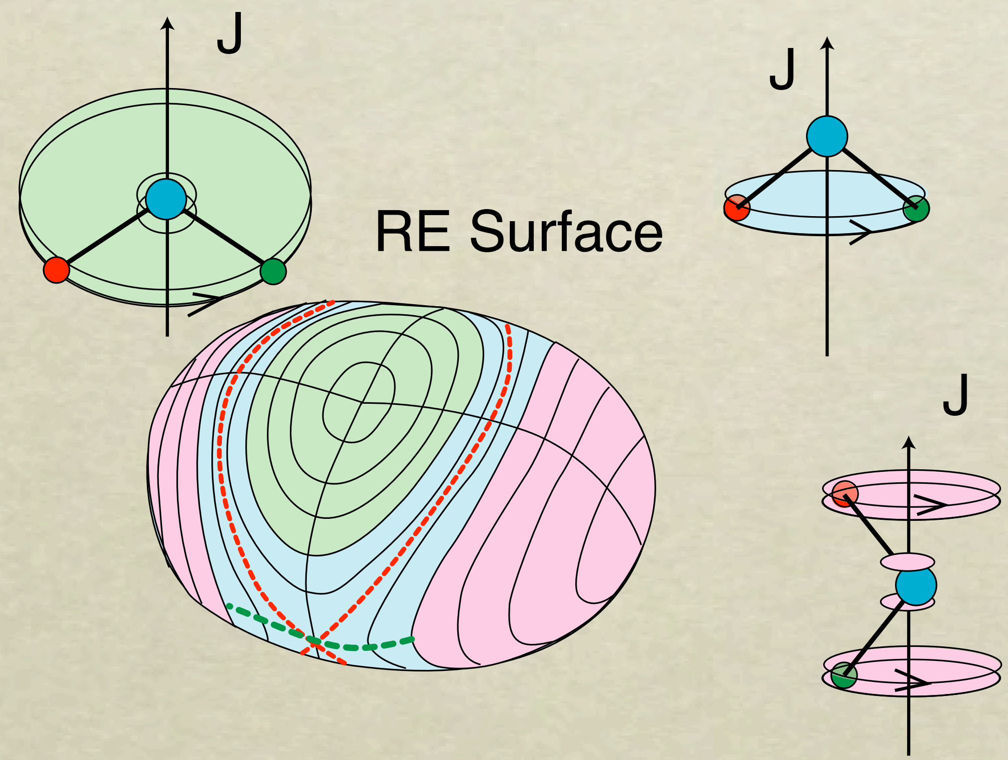

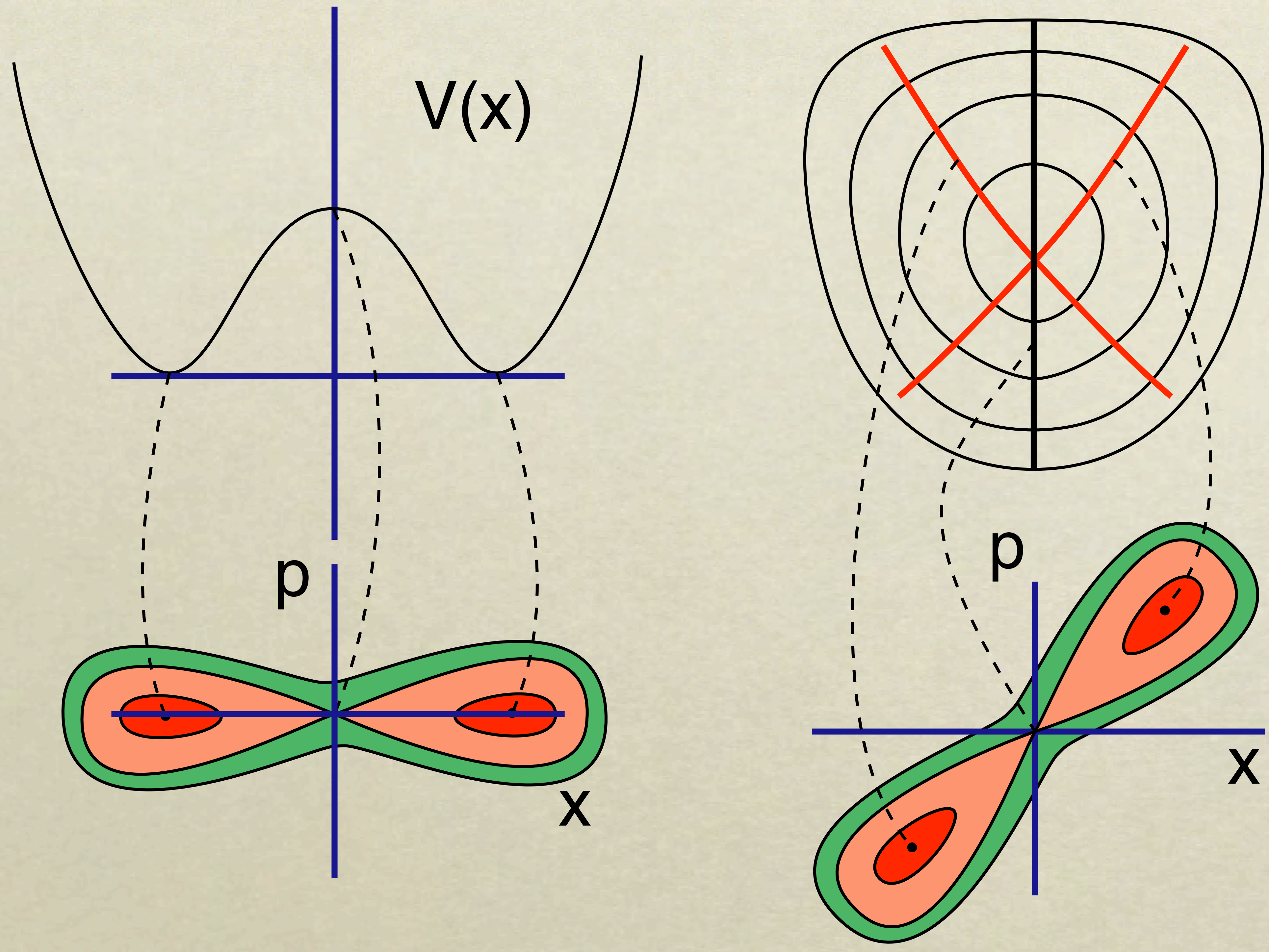
V(x)
p
x
p
x

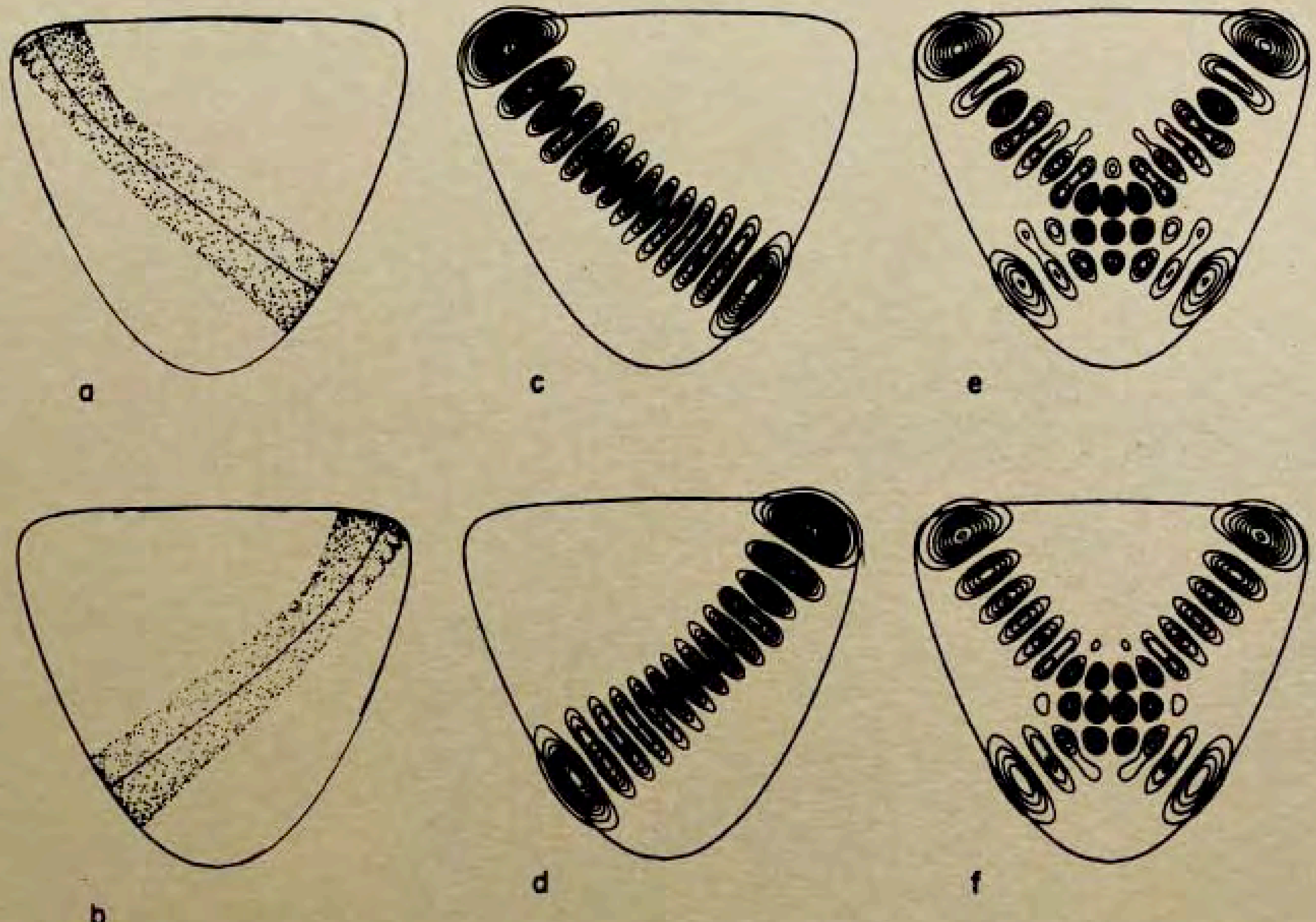
a
b
c
d
e
f

Dynamical Tunneling Examples

van der Waals dissociation

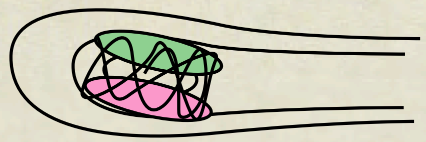

Overtone

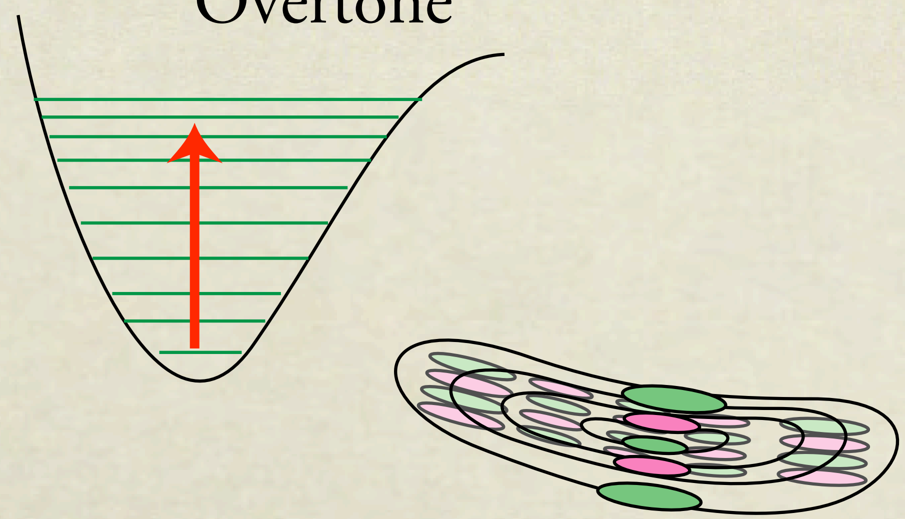

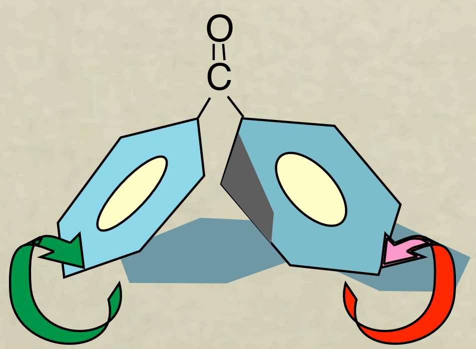

Local Mode

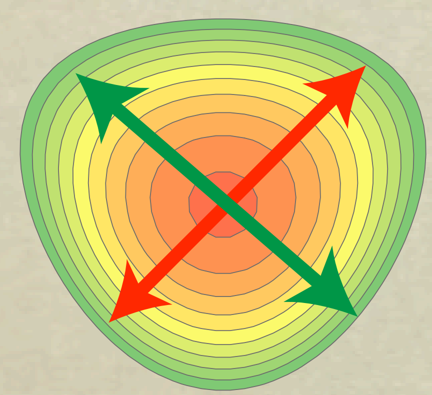

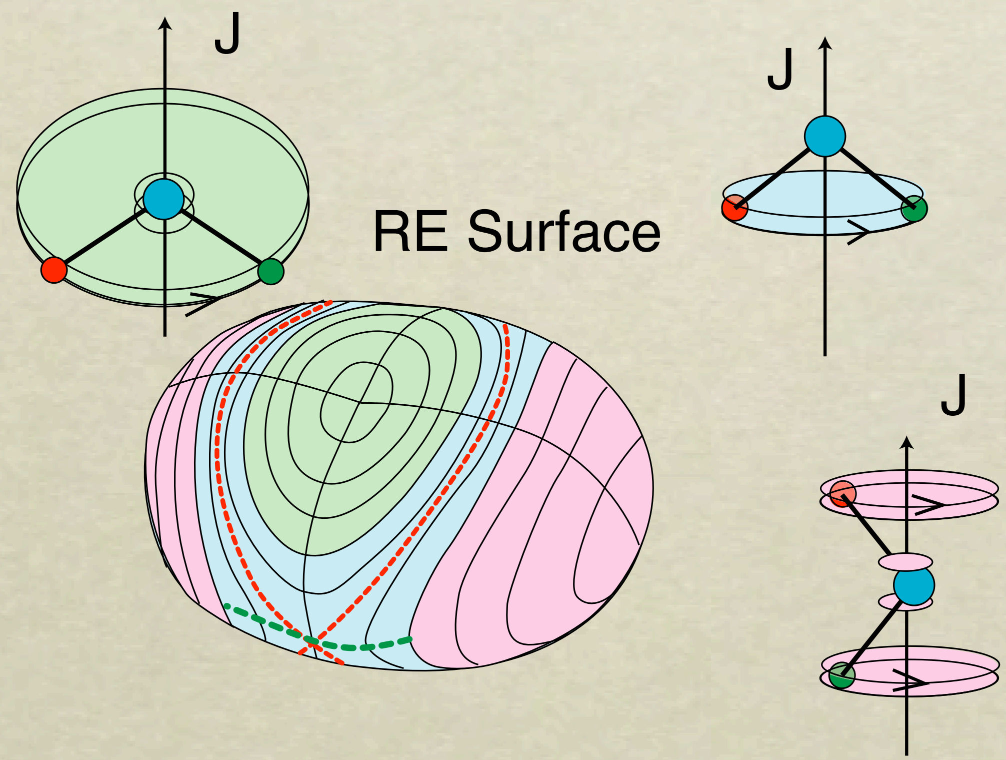

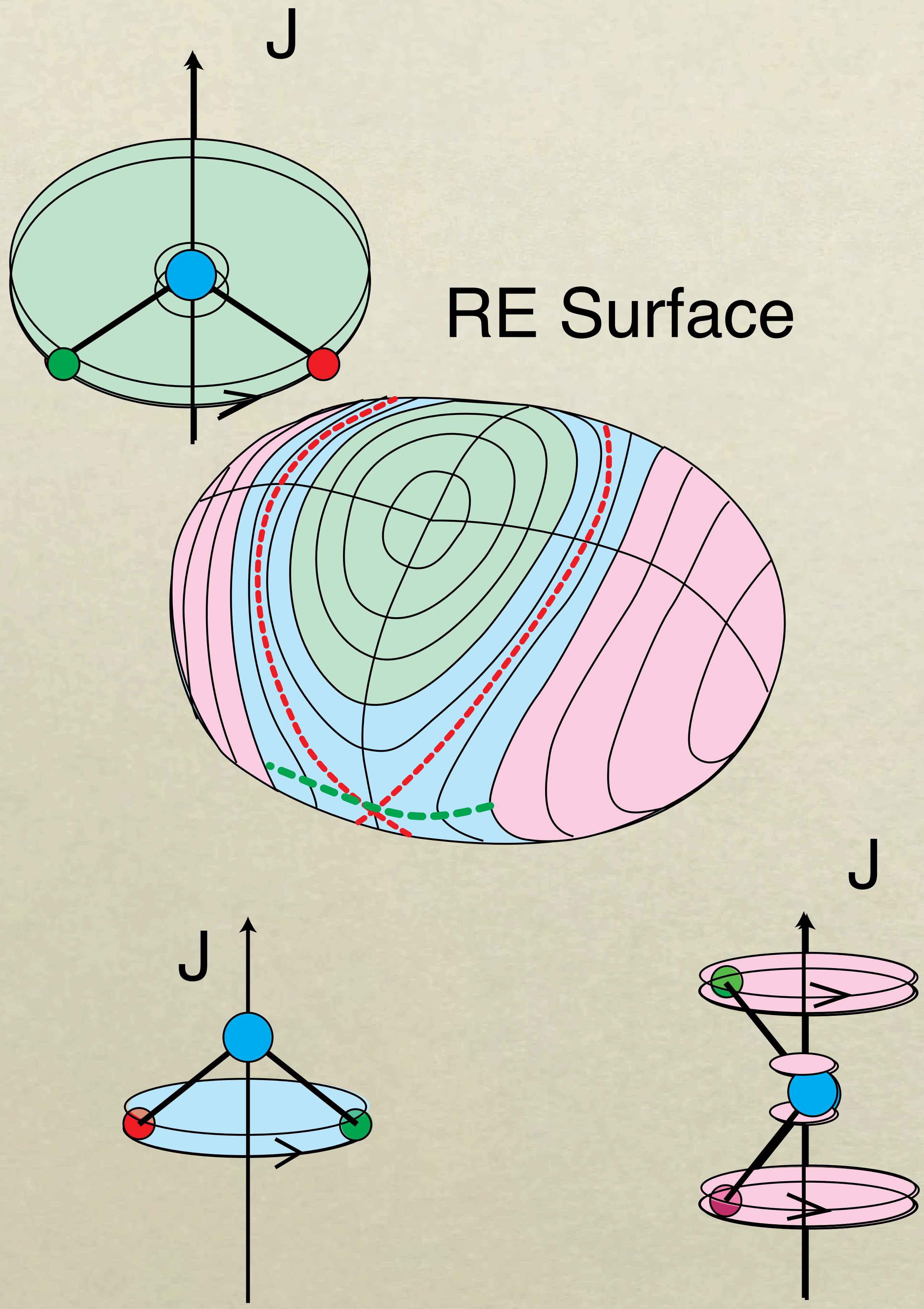
J
RE Surface
J
J

[redacted]

C-C mode chosen so
as not to shake carbon 1

Smalley 1981

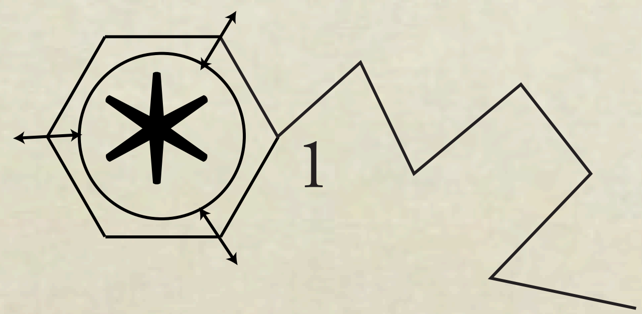

IVR takes place
and is probably
classically forbidden

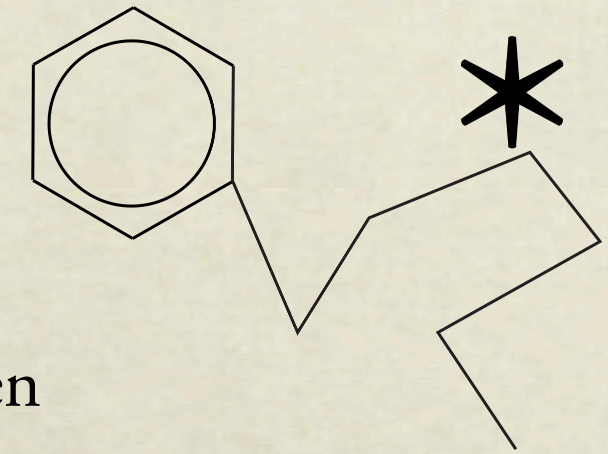

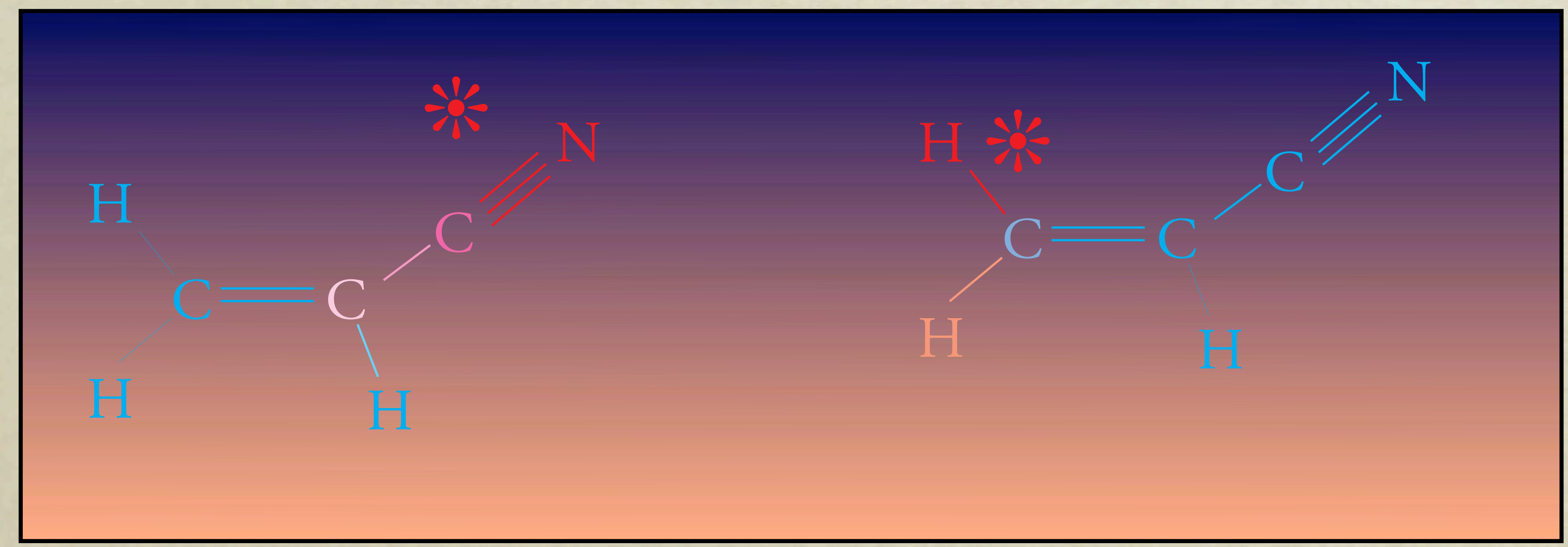

Consider a Hamiltonian in action-angle form

$$H(\mathbf{J},\theta) = H_0(\mathbf{J}) + V(\mathbf{J},\theta)$$

The potential term $V(\mathbf{J},\theta)$ is conveniently expressed as a Fourier series.

$$V(\mathbf{J},\theta) = \lambda \sum_{m,n} V_{m,n}(J_1, J_2)\cos(m\ \theta_1 - n\ \theta_2)$$

For example we might have

$$H = \alpha\ J_1 + \beta\ J_2 + \gamma\ J_1^2/2 + \delta\ J_2^2/2 + \mu J_1\ J_2 + \lambda\ J_1\sqrt{J_2}\sum_{m,n}\cos(m\ \theta_1 - n\ \theta_2)$$

This is always valid because everything is periodic in the angle variables.

Now the frequencies are gradients of the Hamiltonian (from Hamilton's equations of motion):

$$\dot{\theta}_1 = \omega_1(\mathbf{J}) = \frac{\partial H(\mathbf{J})}{\partial J_1} = \alpha + \gamma J_1 + \mu J_2 + \lambda\sqrt{J_2}\sum_{m,n}\cos(m\ \theta_1 - n\ \theta_2)$$

$$\dot{\theta}_2 = \omega_2(\mathbf{J}) = \frac{\partial H(\mathbf{J})}{\partial J_2} = \beta + \delta J_1 + \mu J_2 + \lambda\frac{J_1}{2\sqrt{J_2}}\sum_{m,n}\cos(m\ \theta_1 - n\ \theta_2)$$

and the rest of Hamilton's equations of motion are

$$\dot{J}_1 = -\frac{\partial H}{\partial \theta_1} = \sum_{n,m} V_{m,n}(J_1, J_2)\ m\ \sin(m\ \theta_1 - n\ \theta_2)$$

Then

$$\phi_1 = \theta_1 - \frac{n_0}{m_0}\theta_2; \quad \phi_2 = \theta_2$$

$$J_1 = I_1; \quad J_2 = I_2 - \frac{n_0}{m_0} I_1$$

and

$$H = H_0(I_1, I_2 - \frac{n_0}{m_0} I_1) + \sum_\ell V_{\ell m_0, \ell n_0}(\mathbf{I}) \cos(m_0 \ \ell \ \phi_1)$$

Note that ϕ_2 is missing in H, thus we have

$$\dot{I}_2 = -\frac{\partial H}{\partial \phi_2} = 0$$

$$\dot{\phi}_2 = \frac{\partial H}{\partial I_2} = \omega_2 + \frac{\partial}{\partial I_2} \sum_\ell V_{\ell m_0, \ell n_0}(\mathbf{I}) \cos(m_0 \ \ell \ \phi_1)$$

and

$$\dot{I}_1 = -\frac{\partial H}{\partial \phi_1} = -\sum_\ell V_{\ell m_0, \ell n_0}(\mathbf{I}) m_0 \ \ell \sin(m_0 \ \ell \ \phi_1)$$

$$\dot{\phi}_1 = \frac{\partial H}{\partial I_1} = \omega_1 - \frac{n_0}{m_0}\omega_2 + \frac{\partial}{\partial I_1} \sum_\ell V_{\ell m_0, \ell n_0}(\mathbf{I}) \cos(m_0 \ \ell \ \phi_1)$$

Note that the I_1, ϕ_1 system is autonomous because the ϕ_2 dependence vanishes and I_2 is a constant. Therefore,

$$H^{eff}(I_1, \phi_1) = H_0(I_1, I_2^{res} - \frac{n_0}{m_0} I_1) + \sum_\ell V_{\ell m_0, \ell n_0}(\mathbf{I}) \cos(m_0 \ \ell \ \phi_1)$$

As a further approximation, we expand about I_1^{res}:

$$
\begin{aligned}
H^{eff} \approx\ & H_0(I_1^{res}, I_2^{res} - \frac{n_0}{m_0} I_1^{res}) + (\omega_1^{res} - \frac{n_0}{m_0}\omega_2^{res})\ \delta I_1 + \\
& \frac{1}{2}\left(\frac{\partial \omega_1}{\partial J_1} - \frac{n_0}{m_0}\frac{\partial \omega_1}{\partial J_2} - \frac{n_0}{m_0}\frac{\partial \omega_2}{\partial J_1} + \frac{n_0^2}{m_0^2}\frac{\partial \omega_2}{\partial J_2}\right)\delta I_1^2 \\
& + \sum_\ell V_{\ell m_0, \ell n_0}(\mathbf{I}^{res})\ \cos(m_0 \ell\ \phi_1) \\
& \equiv H_0 + \frac{1}{2} G\ \ \delta I_1^2 + \sum_\ell V_{\ell m_0, \ell n_0}(\mathbf{I}^{res})\ \cos(m_0 \ell\ \phi_1)
\end{aligned}
$$

where we have used $(\omega_1^{res} - \frac{n_0}{m_0}\omega_2^{res}) = 0$. If the lowest $(\ell = 1)$ Fourier component is the most important we can write

$$
H^{eff} = H_0 + \frac{1}{2} G\ \ \delta I_1^2 + V_{m_0, n_0}(\mathbf{I}^{res})\ \cos(m_0\ \phi_1)
$$

This is recognized as a pendulum Hamiltonian. The reduction of a resonance to a pendulum Hamiltonian is an old trick in analysis of Hamiltonian systems with resonances. It is now a simple matter to find the fixed points (stable and unstable) and estimate the resonance width. One just takes the above Hamiltonian literally and finds the separatrices and stable islands. For example for the case

$$
3\omega_1 \approx 2\omega_2
$$

,

$$
F(\theta, \mathbf{I}) = (\theta_1 - \frac{2}{3}\ \theta_2)\ I_1 + \theta_2 I_2
$$

Then

$$
\phi_1 = \theta_1 - \frac{2}{3}\theta_2; \quad \phi_2 = \theta_2
$$

$$
J_1 = I_1; \quad J_2 = I_2 - \frac{2}{3} I_1
$$

On the surface of section, suppose that the green and red dashed tori are both EBK quantized, predicting a degeneracy. In fact, the states will be split, by dynamical tunneling. It may be shown that

$$\langle \psi^{EBK}_{2,5} | H \text{ - } E | \psi^{EBK}_{6,2} \rangle \sim \langle \psi^{EBK}_{2,5} | V^{res}_{4:3} | \psi^{EBK}_{6,2} \rangle$$

where $V^{res}_{4:3}$ is the *classical* resonance interaction "responsible" for a 4 : 3 resonance zone lying between the two tori.

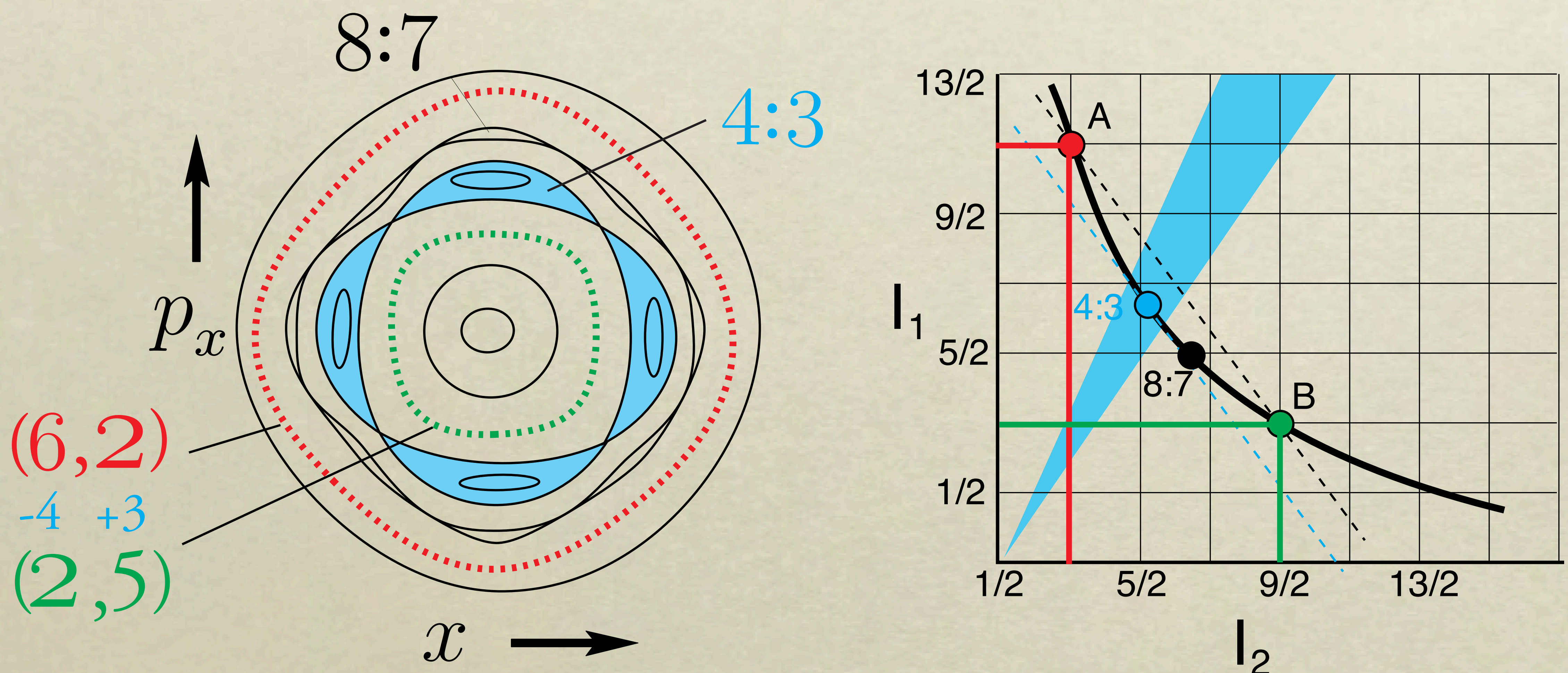

Uzer, Noid, Marcus; Ozorio de Almeida; Jaffe, Reinhardt; EJH

Narrow resonance islands

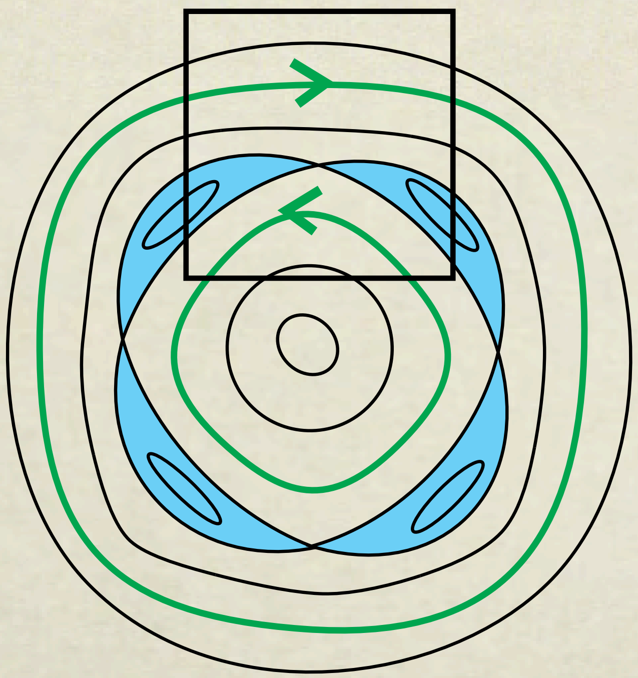

Poincare' S.O.S.

Avoided crossings increase spectral complexity

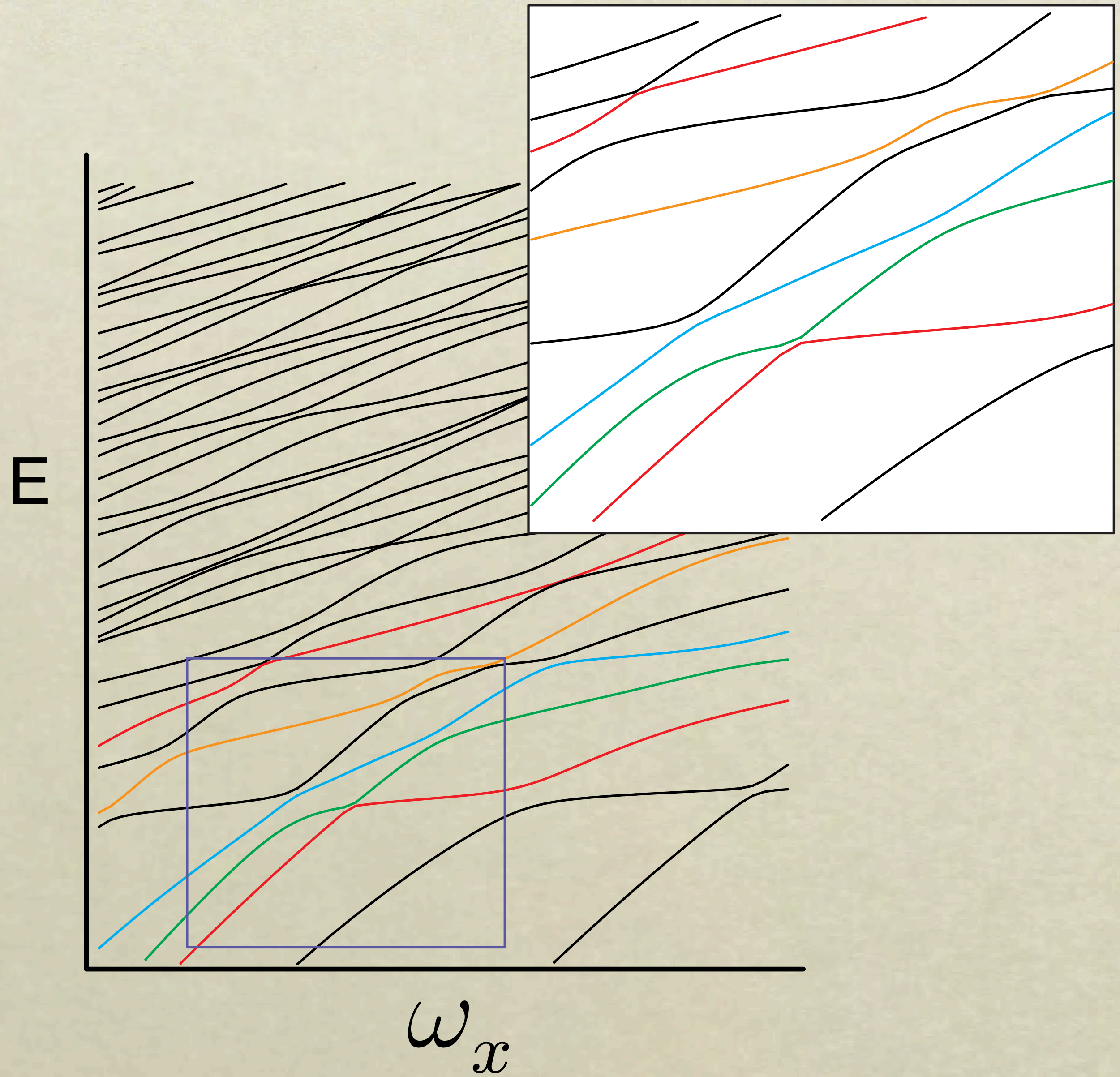

$$H = p_x^2/2 + p_y^2/2 + \omega_x^2 x^2/2 + \omega_y^2 y^2/2 + 0.2x\,y^2$$

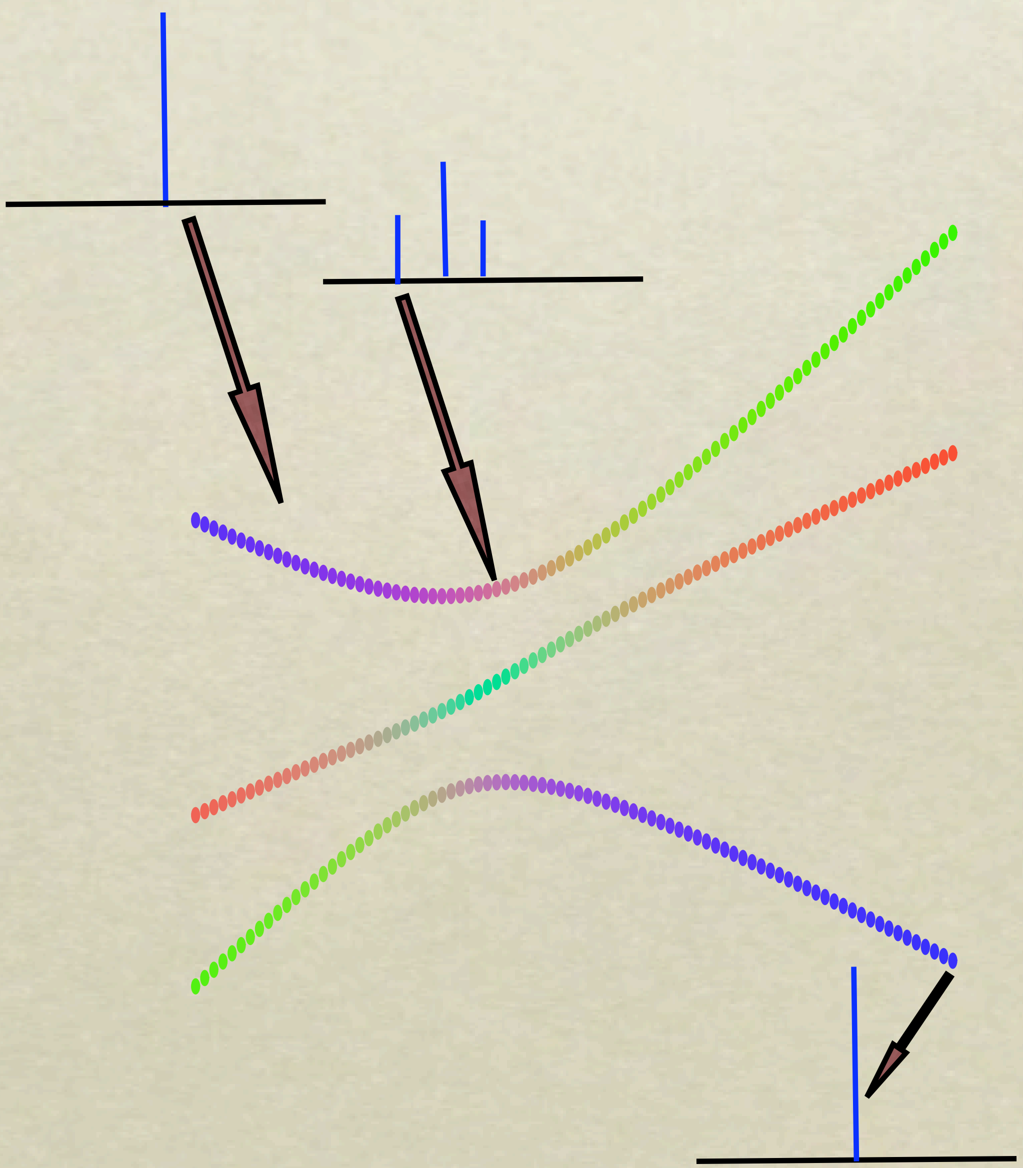

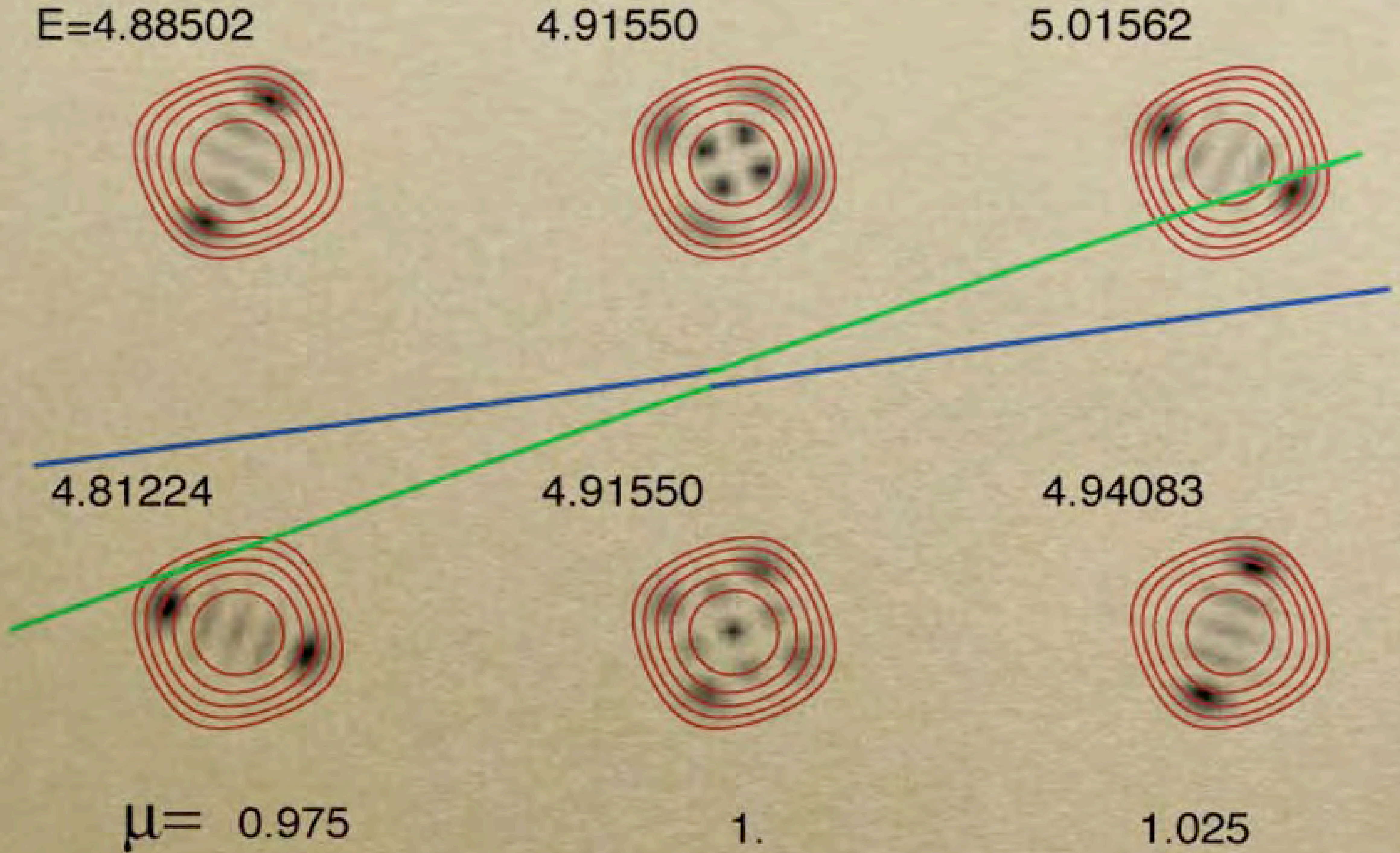
E=4.88502
4.91550
5.01562
4.81224
4.91550
4.94083
μ= 0.975
1.
1.025

Evidence for dynamical tunneling in molecules of moderate size and energy: fractionation in high resolution spectra at 0.01-0.05 cm^{-1}

JOURNAL OF CHEMICAL PHYSICS VOLUME 109, NUMBER 11 15 SEPTEMBER 1998

Intramolecular vibrational energy redistribution in the acetylenic C–H and hydroxyl stretches of propynol

Evan Hudspeth, David A. McWhorter, and Brooks H. Pate
Department of Chemistry, University of Virginia, Charlottesville, Virginia 22901

Received 12 December 1997; accepted 12 June 1998!

The high-resolution infrared spectra of the acetylenic C–H and O–H stretches of propynol have been measured using an electric-resonance optothermal molecular beam spectrometer!. Both spectra display extensive fragmentation of the hydride-stretch oscillator strength characteristic of the intramolecular vibrational energy redistribution (IVR) process. The IVR lifetime is strongly mode-specific. The IVR lifetime of the acetylenic C–H stretch is approximately 400 ps, with a slight increase in the lifetime with increasing values of the K_a quantum number. The lifetime of the O–H stretch is 60 ps and is independent of the rotational quantum numbers. The experimental upper limit for the anharmonic state densities are 30 and 40 states/cm$^{2\ 1}$ for the acetylenic C–H and O–H stretches, respectively. These values are in good agreement with the values obtained by a direct state count ~19 and 32 states/cm$^{2\ 1}$, respectively!. The measured density of states increases with an approximate ($2J+1$)-dependence. These results indicate that all energetically accessible states are involved in the IVR dynamics. However, neither the acetylenic C–H nor the O–H stretch shows a decrease in lifetime as the total angular momentum (J) increases. This result shows that Coriolis coupling of these two hydride stretches to the near-resonant bath states is much weaker than the anharmonic coupling. For the O–H stretch, we are able to obtain the root-mean-squared ~rms! matrix element for the Coriolis coupling prefactor, 0.0015 cm^{2}. The rms anharmonic coupling matrix element is 0.03 cm^{2}. For the low J values measured in the O–H spectrum, the Coriolis-induced IVR rate is much slower than the initial redistribution rate resulting from the stronger anharmonic interactions leading to an IVR process with two distinct time scales. *1998 American Institute of Physics.* @S0021-9606~98!01835-2#

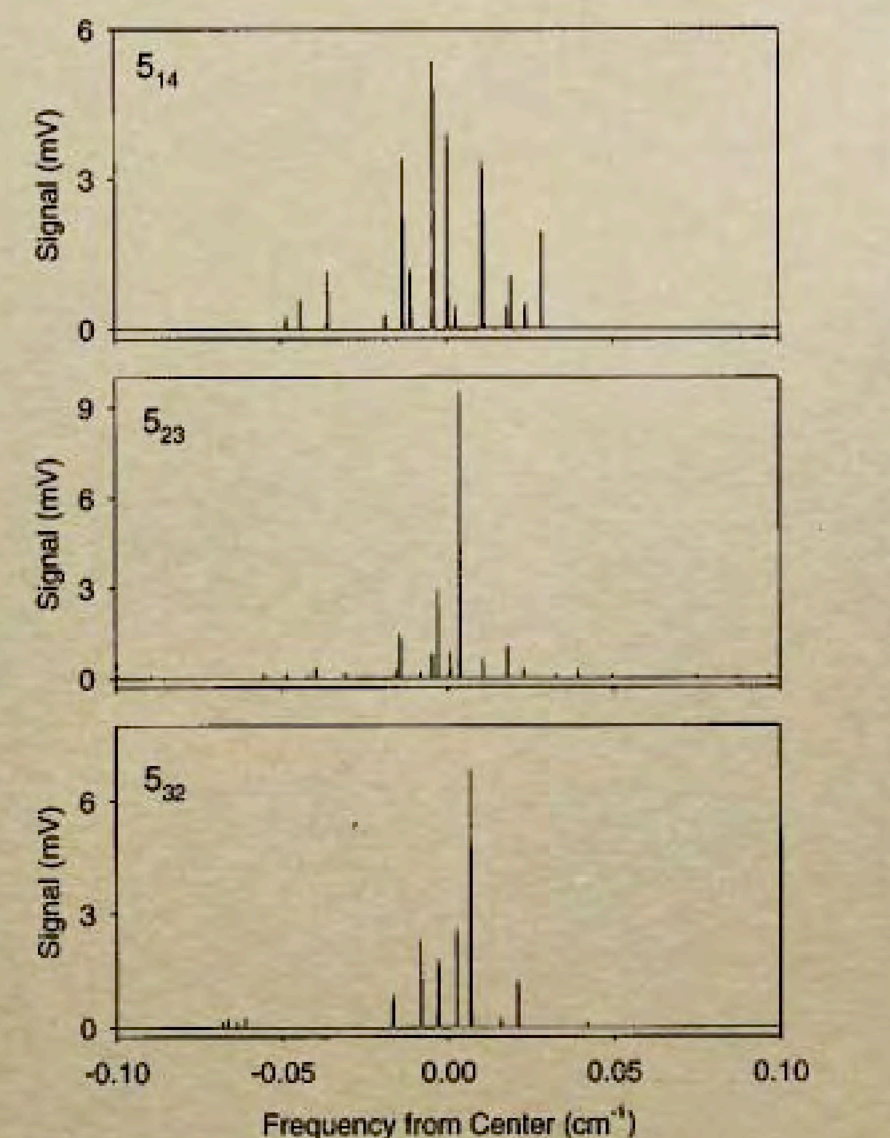

FIG. 6. The $J5$ 5 IVR multiplets of the higher energy asymmetry doublet for the acetylenic C–H stretch. These spectra of the 5_{14}, 5_{23}, and 5_{32} IVR multiplets are computer generated from the measured transition frequencies and intensities ~i.e., noise-free!. The spectra are plotted with respect to the center-of-gravity of each multiplet. For K_a5 2 and 3, the overall line shape appears to be narrower than that of the 5 spectrum.

Experiments by J. Nesbitt, K. K. Lehmann, B. H. Pate, G. Scoles, J. MacDonald, and many others have shown unassignable fractionation of spectra at the ca. 0.05 cm (-1) level in small polyatomic (5-10 atom) molecules at 1000 to 4000 cm (-1). This is a signature of IVR.

IVR is the mechanism responsible for fractionation of high resolution spectra (and thus revealing eigentates of strongly mixed, unassignable parentage). (IVR == unassignable fractionation)

Claim:
Some IVR is due to dynamical tunneling, and dynamical tunneling may even dominate the IVR.

Tunneling Tier Model-
M. Tannenbaum

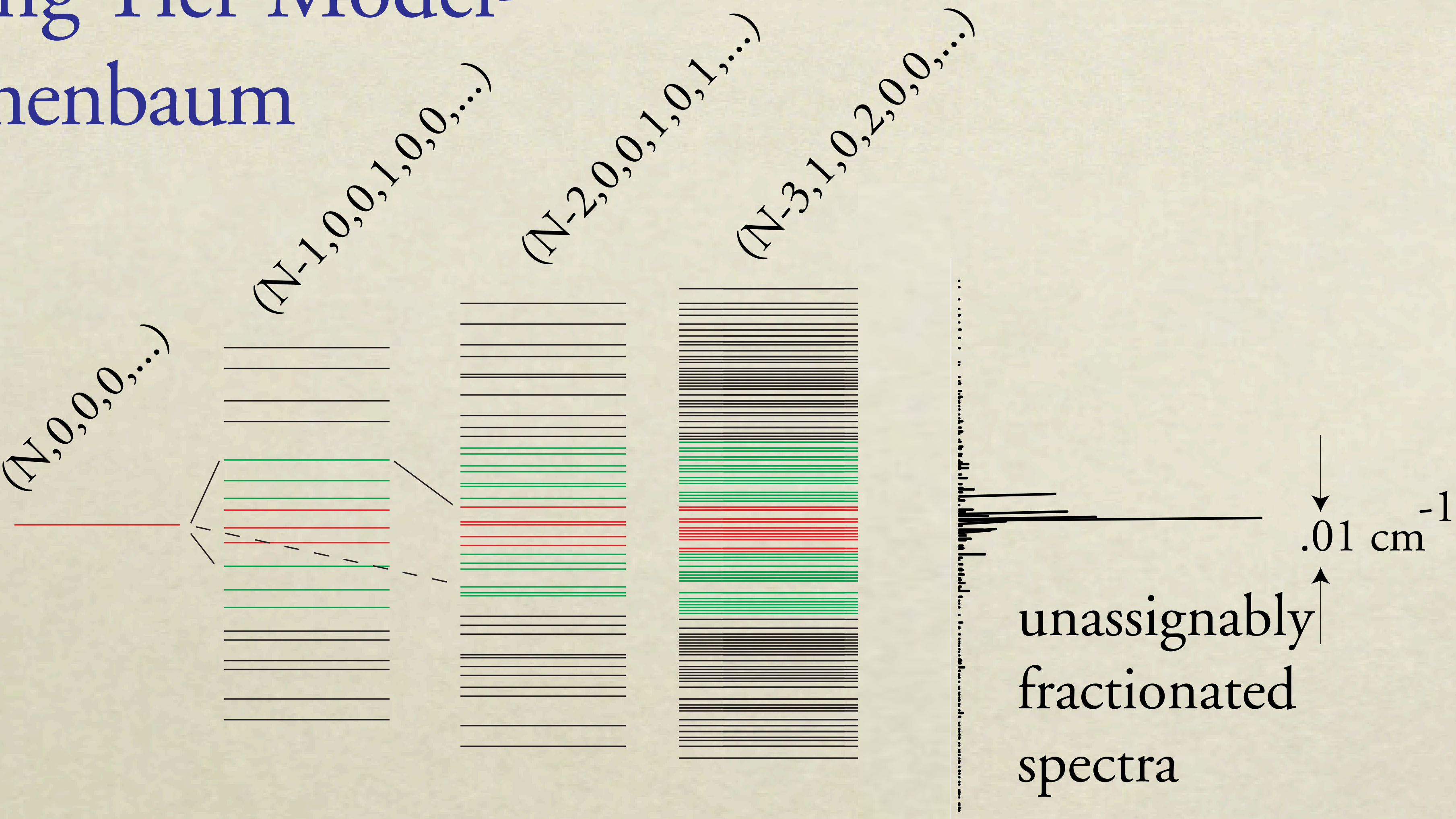

Coupling strenth trends from dynamical tunneling mechanism:

$$\langle J_1 J_2 \cdots J_N | V_{tun} | J_1' J_2' \cdots J_N' \rangle \sim \alpha \ e^{-\gamma \ |\Delta J|}$$

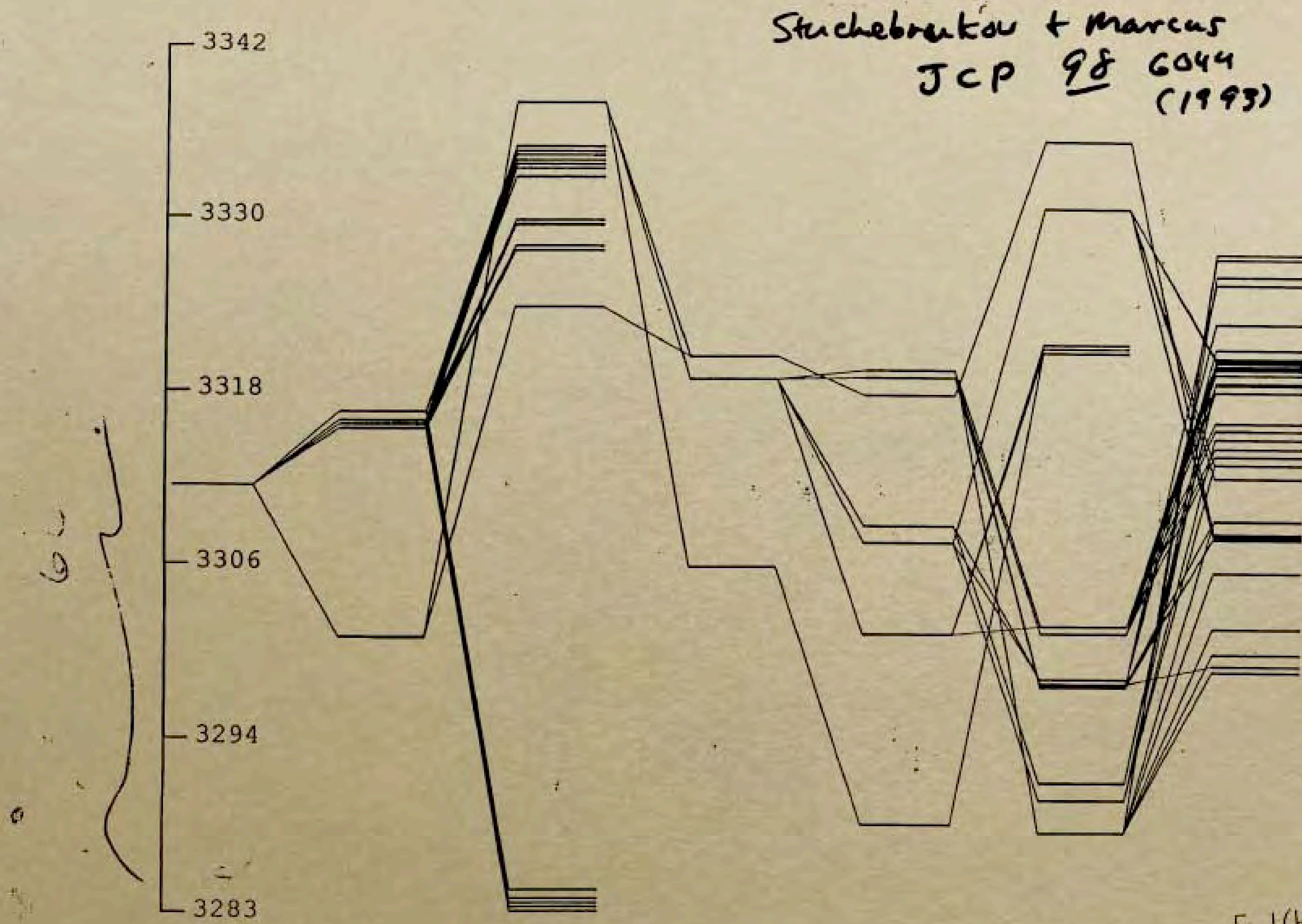

Stuchebrukov + Marcus
JCP 98 6044
(1993)
3342
3330
3318
3306
3294
3283

Traditional perturbation theory:

$$H = H_0 + V_{anharmonic\ coupling}$$

Suggested new perturbation theory:

$$H = H_{classically\ allowed} + V_{tunneling}$$

$$V_{tunneling} = V^{WKB} - V$$

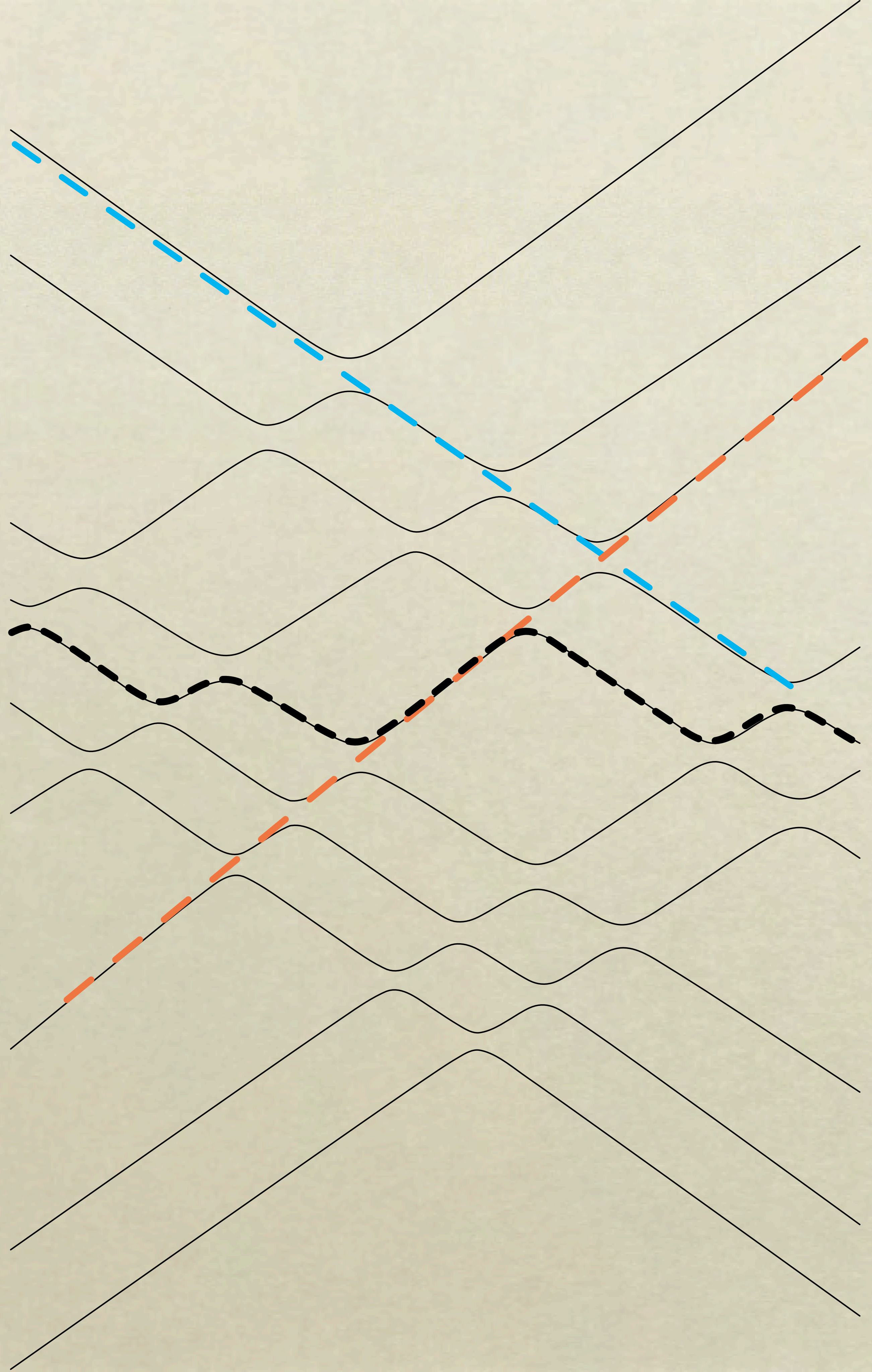

Brooks Pate: Nondeflection of larger molecules in an inhomogeneous field

"IVR" can be tunneling. Candidates:high resolution propyne, acetylene; anticrossing spectra, alkylbenzenes, etc. The tunneling can lead to complete mixing of states in a narrow energy band and lead to spectral clumps with some (but not all) random matrix characteristics.

Nature's Ho: Quantum mechanics without the dynamical tunneling. We are learning how to turn the dynamical tunneling on and off.

Narrow mediating resonance zones far outnumber global and large resonance zones; they dominate the tunneling and can be treated perturbatively but not by classical paths (i.e. they are essentially diffractive).

There may be a localization transition (Logan-Wolynes) as a function of the falloff of the direct tier tunnel coupling. Molecules could live on either side of the transition.

- E. J. Heller. "Dynamical Tunneling and Molecular Spectra", *J. Phys. Chem.*, **99**, 2625 (1995).
- E. J. Heller, book chapter "Spectroscopy and Dynamics in the Wings", in "Molecular Dynamics and Spectroscopy by Stimulated Emission Pumping", Hai-Lung Dai and R. Field, ed., (World Scientific 1995).
- E. J. Heller, "The Many Faces of Tunneling", *J. Phys. Chem.* **103** 10433 (1999).